TURUN
YLIOPISTO
UNIVERSITY
OF TURKU

ACCELERATING INNOVATION IN BIOTECHNOLOGY THROUGH KNOWLEDGE IN CYANOBACTERIAL PHOTOSYNTHESIS

Daniel Solymosi

TURUN YLIOPISTON JULKAISUJA – ANNALES UNIVERSITATIS TURKUENSIS
SARJA – SER. AI OSA – TOM. 657 | ASTRONOMICA – CHEMICA – PHYSICA – MATHEMATICA | TURKU 2021

TURUN
YLIOPISTO
UNIVERSITY
OF TURKU

ACCELERATING INNOVATION IN BIOTECHNOLOGY THROUGH KNOWLEDGE IN CYANOBACTERIAL PHOTOSYNTHESIS

Daniel Solymosi

TURUN YLIOPISTON JULKAISUJA – ANNALES UNIVERSITATIS TURKUENSIS
SARJA – SER. AI OSA – TOM. 657 | ASTRONOMICA – CHEMICA – PHYSICA – MATHEMATICA | TURKU 2021

University of Turku

Faculty of Technology
Department of Life Technologies
Molecular Plant Biology
Doctoral programme in Molecular Life Sciences

Supervised by

Professor, Yagut Allahverdiyeva-Rinne
Photosynthetic Microbes group
Molecular Plant Biology unit
Department of Life Technologies
Faculty of Technology
University of Turku, Finland

Reviewed by

Associate Professor, Joanna Kargul
Head of the Solar Fuels Laboratory
Centre of New Technologies
University of Warsaw, Poland

Professor, Francisco J. Florencio
Instituto de Bioquímica Vegetal y
Fotosíntesis,
Universidad de Sevilla, Spain

Opponent

Professor, Michael Hippler
Institute of Plant Biology and
Biotechnology, University of Münster
Germany

ISBN 978-951-29-8688-0 (PRINT)
ISBN 978-951-29-8689-7 (PDF)
ISSN 0082-7002 (Print)
ISSN 2343-3175 (Online)
Painosalama, Turku, Finland 2021

When we try to pick out anything by itself,
we find it hitched to everything else in the universe.

John Muir

UNIVERSITY OF TURKU
Faculty of Technology
Department of Life Technologies
Molecular Plant Biology
DANIEL SOLYMOSI: Accelerating innovation in biotechnology through knowledge in cyanobacterial photosynthesis
Doctoral Dissertation, 214 pp.
Doctoral Programme in Molecular Life Sciences
November 2021

ABSTRACT

Microalgae are potential hosts for the sustainable production of valuable chemicals using CO_2 as feedstock and light as an energy source. In whole-cell applications, biosynthetic reactions of interest are supplied with cellular reductants (e.g., ferredoxin or NADPH) which are recycled by the native photosynthetic apparatus. Using gene-editing techniques, photosynthesis can be engineered to increase the supply of reductants to the reactions of interest. However, such efforts require specialized knowledge about the photosynthetic machinery. Here, regulatory mechanisms of photosynthesis were investigated using the cyanobacterium *Synechocystis* sp. PCC 6803, a model organism of prokaryotic microalgae. In a primary regulatory process, excess photosynthetic electrons are transferred from ferredoxin to O_2 *via* flavodiiron proteins. However, under controlled cultivation conditions, this process is dispensable and wastes reducing power. Here, it is shown that the heterodimeric flavodiiron proteins Flv1/Flv3 and Flv2/Flv4 have distinct electron sink capacities. Flv1/Flv3 disposes of electrons at a higher capacity and faster rate than Flv2/Flv4. The applicability of such knowledge is demonstrated by disrupting Flv1/Flv3 that consequently, enhanced the supply of reductants to a targeted chemical modification catalysed by a heterologous ene reductase. FLVB, a homolog of Flv3 in green algae has previously been shown to reduce not only O_2 but nitric oxide (NO). This implies that flavodiiron proteins in cyanobacteria may be able to sink photosynthetic electrons into NO. However, it is shown here that NO inhibits photosynthesis in *Synechocystis* thus is unlikely to act as an efficient terminal electron acceptor in photosynthesis. Lastly, the promising cultivation conditions, photomixotrophy, were found to gradually decrease the photosynthetic capacity in *Synechocystis*. This decrease was reversed by deleting the cytochrome c_M protein which appears to regulate the bioenergetic processes under photomixotrophic conditions. For developing an economically feasible and robust chassis to produce targeted compounds, scientific dilemmas are still to be solved at the laboratory scale. It is demonstrated that specialized knowledge created by fundamental research in photosynthesis provides a strong basis for innovative activity in the space of algae (cyanobacteria)-related biotechnologies.

KEYWORDS: photosynthesis, microalgae, cyanobacteria, photomixotrophy, CytM, flavodiiron protein, nitric oxide, bioproduction, biotransformation

TURUN YLIOPISTO
Teknillinen tiedekunta
Bioteknologian laitos
Molekulaarinen kasvibiologia
DANIEL SOLYMOSI: Accelerating innovation in biotechnology through knowledge in cyanobacterial photosynthesis
Väitöskirja, 214 s.
Molekulaaristen biotieteiden tohtoriohjelma
Marraskuu 2021

TIIVISTELMÄ

Mikrolevien avulla voidaan mahdollisesti tuottaa arvokkaita kemikaaleja kestävästi käyttäen raaka-aineena hiilidioksidia ja energianlähteenä valoa. Koko solun sovelluksissa fotosynteesikoneiston kierrättämät solunsisäiset pelkistäjät (esim. ferredoksiini tai NADPH) mahdollistavat kyseiset biosynteettiset reaktiot. Geenieditointitekniikoilla voidaan muokata fotosynteesiä tuottamaan enemmän pelkistäjiä kyseisissä reaktioissa. Tämä vaatii kuitenkin fotosynteesikoneiston erityistä tuntemusta. Tässä työssä tutkittiin fotosynteesin säätelymekanismeja prokaryoottisen mikrolevä malliorganismin, *Synechocystis* sp. PCC 6803 -syanobakteerin, avulla. Primaarisessa säätelyprosessissa ylimääräiset fotosynteettiset elektronit kuljetetaan ferredoksiinilta O_2:lle flavoproteiinien välityksellä. Kontrolloiduissa kasvatusolosuhteissa prosessi on kuitenkin tarpeeton ja tuhlaa pelkistysvoimaa. Tässä työssä osoitetaan, että flavoproteiinien Flv1/Flv3 ja Flv2/Flv4 heterodimeerien elektroninvastaanottajan ominaisuudet ovat erilaiset. Flv1/Flv3 poistaa elektroneja tehokkaammin ja nopeammin kuin Flv2/Flv4. Näiden tietojen sovellettavuus voidaan osoittaa estämällä Flv1/Flv3 heterodimeeri, minkä seurauksena fotosynteettisiä pelkistäjiä saadaan lisää kemialliseen reaktioon, jota katalysoi heterologinen ene-reduktaasi. Aiempi tutkimus on osoittanut, että FLVB, Flv3:n homologi viherlevissä, pelkistää O_2:n lisäksi myös typpioksidia (NO). Syanobakteerien flavoproteiinit pystyvätkin mahdollisesti poistamaan fotosynteettisiä elektroneja typpimonoksidiin. Tässä työssä kuitenkin osoitetaan, että NO estää fotosynteesin Synechocystis-lajissa, joten on epätodennäköistä, että NO toimisi tehokkaana fotosynteesin viimeisenä elektronin vastaanottajana. Fotomiksotrofian, joka on lupaava kasvatusolosuhde, huomattiin asteittain vähentävän Synechocystis-lajin fotosynteettistä kapasiteettiä. Fotosynteettisen kapasiteetin väheneminen kumoutui poistamalla arvoituksellinen sytokromi cM -proteiini, joka ilmeisesti sääntelee bioenergeettisiä prosesseja fotomiksotrofisissa olosuhteissa. Tieteellisiä dilemmoja on vielä ratkaistavana laboratoriotasolla, jotta voidaan kehittää taloudellisesti järkevä ja vankka alusta haluttujen yhdisteiden tuottamiseksi. Tässä työssä osoitetaan, että fotosynteesin perustutkimuksen luoma erityistietous tarjoaa vahvan pohjan innovaatioille leviin (ja syanobakteereihin) liittyvissä bioteknologioissa.

ASIASANAT: fotosynteesi, mikrolevät, syanobakteerit, fotomiksotrofia, CytM, flavodiiron proteiini, typpioksidi, biotuotanto, biotransformaatio

Table of Contents

Table of Contents **6**

Abbreviations **8**

List of Original Publications **11**

1 Introduction **12**
1.1 Principles of oxygenic photosynthesis in cyanobacteria 12
1.1.1 Photosynthetic and auxiliary electron transport 12
1.1.2 State transitions 16
1.1.3 Bioenergetics of PSII 16
1.1.4 Q cycle and cyclic electron transfer 18
1.2 Flavodiiron proteins 19
1.2.1 Molecular function 19
1.2.2 Intra- and interprotein redox chain 20
1.2.3 Physiological role 21
1.3 Nitric oxide 22
1.3.1 Role in photophysiology 22
1.3.2 Biosynthesis 24
1.4 Respiration in cyanobacteria 25
1.4.1 The site of respiration 25
1.4.2 Bioenergetics of Cox 25
1.4.3 Cyd and ARTO in energy generation 26
1.5 C-type cytochromes 26
1.5.1 Cyt c_6 and Cyt c_6-like proteins 26
1.5.2 Cyt c_M protein 29
1.6 Central carbon metabolism 30
1.6.1 A CO_2 fixation interconnected with glycolysis 30
1.7 Photomixotrophy 32
1.7.1 Metabolic modes of cyanobacteria 32
1.7.2 Ecological and biotechnological significance 33
1.7.3 An altered photosynthesis 33
1.7.4 Carbon fluxes 35
1.8 Chemical production in cyanobacterial hosts 36
1.8.1 Engineering PET for improved bioproduction 36

2 Aims of the study **38**

3 Materials and Methods **39**
3.1 Strains and cultivation 39

3.1.1 Construction of transgenic strains ... 39
3.1.2 Cultivation conditions ... 40
3.2 Determining cell properties ... 40
3.2.1 Cell size and number ... 40
3.2.2 Concentration of intracellular chl ... 41
3.2.3 Glucose consumption ... 41
3.3 Photosynthetic activity measurements ... 41
3.3.1 Fluorescence measurements and determining the redox kinetics of P700 and Cyt *f* ... 41
3.4 Monitoring gas exchange ... 42
3.4.1 Clark-type electrode measurements ... 42
3.4.2 Membrane inlet mass spectrometry measurements ... 42
3.5 Transcriptomics ... 43
3.6 Protein analysis ... 43
3.6.1 Western blotting ... 43
3.6.2 Mass spectrometry and data-dependent analysis ... 43
3.6.3 Kinetics parameters of the YqjM enzyme ... 44
3.7 Statistical analysis ... 44

4 Main results ... 45
4.1 Deletion of CytM prevents the gradual inhibition of photosynthesis under photomixotrophic conditions ... 45
4.2 Photomixotrophically cultured ΔCytM accumulates proteins of nutrient uptake systems and cofactor biosynthetic pathways ... 46
4.3 Distinct *in vivo* activity of Flv1/Flv3 and Flv2/Flv4 in *Synechocystis* cultivated under atmospheric conditions ... 48
4.4 NO represses PSII and NDH-1 *in vivo* ... 49
4.5 Deleting Flv1 or Flv3 enhances light-driven whole-cell biotransformation ... 50

5 Discussion ... 52
5.1 Scientific dilemmas when re-designing photosynthesis ... 52
5.2 Inventive activity related to photosynthesis ... 54
5.3 Is algae-tech economically feasible and environmentally sustainable? ... 55

6 Conclusions and future perspectives ... 57

Acknowledgements ... 58

List of References ... 60

Original Publications ... 77

Abbreviations

1,3PG	1,3-bisphosphoglycerate
2PG	2-phosphoglycolate
3PG	3-phosphoglycerate
6PG	6-phosphogluconate
ANOVA	analysis of variance
acetyl CoA	acetyl coenzyme A
ADP	adenosine diphosphate
ATP	adenosine triphosphate
ARTO	alternative respiratory oxidase
CBB	Calvin-Benson-Bassham cycle
CET	cyclic electron transport
Ci	inorganic carbon
chl	chlorophyll
Co	organic carbon
Cox	cytochrome *c* oxidase
Cyd	quinol oxidase
Cys	cysteine
Cyt	cytochrome
DBMIB	2,5-dibromo-3-methyl-6-isopropylbenzoquinone
DCMU	3-(3,4-dichlorophenyl)-1,1-dimethylurea
DCBQ	2,6-dichloro-p-benzoquinone
DDA	data-dependent analysis
DHAP	dihydroxyacetone phosphate
DW	dry weight
ED	Entner-Doudoroff pathway
EMP	Embden-Meyerhof-Parnas pathway
E4P	erythrose 4-phosphate
F6P	fructose 6-phosphate
FBP	fructose 1,6-bisphosphate
Fd	ferredoxin
Fda	fructose-1,6-bisphosphate aldolase

FDP	flavodiiron protein
FQR	ferredoxin quinone oxidoreductase
FMN	flavin mononucleotide
G1P	glucose-1-phosphate
G6P	glucose-6-phosphate
GA3P	glyceraldehyde 3-phosphate
glu	glutamate
Glk	glucokinase
Gnd	6-phosphogluconate dehydrogenase
GSNO	S-Nitrosoglutathione
GWP	global warming potential
HQNO	2-heptyl-4-hydroxyquinoline-N-oxide
KDPG	2-keto-3-deoxygluconate-6-phosphate
LET	linear electron transfer
LIP	loop insertion peptide
MIMS	membrane inlet mass spectrometry
N_2O	nitrous oxide
NAD(PH)	nicotinamide adenine dinucleotide (phosphate)
NDH-1	NADH dehydrogenase-like complex 1
NPQ	nonphotochemical quenching
NROR	Rubredoxin-NADH reductase
NO	nitric oxide
NOFNiR	nitric oxide-forming nitrite reductase
NorB	nitric oxide reductase
NR	nitrate reductase
OCP	orange carotenoid protein
OPP	oxidative pentose phosphate pathway
PBS	phycobilisome
PC	plastocyanin
PEP	phosphoenolpyruvate
PET	photosynthetic electron transfer
PGR5	proton gradient regulation 5
PGRL1	PGR5-like protein 1
PHB	polyhydroxybutyrate
Pi	inorganic phosphate
PM	plasma membrane
Pps	phosphoenolpyruvate synthase
PS	photosystem
PQ	plastoquinone
PQH_2	plastoquinol

Pyr	pyruvate
R5P	ribose 5-phosphate
Rd	rubredoxin
ROS	reactive oxygen species
Ru5P	ribulose 5-phosphate
RuBP	ribulose 1,5-bisphosphate
Rubisco	ribulose 1,5-bisphosphate carboxylase/oxygenase
RTO	respiratory terminal oxidase
S7P	sedoheptulose 7-phosphate
SBP	sedoheptulose 1,7-bisphosphate
sucD	succinate-semialdehyde dehydrogenase
TCA	tricarboxylic acid cycle
TM	thylakoid membrane
Trx	thioredoxin
WOC	water oxidizing complex
Xu5P	xylulose 5-phopsphate
Y(I)	quantum yield of photosystem I
Y(II)	quantum yield of photosystem II
Y(ND)	nonphotochemical quantum yield of PS I equivalent to donor side limitation
Y(NA)	nonphotochemical quantum yield of PS I equivalent to acceptor side limitation
ziaAB	zinc transporter
zwf	glucose-6-phosphate 1-dehydrogenase

List of Original Publications

This dissertation is based on the following original publications, which are referred to in the text by their Roman numerals:

I Solymosi, D., Nikkanen, L., Muth-Pawlak, D., Fitzpatrick, D., Vasudevan, R., Howe, C. J., Lea-Smith, D. J., Allahverdiyeva, Y. Cytochrome c_M decreases photosynthesis under photomixotrophy in *Synechocystis* sp. PCC 6803. *Plant Physiology,* 2020; 183(2): 700–716.

II Santana-Sanchez, A., Solymosi, D., Mustila, H., Bersanini, L., Aro, E.-M., & Allahverdiyeva, Y. Flavodiiron proteins 1–to-4 function in versatile combinations in O_2 photoreduction in cyanobacteria. *ELife*, 2019; 8: 1–22.

III Solymosi, D., Shevela, D., Allahverdiyeva, Y. Nitric oxide represses photosystem II and NDH-1 in the cyanobacterium *Synechocystis* PCC 6803. Accepted manuscript, *BBA – Bioenergy,* 2021.

IV Assil-Companioni, L., Büchsenschütz, H. C., Solymosi, D., Dyczmons-Nowaczyk, N. G., Bauer, K. K. F., Wallner, S., Macheroux, P., Allahverdiyeva, Y., Nowaczyk, M. M., & Kourist, R. Engineering of NADPH Supply Boosts Photosynthesis-Driven Biotransformations. *ACS Catalysis*, 2020; 10(20): 11864–11877

V Nikkanen, L., Solymosi, D., Jokel, M., Allahverdiyeva, Y. Regulatory electron transport pathways of photosynthesis in cyanobacteria and microalgae: Recent advances and biotechnological prospects. *Physiologia Plantarum*, 2021; 173(2): 514–525.

Other scientific articles related to this thesis:

Calzadilla, P. I., Zhan, J., Sétif, P., Lemaire, C., Solymosi, D., Battchikova, N., Kirilovsky, D. The cytochrome b6f complex is not involved in cyanobacterial state transitions. *Plant Cell*, 2019; 31(4): 911–931.

1 Introduction

Cyanobacteria are a group of immensely diverse prokaryotes predominantly carrying out oxygenic photosynthesis. That is, splitting water into O_2, protons, and electrons at the expense of harvested light energy to provide reductants and energy for fixing atmospheric CO_2 into carbohydrates. By producing O_2, ancestors of cyanobacteria facilitated the oxygenation of the atmosphere ~3-2.4 billion years ago, enabling the emergence of complex life forms (Schirrmeister et al., 2015). According to endosymbiotic theory, chloroplasts of algae and plants originate from cyanobacteria which gave rise to the evolution of the green lineage: cyanobacteria, green algae, mosses, gymnosperms, and flowering plants (Keeling, 2010). A widely applied model organism of modern cyanobacteria is the unicellular *Synechocystis* sp. PCC 6803 (hereafter *Synechocystis*), ubiquitous in freshwater (Rippka et al., 1979). The genome of *Synechocystis* has been resolved (Kaneko et al., 1996) and can be modified with relative ease (Berla et al., 2013). Our current understanding of the biology of cyanobacteria is largely based on studies in *Synechocystis*. In the space of biotechnology, cyanobacteria are often grouped with microscopic eukaryotic algae (such as green algae and diatoms) and referred to as microalgae. Strictly speaking, the prokaryotic cyanobacteria are not microalgae but occupy a similar niche to that of microalgae in natural and bioindustrial environments. Hence, cyanobacteria are included in the term microalgae in this work.

1.1 Principles of oxygenic photosynthesis in cyanobacteria

1.1.1 Photosynthetic and auxiliary electron transport

Photosynthetic light reactions in cyanobacteria take place in intracellular lipid bilayer membrane envelopes, the thylakoids. Photons are captured by the reaction centres of photosystem (PS) II and PSI—P680 and P700—consisting of chlorophylls (chl) and absorbing light energy in narrow spectral ranges peaking at 680 nm and 700 nm, respectively (Stanier and Cohen-Bazire, 1977). To expand the spectral range of photosynthetically active radiation, cyanobacteria employ light-harvesting

antenna complexes—phycobilisomes (PBS)—that are composed of phycobiliproteins absorbing light energy in the 490 nm–650 nm range and channelling excitation energy to PSII or PSI (Watanabe and Ikeuchi, 2013).

Absorbed light energy triggers a series of downhill redox reactions in the thylakoids, called the linear electron transfer (LET). Electrons originating from water-splitting at the lumenal side of PSII (Eq. 1) are transferred *via* the plastoquinone (PQ) pool, cytochrome (Cyt) b_6f, Cyt c_6 or plastocyanin (PC), and PSI to the cytoplasmic ferredoxin (Fd) proteins (Fig.1).

$$2\ H_2O = O_2 + 4\ e^- + 4\ H^+ \quad \text{(Equation 1)}$$

In ideal conditions, Fd is primarily oxidized by $NADP^+$ reductase (FNR) to convert $NADP^+$ into the major cellular reductant NADPH, which is utilized for assimilating CO_2 in the Calvin-Benson-Bassham (CBB) cycle (Mullineaux, 2014; Rexroth et al., 2017). The activity of some enzymes in the CBB cycle is tightly linked to the redox state of the Fd pool. Redox signals are conveyed via cytoplasmic thioredoxin (Trx) proteins, which when reduced by e.g., Fd-Trx reductase, activate target enzymes *via* thiol/disulfide exchange (Meyer et al., 2012). This regulatory pathway is essential; depletion of the ubiquitous *m*-type Trx in *Synechocystis* leads to severe redox imbalance (Mallén-Ponce et al., 2021).

In natural conditions however light capture may outpace CO_2 fixation due to sudden increases in light intensity or limited carbon availability. The Fd pool may saturate and place PSI under electron pressure (Kramer et al., 2004), potentially triggering the generation of reactive oxygen species (ROS), which are highly cytotoxic (Khorobrykh et al., 2020). To prevent oxidative damage, cyanobacteria employ various photoprotective mechanisms. Excess absorbed energy may be (i) dissipated as heat by the orange carotenoid protein (OCP) at PBS (Kerfeld et al., 2017; Muzzopappa and Kirilovsky, 2020); (ii) reallocated *via* state transitions (Calzadilla and Kirilovsky, 2020); or (iii) transferred as electrons to electron "outlets" *via* auxiliary electron transfer pathways (Alboresi et al., 2019; Allahverdiyeva et al., 2015b). In cyanobacteria, the major auxiliary electron sinks are flavodiiron proteins (FDP) and NADH dehydrogenase-like complex 1 (NDH-1), which transfer excess electrons from Fd to O_2 and the PQ pool, respectively (Allahverdiyeva et al., 2013; Nikkanen et al., 2020). The pathway *via* NDH-1 is called cyclic electron transport (CET) pathway around PSI since electrons which have traversed through the PQ pool, Cyt b_6f, and PSI, are again transferred to the PQ pool.

Respiratory terminal oxidases (RTO) located in the thylakoid provide additional—albeit lower—capacity to sink excess electrons (Ermakova et al., 2016). The PQ pool can be oxidized by Cyt *c* oxidase (Cox) *via* Cyt b_6f and Cyt c_6/PC (Molina-Heredia et al., 2002; Pils et al., 1997), or directly by quinol oxidase (Cyd)

proteins (Berry et al., 2002). Both RTOs dispose of electrons by reducing O_2 into water. Shared components between photosynthetic and respiratory electron transfer such as the PQ pool, Cyt b_6f, and Cyt c_6/PC complicate regulation but provide flexibility in allocating excess electrons between alternative sink. Indeed, the ability of Cox and Cyd to limit electron flow to PSI has recently been demonstrated *in vivo* (Viola et al., 2021).

Electron transfer in the thylakoid is tightly coupled to the formation of proton motive force (*pmf*), an electrochemical gradient consisting of differences in H^+ concentration (ΔpH) and electric field (ΔΨ) between the lumenal and cytoplasmic side of the thylakoid membrane (Kramer et al., 2003). The ΔpH is generated by processes that accumulate protons in the lumen such as water-splitting at PSII, PQ/PQH_2 oxidoreduction at Cyt b_6f (Q-cycle), and proton-pumping from the cytoplasm to the lumen by NDH-1 and Cox. Moreover, FDP, Cox, and Cyd alkalify the cytosol *via* their oxidase activity. In parallel, ΔΨ builds up due to the ΔpH and transmembrane fluxes of ions such as K^+ (Checchetto et al., 2012). *Pmf* is released among others by ATP synthase which translocates protons from the lumen to the cytoplasm to obtain rotational energy for the conversion of ADP and pyrophosphate into the primary energy carrier ATP (Boyer, 1997). LET is responsible for the bulk of light-induced *pmf* generation although NDH-1 can maintain 40% when PSII is blocked (Miller et al., 2021). To avoid excess production of ATP and maintain ion homeostasis in the thylakoid, lumen acidification triggers PSII to dissipate excess absorbed energy via non-photochemical quenching (NPQ), and imposes photosynthetic control on LET by limiting the activity of Cyt b_6f (Bassi and Dall'Osto, 2021; Foyer et al., 2012). Both are vital regulatory mechanisms in higher oxygenic photosynthetic organisms such as green algae, mosses, gymnosperms, and flowering plants but play a less significant role in cyanobacteria that have a higher PSI/PSII ratio and employ OCP, a protein operating independently of lumen acidification (Kerfeld et al., 2017; Muzzopappa and Kirilovsky, 2020).

In short, the highly branched electron transport network (Fig. 1) provides flexibility for cyanobacteria to safely allocate electrons while meeting metabolic demands in the ever-changing natural environment.

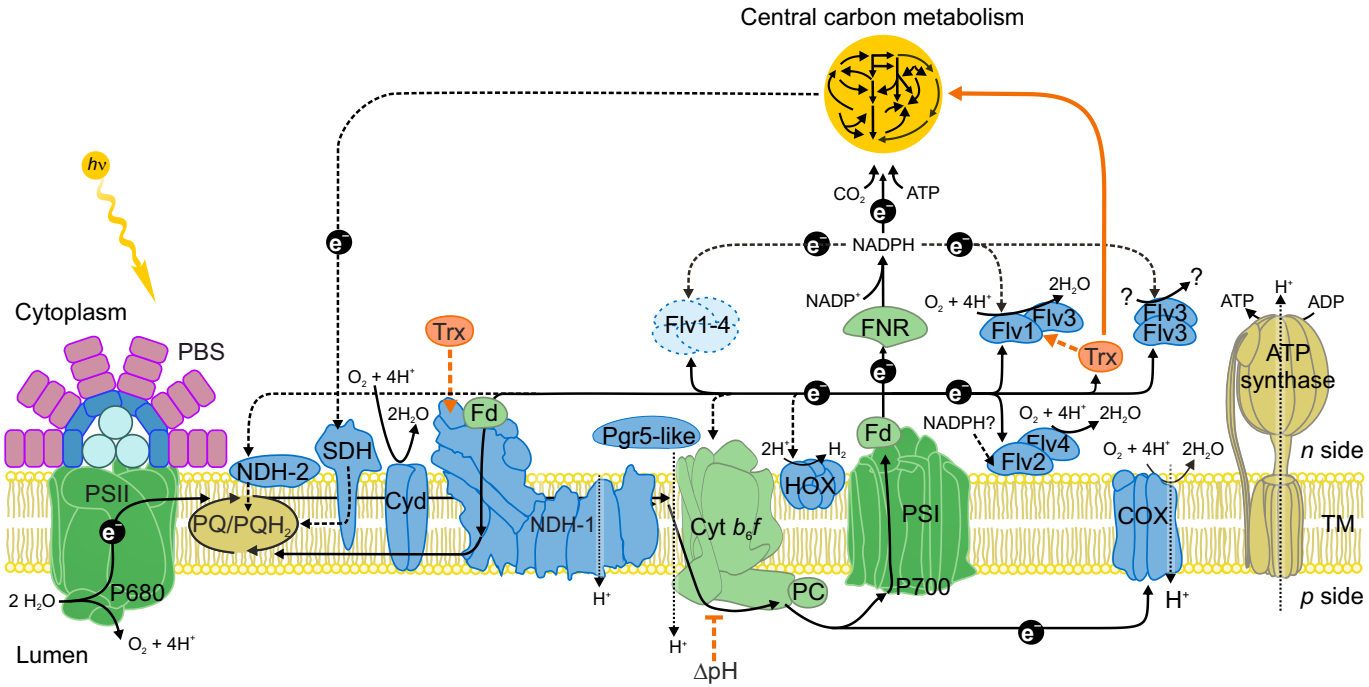

Figure 1. The route of linear electron transport branches into auxiliary electron transport pathways in the thylakoids of *Synechocystis*. ATP and NADPH generated by photosynthesis is utilized in various cellular processes, primarily in CO_2 fixation. The figure is adopted with some modifications from Paper V (Nikkanen et al., 2021).

1.1.2 State transitions

In order to balance unequal excitation pressure on photosystems, the energy absorbed by chl or phycobilin pigments is thought to be dynamically reallocated between PSI and PSII. This reallocation was proposed to account for changes in emission of fluorescence: a decrease in fluorescence by selective excitation of PSII (state II) was interpreted as exporting energy of PSII; and an increase in fluorescence by preferential excitation of PSI (state I) was suggested to reflect the import of energy to PSII (Bruce et al., 1985; Kirilovsky et al., 2014; McConnell et al., 2002; Mullineaux and Allen, 1990). Two mechanisms were hypothesized as means of re-allocating excitation energy; (i) dissociation/association and reversible migration of PBS as means of re-distributing phycobilin-absorbed excitation energy (Joshua and Mullineaux, 2004; Mullineaux et al., 1997) and (ii) spill-over—exciton transfer between PSII and PSI—to balance chl-absorbed energy (Olive et al., 1997). However, it has been shown recently that low fluorescence emission in state II is not the result of excitation energy reallocation via PBS or spill-over but an energy dissipative mechanism in the core of PSII (Bhatti et al., 2020; Ranjbar Choubeh et al., 2018). Dissipation is induced by excessive reduction of the LET chain (Calzadilla et al., 2019) and appears to depend on PSII-PBS interactions (Bhatti et al., 2021). Recently, structural changes in the core of PSII upon illumination was shown to account for some of the changes in fluorescence emission (Sipka et al., 2021), corroborating the idea that dissipation may indeed be associated with the core of PSII. Thus, the classical interpretation of state transitions in cyanobacteria is challenged and a conclusive model remains to be seen.

1.1.3 Bioenergetics of PSII

PSII is a transmembrane pigment-protein complex functioning as a light-driven water-PQ oxidoreductase with chemistry highly conserved among oxygenic photosynthetic organisms (Cardona et al., 2012; Fischer et al., 2016). The core of the PSII monomer consists of (i) the D1/D2 dimer ligating redox cofactors essential for the initial photochemical processes; (ii) CP43 and CP46 inner antenna proteins; (iii) and several small subunits (Loll et al., 2005; Umena et al., 2011; Zouni et al., 2001).

The initial photochemical processes, charge separation and water oxidation, are catalysed at the donor side of PSII in the thylakoid lumen. When P680 is triggered by the energy of an absorbed photon, charge separation occurs that is the formation of a pair of positively charged $P680^+$ and negatively charged $Pheo_{D1}^-$. $P680^+Pheo_{D1}^-$ ejects an electron that is captured by the primary quinone Q_A at the acceptor side of PSII close to the cytoplasm. As a one-electron recipient, the singly reduced Q_A^- rapidly transfers the electron to the secondary quinone Q_B generating the singly reduced Q_B^-. $P680^+$ fills its electron-hole *via* Tyr_Z by an electron derived from the

water-oxidizing complex (WOC) containing a Mn_4CaO_5 cluster. When excited again, P680 transforms to a charge separated state, passes the newly obtained electron to Q_B^- and further oxidizes the Mn_4O_5Ca cluster. In total, 4 charge separations are required to complete the oxidation cycle (Kok-cycle) of WOC, split two water molecules, and release an O_2 molecule. However, Q_B carries only 2 electrons, thus when doubly reduced (and protonated to Q_BH_2 by cytosolic protons), is then replaced to a PQ of the thylakoid membrane (Fig. 2; Rexroth et al., 2017).

Q_A and Q_B are chemically identical PQ molecules but feature distinguishable redox potentials (E_m) essential for electron transfer. The redox potential of Q_A/Q_A^- has long been controversial. Published values have varied but the reasons for differences remained unclear (Krieger et al., 1995). This hindered determining the redox potential of Q_B/Q_B^- (or Q_B/Q_BH_2) resulting in ambiguity at the heart of PSII bioenergetics. Recently, it has been clarified that the presence or absence of a bicarbonate ligand accounts for the differences in published redox potential values of Q_A/Q_A^- (Brinkert et al., 2016). The bicarbonate is ligated to a non-heme iron flanked by Q_A and Q_B (Hienerwadel and Berthomieu, 1995; Zouni et al., 2001). Upon light flashes, the bicarbonate may be released and converted to CO_2 (Shevela et al., 2020) shifting the redox potential of Q_A/Q_A^- from −145 mV to −70 mV (Brinkert et al., 2016). These findings revealed the role of bicarbonate in regulating Q_A-to-Q_B transfer by increasing the energy gap between Q_A and Q_B thus limiting forward electron transfer. By determining the redox potential of Q_B/Q_B^- (90 mV) and Q_B/Q_BH_2 (40 mV) the driving force of Q_A-to-Q_B electron transfer was finally calculated: to be 235 meV (De Causmaecker et al., 2019).

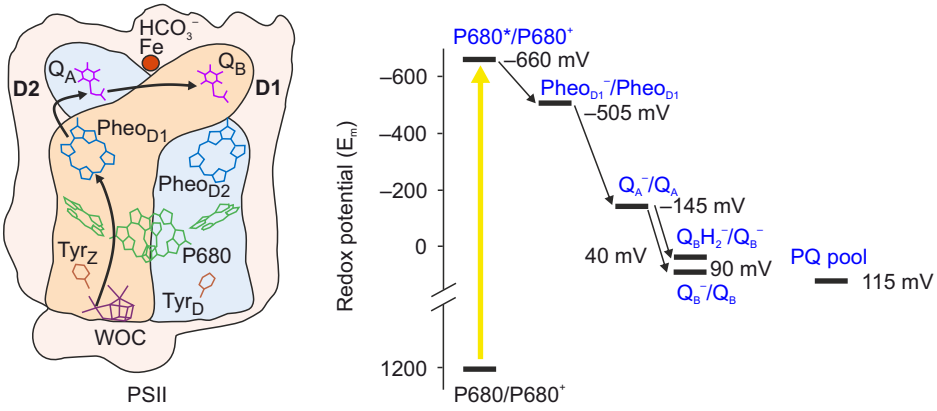

Figure 2. The route of light-induced electron transfer within PSII and the redox potentials of the corresponding redox cofactors. References to E_m values can be found elsewhere (De Causmaecker et al., 2019).

1.1.4 Q cycle and cyclic electron transfer

The most detailed model of the photosynthetic Q cycle is based on the biochemistry and structure of Cyt b_6f in *Chlamydomonas reinhardtii* (hereafter *Chlamydomonas*) which is a common model organism of green algae (Cape et al., 2006; Cramer and Hasan, 2016; Malone et al., 2021). The function and structure of Cyt b_6f are well conserved in oxygenic photosynthetic organisms (Malone et al., 2021) therefore the model of Q cycle established in *Chlamydomonas* is projected onto that in cyanobacteria.

Via the Q cycle, PQH_2 molecules dissociated from PSII are oxidized and deprotonated at the quinol oxidase (Q_o) site of Cyt b_6f. The two electrons of a PQH_2 are split between two transfer routes: (i) the high potential chain consisting of Rieske iron-sulfur protein and Cyt *f* ultimately leading *via* Cyt c_6/PC to PSI; and (ii) the low potential chain composed of heme b_L, b_H, and c_i dedicated to the regeneration of a fresh PQ to PQH_2 at the quinone reductase (Q_i) site of Cyt b_6f (Fig. 3). To conserve redox power, *pmf* is generated: the two protons of a PQH_2 at the Q_o site are released to the lumen, and an additional proton is picked up from the cytosol at the Q_i site to protonate PQ. In the canonical model of the Q cycle, regeneration of PQ to PQH_2 proceeds *via* a singly reduced $PQH^{\bullet}$ radical intermediate and is only finalized when a second PQH_2 is oxidized at the Q_o site. However, $PQH^{\bullet}$ is highly reactive and may produce the toxic ROS in $O_2^{\bullet-}$ (Cape et al., 2006).

An alternative model has been proposed where heme c_i coupled with heme b_H is preloaded with an electron originating from Fd, therefore, enabling quasi two-electron reduction of PQ and circumventing the production of $PQH^{\bullet}$ intermediate (Cramer and Hasan, 2016; Mulkidjanian, 2007). Such *modus operandi* requires the Cyt b_6f to function as a Fd-PQ reductase (FQR), in other words, redirecting photosynthetic electrons back to the PQ pool via CET. Recent spectroscopic studies suggest that Cyt b_6f indeed operates as FQR in *Chlamydomonas* when exposed to anoxic conditions (Buchert et al., 2020). These conditions are known to induce CET likely by triggering the formation of PSI-LHCI-Cyt b_6f supercomplexes (Finazzi et al., 1999; Steinbeck et al., 2018). It was proposed that the proton gradient regulation 5 (PGR5) and PGR5-like protein 1 (PGRL1) assist in tethering FNR and Fd to Cyt b_6f (Mosebach et al., 2017). Indeed, Cyt b_6f-assisted CET was hindered in PGR5-deficient *Chlamydomonas* when exposed to anoxic conditions (Buchert et al., 2020). In *Synechocystis*, NDH-1 rather than Cyt b_6f appears to be the major FQR (Miller et al., 2021). Accordingly, deleting the homolog of PGR5 has minor effects on the physiology of *Synechocystis* (Margulis et al., 2020; Yeremenko et al., 2005). Genes encoding PGRL1 are absent in cyanobacterial genomes (Peltier et al., 2010), although a putative uracil-DNA glycosylase of *Synechocystis* was recently suggested to function in a manner analogous to PGRL1 of plants (Dann and Leister, 2019).

Regardless of which complex acts as FQR, CET always generates *pmf* since the rerouted electrons originating from Fd participate in additional Q-cycles, thus promoting lumen acidification and ATP production (Fig. 3). Importantly, CET decreases NADPH output since FQR oxidizes Fd proteins which would have otherwise been allocated to FNR. Thus, CET is widely regarded as a mechanism to adjust the ATP/NADPH ratio. Recently, it was estimated that ~35% of electrons passing through PSI are circulating *via* CET in *Synechocystis* exposed to constant illumination, demonstrating the vital importance of CET in cyanobacteria (Theune et al., 2020).

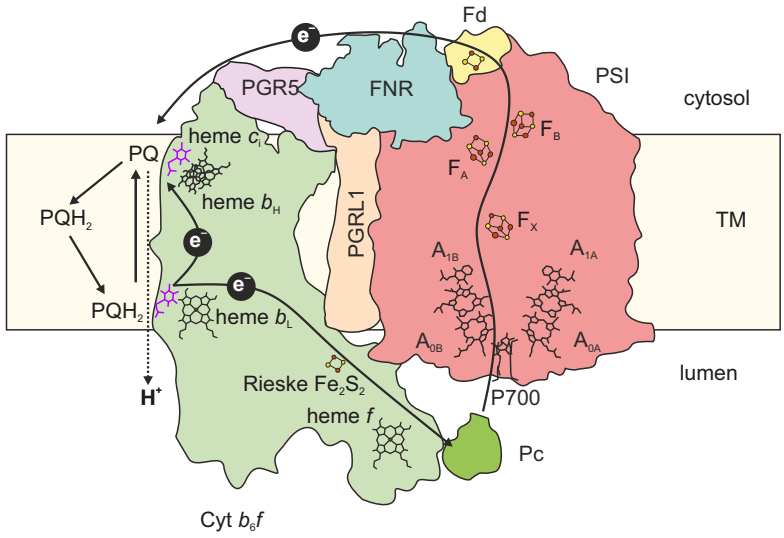

Figure 3. Model of the Q-cycle assisted by Cyt b_6f-dependent cyclic electron flow in *Chlamydomonas*.

1.2 Flavodiiron proteins

1.2.1 Molecular function

FDPs are widespread in all the three Domains of living organisms; Bacteria, Archaea, and Eukarya. Their primary molecular function is reducing O_2 to water (Eq. 2) or nitric oxide (NO) to nitrous oxide (N_2O, Eq. 3) without generating reactive intermediates.

$$O_2 + 4\ e^- + 4\ H^+ = 2\ H_2O \text{ (Equation 2)}$$

$$NO + 2\ e^- + 2\ H^+ = ½\ N_2O + ½\ H_2O \text{ (Equation 3)}$$

Cyanobacteria possess 2-6 FDP gene paralogs (*flv1A, flv1B, flv2, flv3A, flv3B, flv4*) that are divided into cluster A (Flv1A, Flv1B, Flv2) and B (Flv3A, Flv3B, Flv4)

based on amino acid sequence similarities (Zhang et al., 2009). Co-transcription of *flv2* with *flv4* is ensured by organizing these genes into *flv4-open reading frame-flv2* operons in *β*-cyanobacteria where *Synechocystis* belongs. The arrangement of *flv1* and *flv3* genes is not conserved (Allahverdiyeva et al., 2015a). Nonetheless, Flv1 and Flv3 proteins were shown to accumulate co-dependently in *Synechocystis* (Mustila et al., 2016). Flv1 and Flv3 thus likely form functional pairs, and indeed, photoreduction of O_2 *in vivo* was only observed when both proteins were expressed (Allahverdiyeva et al., 2011; Helman et al., 2003). Interestingly, Flv3 proteins are substantially more abundant than Flv1 in *Synechocystis* (Allahverdiyeva et al., 2013) suggesting that alternative oligomerization may occur *in vivo*. In line with this, Flv3/Flv3 homodimers have been detected in *Synechocystis* (Mustila et al., 2016). Although such homodimers are capable of reducing O_2 *in vitro* (Brown et al., 2019), *in vivo* studies suggest yet an alternative function of Flv3/Flv3 homodimers (Mustila et al., 2016). Arrangements other than monomeric arrangements cannot be excluded, tetramerization of Flv1 and Flv3 in 1:3 ratio or combination with Flv2 and Flv4 may occur (Santana-Sanchez et al., 2019). However, direct evidence is yet to be seen.

1.2.2 Intra- and interprotein redox chain

The core of an FDP monomer consists of two domains; the N-terminal metallo-*β*-lactamase-like domain containing the catalytic diiron centre and the C-terminal flavodoxin-like domain harbouring a flavin mononucleotide (FMN) cofactor (Romão et al., 2016). The minimal functional unit of the majority of FDPs is a homodimer or homotetramer arranged into a head-to-tail orientation, bringing the catalytic diiron "head" near to the FMN "tail", enabling interprotein electron transfer from FMN to the diiron centre (Hayashi et al., 2010; Helman et al., 2003; Vicente et al., 2002).

Ancient FDPs (class A) found in many prokaryotes and archaea comprised only the two N- and C-terminal core modules (Folgosa et al., 2018). Class A FDPs thus require additional redox partners which provide electrons for the FMN cofactor (Gonçalves et al., 2011). In the primitive Proteobacteria *Desulfovibrio gigas* and Firmicutes *Clostridium acetobutylicum*, FDP has two redox partners, Rubredoxin (Rd) serving as the electron donor for FMN, and Rubredoxin-NADH reductase, (NROR) keeping the Rd pool reduced at the expense of NADH (Hayashi et al., 2010; Hillmann et al., 2009; Silaghi-Dumitrescu et al., 2003). During the course of evolution, different redox partners were fused to the core domains of FDP resulting in more complete electron transfer condensed into a single polypeptide chain which simplified the operation of these enzymes. In modern Proteobacteria such as *Escherichia coli*, Rd is fused to the C-termini of FDP (class B) thus only one redox partner, NROR, is required to transfer electrons from NADH to FDP (Folgosa et al.,

2018). In oxygenic photosynthetic organisms and some protozoa, an NAD(P)H-flavin oxidoreductase-like domain is fused to the C-termini (class C) instead of Rd, enabling a complete interprotein electron transport chain from NAD(P)H to O_2 or NO (Vicente et al., 2002). Accordingly, the class C FDP Flv1 and Flv3 purified from *Synechocystis* was shown to reduce O_2 to water at the expense of NAD(P)H *in vitro* in the absence of additional redox partners (Vicente et al., 2002; Brown et al., 2019). Curiously, however, Flv1 and Flv3 in *Synechocystis* appear to favour Fd over NAD(P)H as the electron donor *in vivo* (Nikkanen et al., 2020; Sétif et al., 2020). In line with this, a class A FDP purified from the protozoan *Entamoeba histolytica* was shown to oxidize Fd *in vitro* (Cabeza et al., 2015). Both Fd and Rd contain an iron-sulfur cluster, utilizing iron-sulfur proteins as electron donors of FDP thus appears to be evolutionarily conserved.

1.2.3 Physiological role

The physiological role of FDPs varies among host organisms. Anaerobic prokaryotes such as the acetogenic *Moorella thermoacetica* utilizes FDPs to maintain intracellular anoxic conditions (Silaghi-Dumitrescu et al., 2003), and denitrifying prokaryotes e.g. *Paracoccus denitrificans* may scavenge excess endogenous NO by FDPs (Gomes et al., 2002). In oxygenic photosynthetic organisms possessing FDPs (the majority except for flowering plants and red algae), the primary physiological function of these proteins is safeguarding the photosynthetic apparatus. Flv1 (or FLVA) and Flv3, or their homologs in higher organisms the FLVA and FLVB, respectively, keep PSI oxidized by transferring surplus electrons from Fd to O_2, thus preventing the generation of ROS (Alboresi et al., 2019; Allahverdiyeva et al., 2015a). Since Flv1 and Flv3 reduce O_2 to water by electrons originating from water-splitting at PSII, the reaction can be considered as a water-to-water cycle. A similar reaction —the so-called Mehler-reaction— occurs when excessively reduced components of the LET (e.g. Fd) reduce O_2 to O_2^- which is neutralized to water by a superoxide dismutase and peroxidase *via* the H_2O_2 intermediate (Asada, 1999; Kozuleva et al., 2020). Due to similarities between Mehler-reactions and that catalysed by Flv1 and Flv3, the latter is denoted as the Mehler-like reaction (Allahverdiyeva et al., 2011). Importantly, FDPs appear to have higher catalytic efficiency (10^5 M^{-1} s^{-1}, purified Flv3 *in vitro*) than the Mehler-reaction (10^3 M^{-1} s^{-1}, purified Fd *in vitro*) thus outcompeting the latter (Brown et al., 2019; Kozuleva and Ivanov, 2010).

High catalytic efficiency is combined with high capacity. Flv1 and Flv3 in *Synechocystis* was shown to transfer ~40-60% of photosynthetic electrons to O_2 at dark-to-light transitions (Allahverdiyeva et al., 2011; Helman et al., 2005). Accordingly, loss of Flv1 (or FLVA) and Flv3 (or FLVB) is lethal when

Synechocystis, *Chlamydomonas*, or the moss *Physcomitrella patens* are exposed to abrupt and intense light strokes, demonstrating that the Mehler-like reaction is indispensable in these organisms which habitually experience intensely fluctuating light (Allahverdiyeva et al., 2013; Gerotto et al., 2016; Jokel et al., 2018).

Apart from relieving PSI of electron pressure, Flv1, Flv3, and the FLVA, and FLVB homologs in green algae accelerate LET. This was evidenced by lower rates of gross O_2 production in FLVB-deficient *Chlamydomonas* when compared to the wild type (Chaux et al., 2017). Accelerated LET in turn generates *pmf* and initializes the CBB cycle. Indeed, a loss of FDPs was required for building up ΔpH under dark-to-light transitions in *Synechocystis*, *Chlamydomonas*, and the mosses *Physcomitrella patens,* and *Marchantia polymorpha* (Chaux et al., 2017; Gerotto et al., 2016; Nikkanen et al., 2020; Shimakawa et al., 2017) and for kick-starting the CBB cycle in *Chlamydomonas* shifted from dark anaerobic to light oxic conditions (Burlacot et al., 2018). Recently, it was shown that FDPs in *Chlamydomonas* catalyse the light-induced reduction of NO to N_2O *in vivo* demonstrating that *via* dual substrate specificity, the role of FDP in green algae extends to NO detoxification (Burlacot et al., 2020). Dual substrate specificity was earlier demonstrated in FDP isolated from the prokaryote *Moorella thermoacetica* (Silaghi-Dumitrescu et al., 2003). The structural features determining substrate specificity of FDPs and whether cyanobacterial FDPs can reduce NO remain to be elucidated.

The role of Flv2 and Flv4, the paralogs of Flv1 and Flv3 in *β*-cyanobacteria is less understood. Earlier it has been proposed to protect PSII in *Synechocystis via* transferring excess electrons from Q_B^- or the PQ pool to an unknown electron acceptor (Bersanini et al., 2014; Chukhutsina et al., 2015; Zhang et al., 2012, 2009). However, a recent study revealed the protection attributed to Flv2 and Flv4 was in fact facilitated by the sll0218 protein that is co-expressed with Flv2 and Flv4 proteins due to the arrangement of the encoding genes into the *flv4-sll0218-flv2* operon (Bersanini et al., 2017). The sll0218 protein was shown to contribute to the repair and structural stability of PSII (Bersanini et al., 2017), the function of Flv2 and Flv4 however remains to be seen.

1.3 Nitric oxide

1.3.1 Role in photophysiology

NO has been shown *in vivo* to act as an electron acceptor for FLVB in green algae (Burlacot et al., 2020). Similarly, Flv3, the homolog of FLVB in *Synechocystis*, may transfer electrons to NO. In other words, NO may function as a sink of photosynthetic electrons in cyanobacteria. However, NO is a gaseous radical highly reactive towards O_2, transition metals (e.g., Fe, Mn, Co), and redox-active moieties

of biological macromolecules such as cysteine (Cys) residues within proteins (Astier et al., 2011; Ford and Lorkovic, 2002). Hence, understanding the effects of NO on the photosynthetic apparatus is imperative to uncover whether NO can act as an electron acceptor.

NO functions as a signalling molecule in numerous cellular processes such as growth, nutrient uptake, and biotic or abiotic stresses in flowering plants and green algae (Astier et al., 2021; Kolbert et al., 2019). The primary NO signalling mechanism in these organisms is S-nitrosation, a post-translational modification of proteins that is the conversion of thiolate of Cys residues into S-nitrosothiol predominantly by NO-derived molecules such as N_2O_3 (Astier et al., 2011; Lamotte et al., 2015). When the flowering plant *Arabidopsis* and green algae *Chlamydomonas* were exposed to the NO donor S-nitrosoglutathione (GSNO) peptide, several photosynthetic proteins were found to be S-nitrosated such as PSII, Cyt b_6f, PSI, or the ribulose-1,5-bisphosphate carboxylase/oxygenase (Rubisco) enzyme (Lindermayr et al., 2005; Morisse et al., 2014). S-nitrosation was shown to facilitate the degradation of Cyt b_6f and Rubisco thus regulating the composition of thylakoids and the capacity of CO_2 fixation, respectively (De Mia et al., 2019; Wei et al., 2014). Little is known about the physiological role of NO in cyanobacteria.

Apart from S-nitrosation, NO affects photosynthesis by binding to metal cofactors of the photosynthetic apparatus. It has been demonstrated that NO binds and chemically reduces the water-oxidizing Mn_4O_5Ca cluster *in vitro* in thylakoids and PSII complexes isolated from spinach and the cyanobacterium *Thermosynechococcus elongatus*, respectively (Goussias et al., 1997; Sarrou et al., 2003; Schansker et al., 2002). Ferrous iron (Fe^{2+}), abundant in the photosynthetic apparatus, is especially susceptible to NO (Ford and Lorkovic, 2002). The ferrous non-heme iron positioned between Q_A and Q_B was found to ligate NO in isolated spinach thylakoids leading to substantially slower Q_A-to-Q_B electron transfer and decreased PSII photochemical efficiency *in vitro* (Diner and Petrouleas, 1990; Petrouleas and Diner, 1990). These modifications substantially decreased PSII efficiency *in vivo*, as evidenced by studies on leaf discs of pea (*Pisum sativum*) and epidermal strips of bean (*Vicia faba*) exposed to GNSO under atmospheric conditions, respectively (Ördög et al., 2013; Wodala et al., 2008). Moreover, NO was shown to bind the heme c_i of Cyt b_6f under anoxic conditions *in vitro* (Twigg et al., 2009). These studies elucidated that NO limits the photochemical activity in higher photosynthetic organisms (Fig. 4). Nonetheless, the impacts of NO on photosynthesis in cyanobacteria *in vivo* remains to be elucidated.

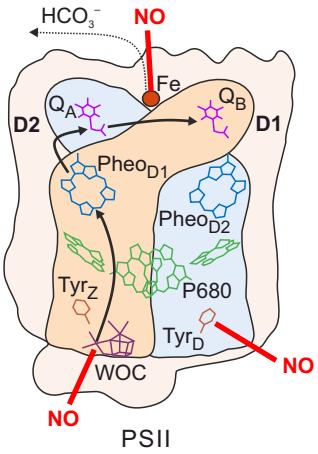

Figure 4. The main target sites of NO in PSII based on *in vitro* studies.

1.3.2 Biosynthesis

To avoid extensive damage to the photosynthetic apparatus, oxygenic photosynthetic organisms must tightly regulate the generation and turnover of NO. Production of NO in green algae and flowering plants appears to depend on nitrate reductase (NR), a key enzyme in N-assimilation (Planchet et al., 2005; Sakihama et al., 2002). However, rather than directly catalysing the biosynthesis of NO, NR seems to provide electrons originating from NADPH to a molybdoenzyme dubbed the NO-forming nitrite reductase (NOFNiR) enzyme (Chamizo-Ampudia et al., 2016). It was proposed that in *Chlamydomonas*, the NR-NOFNiR dual system is assisted by the truncated hemoglobin 1 (THB1) protein that recycles excessively produced NO into nitrate (Sanz-Luque et al., 2015b, 2015a).

The origin of NO in cyanobacteria is unclear. Production of NO has been observed previously (Mallick et al., 1999). However, the existence of the NR-NOFNiR system however has not been investigated. Alternative endogenous sources of NO may be present in cyanobacteria. An active protein homologous to the prototypic mammalian L-arginine-dependent NO synthase was discovered in the cyanobacterium *Synechococcus* sp. 7335, the encoding gene however does not seem to be conserved in cyanobacteria (Correa-Aragunde et al., 2018). Moreover, it was demonstrated that cyanoglobin (GlbN) isolated from *Synechocystis* is able to convert nitrite into NO under anoxic conditions *in vitro* (Sturms et al., 2011). Cyanobacteria (and green algae) may encounter extracellular NO in natural habitats. Several cyanobacterial species were shown possessing cyanoglobins protecting the cells from NO stress likely by converting exogenous NO to nitrate *via* NO dioxygenase activity (Scott et al., 2002; Scott and Lecomte, 2008; Thorsteinsson et al., 1999).

Cyanoglobins may be recycled by cognate Hb reductases thus providing an efficient NO scavenging mechanism to host cells (Uppal et al., 2020). Another layer of defence is nitric oxide reductase (NorB) that has been shown to convert NO into N_2O in *Synechocystis* (Büsch et al., 2002). In short, the production and turnover of NO in cyanobacteria is yet to be clarified.

1.4 Respiration in cyanobacteria

1.4.1 The site of respiration

Respiration is a membrane-associated transport of electrons from metabolized organic substrates to a terminal electron acceptor, which is predominantly molecular O_2 in cyanobacteria. Cyanobacteria possess three different RTO complexes, the aa_3-type heme-copper oxidase Cox (encoded by *coxBAC*), the alternative respiratory terminal oxidase ARTO (encoded by *CtaCDEII*), and the *bd*-type quinol oxidase Cyd (Hart et al., 2005). The cellular site of respiration has been long debated. ARTO was unambiguously located to the plasma membrane (Agarwal et al., 2010; Huang et al., 2002; Kranzler et al., 2014) Cox and Cyd, however, seemed to reside in both the thylakoid and plasma membrane (Lea-Smith et al., 2016a). Since Cyt b_6f can be found only in the thylakoid, the respiratory electron transport chain toward Cox would be incomplete in the plasma membrane (Schultze et al., 2009). Recent studies applying more sophisticated separation and tagging techniques located both Cox and Cyd exclusively to the thylakoid membranes of *Synechocystis*, thus disproving the existence of the incomplete respiratory electron transport in the plasma membrane (Baers et al., 2019; Cohen et al., 2020).

1.4.2 Bioenergetics of Cox

The major terminal oxidase in cyanobacteria appears to be Cox. The majority of cyanobacteria contain the encoding *coxBAC* genes (Lea-Smith et al., 2013), and deletion of the complex arrests cell growth in the dark (Pils et al., 1997; Stebegg et al., 2012). The chemistry of Cox in cyanobacteria is based on structural and biochemical studies of Cox complexes from prokaryotes *Paracoccus denitrificans* (Iwata et al., 1995; Koepke et al., 2009)*, Rhodobacter sphaeroides* (Svensson-Ek et al., 2002), and *Thermus thermophilus* (Lyons et al., 2012). In a single-turnover event, 2 electrons originating of 2 reduced Cyt c_6/PC proteins are transferred to the binuclear catalytic centre (copper Cu_B-heme a_3). Coupled with the electron transfer, six protons from the cytoplasm diffuse through a proton-conducting water chain, four to the lumen and two to the catalytic centre. Since reducing O_2 to water requires 4 electrons and protons, a second turnover rapidly follows. Proton-pumping at 2

H^+/e^-/ratio assists in generating *pmf* in the dark thus powers cellular processes when the photosynthetic apparatus is idle. Interestingly, Cox purified from the prokaryote *Pseudomonas stutzeri* was shown *in vitro* to reduce NO (Forte et al., 2001) and H_2O_2 (Xie et al., 2014). Whether Cox in cyanobacteria possesses such capabilities remains to be elucidated.

1.4.3 Cyd and ARTO in energy generation

The molecular function of Cyd in cyanobacteria is predominantly based on biochemical studies of bioenergetics membranes isolated from *Escherichia coli*. Cyd lacks proton-pumping activity, as evidenced by the generated transmembrane potential in a H^+/e^- ratio during a single turnover event of oxidizing 1 PQH_2 molecule to PQ (Borisov et al., 2020, 2011). Indeed, the recently resolved crystal structure of Cyd from *E. coli* and *Geobacillus thermodenitrificans* confirmed the absence of trans-membrane proton-conducting channels (Safarian et al., 2019, 2016). Cyd, therefore, contributes to energy conservation by extracting 4 protons from the cytoplasm for the 4-electron reduction of O_2 to water, alkalifying the cytosol, and releasing 2 protons/PQH_2 to the lumen. Less efficient in energy generation than Cox, Cyd may play a pivotal role under low-O_2 conditions, given the higher affinity to O_2 (K_m = 0.35 μM) when compared to that of Cox (K_m = 7 μM) in *Synechocystis* (Pils and Schmetterer, 2001). Cox and Cyd moreover are vital when diurnal light/dark periods sharply alter (Lea-Smith et al., 2013), likely providing energy to repair the photosynthetic apparatus in the dark (Nikkanen et al., 2021). Besides this, Cyd can contribute to the oxidation of the PQ pool, however, only to a minor extent and under adverse conditions when the capacity of FDPs is limited and the PET chain is strongly reduced (Ermakova et al., 2016).

The role of ARTO in energy generation is less obvious. Although homologous to Cox, ARTO seems to participate primarily in iron acquisition in *Synechocystis* by reducing periplasmic iron (Kranzler et al., 2014). Regardless of the chemical nature of the electron acceptor (and donor), ARTO may pump protons from the cytoplasm into the periplasm, energizing the plasma membrane. The crystal structure is yet to be resolved thus the bioenergetics of ARTO remains to be elucidated.

1.5 C-type cytochromes

1.5.1 Cyt c_6 and Cyt c_6-like proteins

The class I *c*-type Cyt family consists of soluble, small molecular weight proteins, harbouring a *c*-type monoheme —a porphyrin compound, coordinating an iron atom— covalently attached to a conserved peptide motif. Cyanobacterial class I *c*-

type Cyt proteins engage in various cellular processes. Cyt c_{555} (PsbV) is an extrinsic lumenal component of PSII and by maintaining the proper ion environment of the manganese complex, it stabilizes WOC (Shen et al., 1998; Shen and Inoue, 1993). Cyt c_6 transfers electrons from Cyt b_6f to PSI and Cox (see in section 1.1.1), substituting PC when Cu, the cofactor of PC, is depleted (Durán et al., 2004). Abundance of PC and Cyt c_6 is regulated by the transcription factor PetR, which represses the expression of the *petE* gene (PC) and induces that of the *petJ* gene (Cyt c_6). When Cu is replete, the protease PetP degrades PetR, enabling the expression of PC (García-Cañas et al., 2021).

The class I *c*-type Cyt family underwent an expansion and diversification during the course of evolution (Howe et al., 2016). According to the most recent model of Cyt c_6 phylogeny, the ancestral *petJ* gene encoding Cyt c_6 duplicated in cyanobacteria, giving rise to the canonical Cyt c_6 and Cyt c_{6B} proteins (Slater et al., 2021). By accumulating point mutations, ancestral Cyt c_{6B} forked into groups of the low-redox-potential Cyt c_{6B} and Cyt c_{6C} proteins which are widespread in cyanobacteria (Bialek et al., 2008). In gymnosperms and flowering plants, Cyt c_{6B} (and Cyt c_{6C}) were replaced by a new ortholog, Cyt c_{6A}, which acquired a 12-amino-acid-long loop insertion peptide (LIP) motif (Howe et al., 2006; Slater et al., 2021). However, Cyt c_6 disappeared in the green lineage after the mosses, thus Cyt c_{6A} appears to be the only Cyt *c* in higher oxygenic photosynthetic organisms. It has been suggested that iron became less available as early plants conquered dry lands thus favouring PC over Cyt c_6 as the primary electron carrier (De La Rosa et al., 2002; Kerfeld and Krogmann, 1998).

The physiological role of low-potential Cyt $c_{6A,\ B,\ C}$ proteins remains to be elucidated. The three-dimensional structures of those orthologs with resolved crystal structure closely resemble that of Cyt c_6 (Marcaida et al., 2006; Zatwarnicki et al., 2014), fulfilling a role as an electron carrier to PSI appears to be plausible. The binding of Cyt c_6 and PC to PSI is governed by electrostatic interactions (Hervás et al., 1995; Hippler et al., 1997). Importantly, the surface charge distributions of Cyt $c_{6A,\ B,\ C}$ differ markedly from that of Cyt c_6, likely weakening their eventual electrostatic interactions with PSI (Bialek et al., 2014; Marcaida et al., 2006; Zatwarnicki et al., 2014). Moreover, the low redox potential of Cyt $c_{6A,\ B,\ C}$ substantially increases the energetic barrier between Cyt *f* and Cyt $c_{6A,\ B,\ C}$ (Table 1). In line with this, it was demonstrated that an *Arabidopsis thaliana* mutant deficient in PC was unable to grow due to blocked PET, and over-expression of the *atc6* gene encoding Cyt c_{6A} did not rescue the lethal phenotype (Weigel et al., 2003). Similarly, *Synechocystis* fails to grow when Cyt c_6 and PC are not expressed (Durán et al., 2004). In conclusion, $c_{6A,\ B,\ C}$ is unlikely to participate in canonical LET. Interestingly, however, Cyt c_{6A} was shown to reduce PC *in vitro* (Wastl et al., 2004). Since accepting electrons from Cyt *f* is unlikely, Cyt c_{6A} might oxidize PQH_2, thus

bypassing Cyt b_6f when the PQ pool is strongly reduced (Howe et al., 2016). In line with this, Cyt c_{6A} of *Arabidopsis* was located in the thylakoid lumen of chloroplasts (Gupta et al., 2002).

Little is known about Cyt c_{6B} and c_{6C} proteins. The crystal structure of Cyt c_{6B} from *Synechococcus* WH 0182 was resolved at 1.4 Å resolution (Zatwarnicki et al., 2014) providing, however, little insight into the molecular function of the protein. Recently, it was discovered that a Cyt c_{6C}-like protein (dubbed Cyt c_{6-3}) has redox potential comparable to Cyt c_6 (Table 1). Transcriptomics and immunofluorescence analysis of the filamentous heterocyst-forming *Nostoc* sp. PCC 7119 revealed that Cyt c_{6-3}, is specifically repressed in heterocysts when cultures were shifted to N_2-fixing conditions (Torrado et al., 2017). Homologs of this protein appear to be present predominantly in genomes of heterocyst-forming species, suggesting some role related to heterocysts (Bialek et al., 2008; Torrado et al., 2017).

Table 1. Midpoint redox potential of electron carriers and Cyt $c_{6A, B, C}$ in cyanobacteria.

Protein	Redox potential (E_m)	Reference
PQ pool	+80-110 mV	(De Causmaecker et al., 2019; Okayama, 1976)
PC	+360 mV	(Molina-Heredia et al., 2002)
Cyt c_6	+310-390 mV	(Cho et al., 1999; Molina-Heredia et al., 1998)
Cyt c_{6A}	+140 mV	(Molina-Heredia et al., 2003; Worrall et al., 2007)
Cyt c_{6B}	+110 mV	(Bialek et al., 2008; Zatwarnicki et al., 2014)
Cyt c_{6C}	+150-200 mV	(Bialek et al., 2008; Reyes-Sosa et al., 2011)
Cyt c_{6-3}	+340 mV	(Torrado et al., 2017)
Cyt c_M	+150 mV	(Cho et al., 2000)
Cyt *f*	+270-330 mV	(Albarrán et al., 2005; Baymann et al., 2001)

1.5.2 Cyt c_M protein

Akin to Cyt $c_{6A,\ B,\ C}$ proteins, the molecular function of the Cyt c_M orthologue (encoded by *cytM*) has been enigmatic. CytM is widespread in cyanobacteria, nearly every sequenced species carries the *cytM* gene (Bialek et al., 2016). Expression of *cytM* in *Synechocystis* is negligible under moderate photosynthetic conditions (Malakhov et al., 1999) and accordingly, deletion of *cytM* does not affect cell growth or net photosynthetic O_2 production under these conditions (Malakhov et al., 1994). It has been shown that CytM is unable to reduce PSI *in vitro*, possibly due to the electrically positive surface area surrounding the heme cleft, and the loss of a positively charged arginine that is critical for interacting with PSI (De La Cerda et al., 1999; Molina-Heredia et al., 2002). Moreover, the redox potential of the protein is substantially lower than that of Cyt c_6 or PC (Table 1). Therefore, it is unlikely that CytM could substitute Cyt c_6 or PC in canonical PET. However, stress-induced transcriptional co-regulation between the genes of CytM, Cyt c_6, and PC has been demonstrated, thus a role related to Cyt c_6, or PC cannot be excluded (Malakhov et al., 1999).

The physiological relevance of CytM becomes apparent when cells are exposed to glucose. A dark-adapted variant of the filamentous *Leptolyngbya boryana* was found to grow rapidly when exposed to glucose in the dark—heterotrophic conditions—and genome re-sequencing revealed that the fast-growing strain carried a disrupted *cytM* gene. Accordingly, a *cytM* deletion mutant of *Synechocystis* demonstrated a growth advantage over the wild type when cells were exposed to glucose in the dark or light (photomixotrophic conditions). Based on the elevated net photosynthetic O_2 production and respiratory O_2 consumption, CytM was suggested to be: (i) a transcriptional regulator; (ii) an electron transporter between Cyt b_6f and Flv1/Flv3; or (iii) a repressor of Cox (Hiraide et al., 2015). Cox appears to be an electron acceptor of CytM. Subunit II of Cox, harbouring the Cu_A centre, is reduced by CytM *in vitro* at physiologically relevant rates (Bernroitner et al., 2009). CytM, moreover, shares sequence similarities with the C-termini of Cox subunit II of *Thermus* sp. and *Bacillus* sp., hinting that CytM might be structurally associated with Cox in cyanobacteria (Manna and Vermaas, 1997). Given the role of Cox in regulating electron flow to PSI (Viola et al., 2021), CytM may contribute to regulating auxiliary electron transfer. To interact with the Cu_A centre that faces the thylakoid lumen, however, CytM should be located in the thylakoid lumen.

In an earlier report, the CytM protein was localized both to the thylakoid and the plasma membrane of *Synechocystis* (Bernroitner et al., 2009). However, the purity of the membrane extracts was not determined and cross-contamination is a known issue of the applied separation technique (Schultze et al., 2009; Sonoda et al., 1997). A recent proteomics study, using more efficient subcellular fractionation, did not detect or localize CytM (Baers et al., 2019). Nevertheless, the hydrophobic N-

terminus resembles the signal peptide of Cyt c_6 (Bernroitner et al., 2009), an alpha-helical domain that anchors the protein into the thylakoid membrane. For penetrating the lumen, terminal processing must occur and indeed, CytM appears to carry a conserved cleavage site (Malakhov et al., 1994). Yet processing does not seem to occur *in vivo*. A processed mature form is predicted to be 8.3 kDa (Malakhov et al., 1994), while the protein extracted from various cyanobacterial species, including *Synechocystis*, the marine, unicellular *Synechococcus elongatus* PCC 6301, and the filamentous *Anabaena* sp. PCC 7120, was found to be heavier than 8.3 kDa (Bernroitner et al., 2009; Cho et al., 2000). CytM thus might retain the putative signal peptide, which could serve as a membrane anchor. In summary, the exact role of CytM in bioenergetics processes remains to be elucidated.

1.6 Central carbon metabolism

1.6.1 A CO_2 fixation interconnected with glycolysis

The metabolism of cyanobacteria is optimized to assimilate inorganic carbon (CO_2, HCO_3^-) as the primary carbon source. The principal process to fix CO_2 is the Calvin-Benson-Bassham (CBB) cycle, which is divided into two phases. In the first phase, Rubisco converts ribulose 1,5-bisphosphate (RuBP) and CO_2 into two 3-phosphoglycerate (3PG) molecules. In the second phase, the precursor RuBP is regenerated by various enzymes at the expense of ATP and NADPH, both predominantly generated by the photosynthetic apparatus. Rubisco is notorious for catalytic inefficiency, the turnover rate is slow at a rate-limiting partial pressure of CO_2 and the abundant O_2 is readily confused with CO_2 for a substrate, leading to oxidation of RuBP into a useful 3PG and wasteful 2-phosphoglycolate (2PG) molecule (Farquhar et al., 1980). 2PG inhibits the enzymes of the CBB cycle thus it is metabolized *via* photorespiratory salvage pathways which, however, require extra energy and waste fixed carbon by releasing CO_2 (Eisenhut et al., 2019). To minimize photorespiration, Rubisco in cyanobacteria is encapsulated in proteinaceous compartments, called carboxysomes, where CO_2 is enriched *via* carbon concentrating mechanisms (CCM) to a level approximately~ one thousand times higher than in the extracellular space (Badger and Price, 2003; Kaplan and Reinhold, 1999; Kerfeld and Melnicki, 2016).

Surplus fixed carbon is stored in the glucose polymer glycogen. In the dark, glycogen is hydrolysed and converted into various metabolites *via* catabolic pathways. The conventional glycolytic route in prokaryotes, the Embden-Meyer-Parnas (EMP) pathway, concludes at pyruvate—an important anabolic precursor (Mills et al., 2020). An alternative pathway, that was only recently shown to exist in cyanobacteria, the Entner-Doudoroff (ED) pathway, provides a less energy-

consuming source of pyruvate via alternative intermediates (Chen et al., 2016). A third glycolytic route, the oxidative pentose phosphate (OPP) pathway, concludes in glyceraldehyde 3-phosphate (GA3P) via intermediates shared with CBB cycle (Fig. 5). The OPP pathway is the primary glycolytic process in the dark (Yang et al., 2002). In the first two steps of the OPP pathway, a glucose-6-phosphate (G6P) molecule is converted into 6-phospho-gluconate (6PG) then ribulose-5-phosphate (Ru5P) by the G6P dehydrogenase (Zwf) and 6P-gluconate dehydrogenase (Gnd) enzymes, respectively. These two steps yield two NADPH molecules providing reducing power in the dark (Jansén et al., 2010; Yang et al., 2002). However, the second step involves a decarboxylation reaction during which a CO_2 molecule is released therefore a fixed carbon molecule is lost.

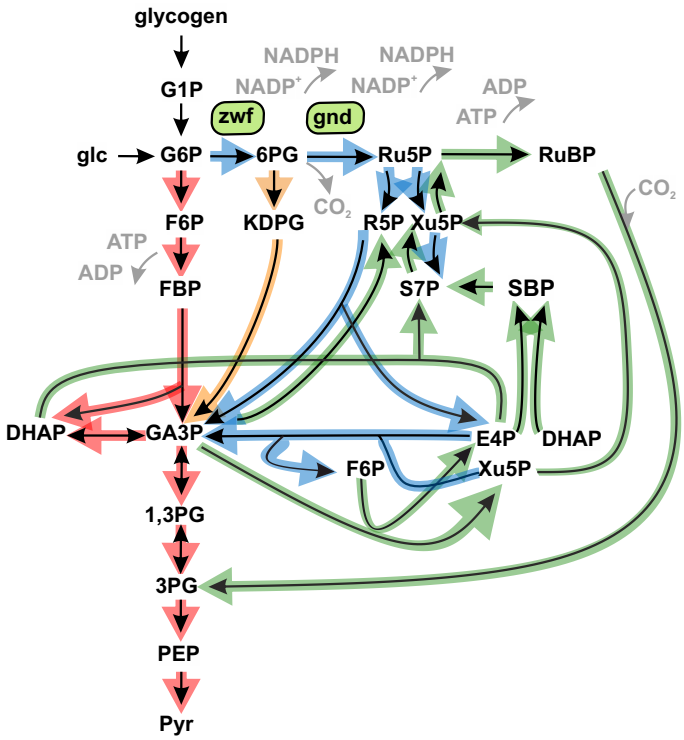

Figure 5. Simplified scheme of the central carbon metabolism in *Synechocystis*. The EMP (red), ED (orange), and PP (blue) pathways, and the CBB cycle (green) are interconnected *via* shared intermediates. 1,3PG, 1,3-bisphosphoglycerate; 3PG, 3-phosphoglycerate; 6PG, 6-phosphogluconate; DHAP, dihydroxyacetone phosphate; E4P, erythrose 4-phosphate; F6P, fructose-6-phosphate; FBP, fructose 1,6-bisphosphate; G1P, glucose-1-phosphate; G6P, glucose-6-phosphate; GA3P glyceraldehyde 3-phosphate; KDPG, 2-keto-3-deoxygluconate-6-phosphate; PEP, phosphoenolpyruvate; Pyr, pyruvate; R5P, ribose 5-phosphate, Ru5P, ribulose 5-phosphate; RuBP, ribulose 1,5-bisphosphate; S7P, sedoheptulose 7-phosphate; SBP; sedoheptulose 1,7-bisphosphate; Xu5P, xylulose 5-phosphate.

The apparent activity of Zwf and Gnd enzymes in light was long considered as a wasteful result of incomplete suppression (Knoop et al., 2013; Young et al., 2011). Importantly, however, Ru5P is an intermediate of the CBB cycle and appears to be replenished by Zwf and Gnd in the light. In this way, glycogen reserves could be tapped when regeneration of the Ru5P pool is otherwise insufficient e.g., at dark-to-light transitions (Makowka et al., 2020; Shinde et al., 2020). The glycolytic routes are thus interconnected with CO_2 fixation and are crucial not only to metabolize organic but inorganic carbon sources.

1.7 Photomixotrophy

1.7.1 Metabolic modes of cyanobacteria

Several cyanobacterial species invest in multiple nutritional acquisitions and bioenergetics systems to utilize a variety of energy and carbon sources (Table 2). Photomixotrophy, a metabolic mode, has multiple definitions: (i) a form of alternative carbon acquisition; (ii) the facultative utilization of external amino acids, alternative sources of phosphorous and sulfur; or (iii) a combination of different nutritional pathways in a single organism (Stoecker et al., 2017). In this work, photomixotrophy indicates photosynthetic CO_2 assimilation simultaneously with the metabolization of exogenous organic carbon sources, primarily glucose. The successful coexistence of photomixotrophic and obligate photosynthetic cyanobacterial species in nature indicates that the profit must outweigh the cost of investing in multiple sensory, uptake, and metabolic systems (Muñoz-Marín et al., 2020).

Table 2. Trophic modes of cyanobacteria based on the source of energy and origin of utilized carbon. Photoheterotrophy only occurs in the presence of artificial chemical inhibitors of photosynthesis.

Metabolic mode	Energy source	Carbon source
photoautotrophy	light	inorganic carbon
photoheterotrophy	light	organic carbon
photomixotrophy	light, organic carbon	inorganic and organic carbon
chemoheterotrophy	organic carbon	organic carbon

1.7.2 Ecological and biotechnological significance

A long-lasting dogma is that cyanobacteria are predominantly photoautotrophic organisms and only in special cases, facultatively heterotrophic (Rippka, 1972; Smith, 1983; Stal and Moezelaar, 1997). This dogma seems to change as the ecological importance of photomixotrophy becomes more evident. Recently, the most abundant phototrophs on Earth—*Prochlorococcus* and *Synechococcus*—were shown to utilize glucose in daylight (Duhamel et al., 2018; Zubkov and Tarran, 2008) indicating the significance of photomixotrophy in global biogeochemical cycles (Moore, 2013; Muñoz-Marín et al., 2020). Although the concentration of glucose in natural waters tends to be low, ranging from 10 to 400 nM in open oceans (Vaccaro et al., 1968), during phytoplankton blooms glucose is more abundant (Ittekkot et al., 1981; Teeling et al., 2012).

Supplementing the growth of cyanobacteria with carbohydrates enhances biomass production, providing advantages for bioindustrial applications (Matson and Atsumi, 2018). It has been reported that applying photomixotrophic conditions increased yields of potential biofuels such as 2,3-butanediol (Kanno et al., 2017; Kanno and Atsumi, 2017), isobutanol (Varman et al., 2013), or chemical commodities e.g., polyhydroxybutyrate (PHB) polymers (Khetkorn et al., 2016), and ethylene (Lee et al., 2015). Importantly, several cyanobacteria are capable of assimilating polysaccharides (like starch or maltodextrin) di- and monosaccharides (maltose, sucrose, glucose, fructose, mannose), organic acids (acetate), or glycerol (Francisco et al., 2014; Schneegurt et al., 1997). By introducing heterologous transporters and catabolic enzymes, transgenic *Synechocystis* was shown to metabolize molecules with low bioavailability such as the wood-derivate xylose (Ranade et al., 2015). Therefore, various industrial side streams can potentially serve as feedstocks for photomixotrophic cultivation. These studies demonstrate the potential of applying photomixotrophic conditions in production platforms.

Carbohydrates, however, raise the possibility of microbial contamination of microalgal cultures, thus adding complexity to operating production platforms (Perez-Garcia et al., 2015). Also, the release of CO_2 upon metabolizing carbohydrates generally increase the net CO_2 emission of photomixotrophic platforms (Patel et al., 2021). However, this may be offset by CO_2 uptake of separate photoautotrophic cultures. Indeed, it was shown that the growth of photoautotrophic green algae cultures can be supplied by CO_2 released by a heterotrophic cultures. (Sim et al., 2019).

1.7.3 An altered photosynthesis

Shifting the carbon metabolism towards glucose assimilation involves alterations in thylakoid electron transfer. The most evident change is the increased respiratory

activity in the thylakoid that can be observed a few minutes after exposure to glucose, as evidenced by enhanced O_2 and NADPH consumption in *Synechocystis* exposed to dark (Lee et al., 2007). The effects of glucose on photosynthesis are less evident and the scientific literature is rich in contradictory results. It seems clear that photosynthesis becomes partially inhibited and net photosynthetic O_2 production decreases in the presence of glucose (Haury and Spiller, 1981; Lee et al., 2007; Nieva and Valiente, 1996; Reyes et al., 1993; Takahashi et al., 2008; Zilliges and Dau, 2016). It is generally accepted that such a decrease in photosynthetic activity is triggered by cytosolic reductants (generated *via* glycolysis) that strongly reduce the thylakoid electron transfer chain. Contrary to this, however, the maximum photosynthetic capacity was shown to increase in various cyanobacterial species exposed to glucose or fructose in light (Haimovich-Dayan et al., 2011; Kang et al., 2004; Sakuragi et al., 2006; Yu et al., 2009).

Regulation of photosynthesis in photomixotrophically cultivated cyanobacteria thus remains obscure. Earlier it was found that disrupting the serine/threonine kinase homolog PmgA (**p**hoto**m**ixotrophic **g**rowth) retards the growth of *Synechocystis* under photomixotrophic conditions (Hihara and Ikeuchi, 1997). The slow growth of the ΔPmgA cells was attributed to the inability to regulate the PSI/PSII ratio leading to redox imbalance (Hihara et al., 1998). The PSI/PSII ratio thus appears to be an important regulatory factor, yet that has never been confirmed independently. The PS ratio was determined in *Synechocystis* exposed to glucose for 2 h which was likely too short for altering PS content and indeed, no change was observed. (Haimovich-Dayan et al., 2011). Another key regulatory factor appears to be the redox state of the NADP(H) and NAD(H) pools. The thylakoid-localized pyridine nucleotide transhydrogenase, PntAB, that controls NADPH/NAD^+ and $NADP^+$/NADH ratios in *Synechocystis*, was shown to be vital under low-light photomixotrophic conditions (Kämäräinen et al., 2016). Such ratios are crucial for enzymes regulated by redox cofactor feedback, linking PntAB to the wider metabolism.

Via determining incorporation of radioactively labelled inorganic carbon in *Synechocystis*, earlier studies demonstrated that glucose induces a rapid loss in the capacity of inorganic carbon uptake (Beuf et al., 1994; Bloye et al., 1992), a process mediated, among others, by the thylakoid-localized NDH-1_3 isoform. However, a latter study of real-time gas fluxes employing membrane inlet mass spectrometry (MIMS) contradicted these findings (Benschop et al., 2003). Nonetheless, NDH-1_3 seems to have a crucial role in the growth of photomixotrophic cells. Spontaneous point mutations of genes encoding subunits specific to NDH-1_3 e.g., NdhF3, or CupA, reverted the growth deficiency of ΔPmgA *Synechocystis* under photomixotrophic conditions (Nishijima et al., 2015). How the mutations altered the functionality of NDH-1_3 is yet to be determined. In summary, much ambiguity

remains about the status and the regulation of the photosynthetic machinery under photomixotrophic conditions.

1.7.4 Carbon fluxes

Metabolizing glucose under photomixotrophic conditions was long thought to proceed independently of photosynthesis (Marquez et al., 1993; Ogawa and Aiba, 1981). However, through the application of metabolomics techniques and metabolic flux analysis, it has been demonstrated that the central carbon metabolism rearranges to assimilate CO_2 simultaneously with glucose in *Synechocystis* cultivated under long-term photomixotrophic conditions (Fig. 6; Nakajima et al., 2014; Yang et al., 2002; You et al., 2014). Compared to a purely photoautotrophic metabolism, carbon flux in photomixotrophic cells *via* the CBB cycle decreases (Nieva and Valiente, 1996; Takahashi et al., 2008), presumably by CP12-mediated repression of key CBB enzymes Phosphoribulokinase (Prk) and Glyceraldehyde-3-phosphate (GA3P) dehydrogenase (Takahashi et al., 2008; Tamoi et al., 2005). In line with this, carbon fluxes *via* Zwf and Gnd have been shown to increase in cells cultured photomixotrophically (Nakajima et al., 2014; Takahashi et al., 2008; Yoshikawa et al., 2013; You et al., 2014), the rate however remained unclear due to the different culturing conditions applied in the studies. A recent report clarified that the importance of Zwf in photomixotrophic metabolism is light-dependent; loss of Zwf in *Synechocystis* severely limited growth under low-light but not under moderate-light photomixotrophic conditions. This implies that the first steps of the OPP pathway are crucial for maintaining redox balance in photomixotrophic cells (Ueda et al., 2018), and perhaps assist in replenishing intermediates of the CBB cycle, as was suggested recently (Makowka et al., 2020). The activity of the CBB cycle affects the photosynthetic electron transport *via* feedback regulation. Therefore, understanding the regulation of carbon fluxes is vital for deciphering photosynthesis under photomixotrophic conditions.

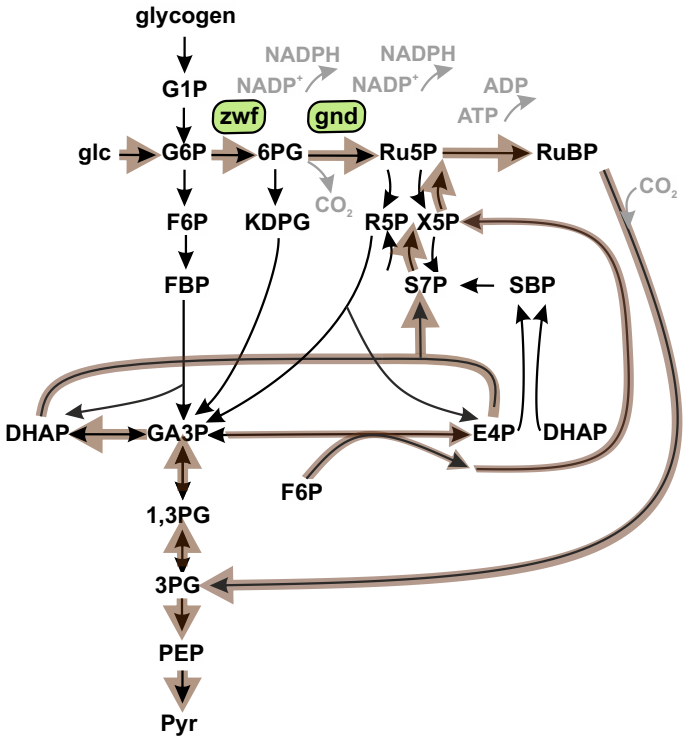

Figure 6. The most pronounced carbon fluxes (brown) in *Synechocystis* cultured photomixotrophically was reconstructed based on metabolomics studies and ^{13}C metabolic flux analysis (Nakajima et al., 2014).

1.8 Chemical production in cyanobacterial hosts

1.8.1 Engineering PET for improved bioproduction

Cyanobacteria have great potential as sustainable solar-driven microfactories producing targeted valuable chemicals. However, productivity is limited by several bottlenecks such as the costly cultivation and downstream processes or the inefficiencies in microalgal photochemistry. An increasingly attractive strategy to alleviate inefficiencies in photosynthesis is engineering electron transfer routes in thylakoids to enhance the flux of photosynthetic electrons, or redirect electrons towards the biosynthesis of targeted chemicals. The rapid development of gene-editing tools for microalgae is largely contributing to these efforts (Santos-Merino et al., 2019; Vijay et al., 2019).

An example of this is the expression of a heterologous electron sink, an Fd-dependent Cyt P450 monooxygenase, in *Synechococcus* PCC 7002 which was shown to accelerate intersystem electron flux leading to higher ATP and NADPH

levels (Berepiki et al., 2018, 2016). The photosynthetic electron flux can be further accelerated by combining the expression of Cyt P450 protein with a metabolic sink such as sucrose export (Santos-Merino et al., 2021). Alternatively, eliminating CET proteins or native photoprotective electron sinks such as FDP may increase the supply of reductants (NADPH and reduced Fd) for desired reactions. Indeed, it was shown that L-lactate yields can be increased in *Synechocystis* by repressing the expression of genes encoding proteins involved in CET such as subunits of the NDH-1 complex (Yao et al., 2020). In line with this, the deletion of Flv1, Flv3, or the PGR5 homolog in *Synechococcus* sp. 7002 expressing a heterologous NADPH-dependent D-lactate dehydrogenase improved production of D-lactate when the mutants were exposed to constant illumination at mild temperature and atmospheric CO_2. At higher temperature and/or CO_2 levels, however, the production of D-lactate in the mutants was comparable to that in the reference strain (Selão et al., 2020). Similar results were reported in a study utilizing sucrose as a marker compound in an engineered salt-stressed *Synechocystis* strain. Under mild illumination (at 1% CO_2), the ΔFlv3 mutant demonstrated higher sucrose yields than the reference strain, however, when light intensity was increased the production advantage of the mutant disappeared. *In silico* modelling of carbon fluxes suggested that fixed carbon was reallocated towards PHB production and the deletion of Flv3 likely exacerbated that shift (Thiel et al., 2019).

Alternatively, NADPH or reduced Fd can be utilized by oxidoreductase enzymes that catalyse specific chemical alterations of targeted compounds in a process called biotransformation. The ene reductases belonging to the Old yellow enzyme protein family are promising alternatives for chemical catalysts due to their ability to convert various alkane substrates (e.g., aldehydes and maleimides) into valuable chemicals *via* high regio-, stereo- and enantioselectivity (Toogood and Scrutton, 2018). Such reactions can be directly coupled to photosynthesis, as was evidenced by a recent study showing that *Synechocystis* cells can supply photosynthetic reductants to a heterologously expressed Old yellow enzyme homolog, the NADPH-dependent YqjM protein (Köninger et al., 2016). Whether the availability of NADPH can be improved by removing electron sinks remains to be elucidated.

These studies demonstrate that electron sink engineering is a promising strategy for improving chemical production in microalgae. However, developing robust strains requires a better understanding of the regulatory links between photosynthesis and central carbon metabolism.

2 Aims of the study

Understanding the regulation of photosynthesis is crucial for developing economically feasible microalgal chassis producing valuable chemicals. Using the model cyanobacterium *Synechocystis*, the current study sheds light on regulatory components of the photosynthetic apparatus to bring microalgae a step closer to bioindustrial applicability.

The study was based on the following framework:

I. Characterizing the photosynthetic apparatus and the role of CytM in *Synechocystis* cultured under bioindustrially relevant photomixotrophic conditions.

II. Distinguishing between the activity of Flv1/Flv3 and Flv2/Flv4 in *Synechocystis in vivo*. These proteins are engineering targets in microalgae.

III. Investigating the *in vivo* effects of exogenous NO on photosynthesis to understand whether NO can act as a terminal electron acceptor in cyanobacteria. NO was shown to be an electron acceptor of FLVB, a homolog of Flv3 in green algae.

IV. Improving a model biotransformation reaction in *Synechocystis* cells by inactivating the Flv1/Flv3 heterodimer.

V. Reviewing the current understanding about regulation of photosynthetic electron transfer and the efforts of engineering photosynthesis in microalgae.

3 Materials and Methods

3.1 Strains and cultivation

Table 3. *Synechocystis* strains used in this work. Construction of the transgenic strains are detailed in the original publications. Indexes ^{OE}, $^{-}$ and $^{+}$ indicate overexpression, deletion or introduction of the corresponding genes, respectively.

Strain	Genetic modification	Published	Paper
Wild type		(Williams, 1988)	I-IV
ΔCox/Cyd	*ctaC1*$^{-}$*, ctaD1*$^{-}$*, ctaE1*$^{-}$*, cydA*$^{-}$*, cydB*$^{-}$	(Lea-Smith et al., 2013)	I
ΔCytM	*cytM*$^{-}$	Paper I	I
ΔCox/Cyd/CytM	*ctaC1*$^{-}$*, ctaD1*$^{-}$*, ctaE1*$^{-}$*, cydA*$^{-}$*, cydB*$^{-}$*, cytM*$^{-}$	Paper I	I
M55	*ndhB*$^{-}$	(Ogawa, 1991)	II
ΔFlv1/Flv3	*flv1*$^{-}$*, flv3*$^{-}$	(Allahverdiyeva et al., 2013)	II
ΔFlv2	*flv2*$^{-}$	(Zhang et al., 2012)	II
ΔFlv4	*flv4*$^{-}$	(Zhang et al., 2012)	II
ΔSll0218	*sll0218*$^{-}$	(Helman et al., 2003)	II
ΔSll0218/Flv2	*sll021*$^{-}$, *flv2*$^{-}$	(Helman et al., 2003)	II
ΔFlv3/4	*flv3*$^{-}$*, flv4*$^{-}$	(Helman et al., 2003)	II
Flv4-Flv2 OE	*flv4*^{OE}, *sll0218* ^{OE}, *flv2* ^{OE}	(Bersanini et al., 2014)	II
Syn:P_{cpc}YqjM	*YqjM*$^{+}$	Paper IV	IV
ΔFlv1:YqjM	*flv1*$^{-}$, *YqjM*$^{+}$	Paper IV	IV
ΔFlv3:P_{cpc}YqjM	*Flv3*$^{-}$, *YqjM*$^{+}$	Paper IV	IV

3.1.1 Construction of transgenic strains

All strains in this study are derived from the glucose-tolerant, non-motile *Synechocystis* sp. PCC 6803 (Williams, 1988). As a control strain, wild type *Synechocystis* was employed. In Paper I, wild type and previously published ΔCox/Cyd strains (Lea-Smith et al., 2013) were used as genetic backgrounds to construct unmarked ΔCytM and ΔCox/Cyd/CytM mutants lacking *cytM via* a two-

step homologous recombination protocol (Lea-Smith et al., 2016b). The rest of the mutants were generated according to the references listed in Table 3.

3.1.2 Cultivation conditions

Synechocystis strains were kept in cryogenic storage and revived on BG-11 agar plates at 3% (V/V) CO_2. In every case, pre-experimental cultures (pre-cultures) were inoculated at ~ OD_{750} 0.1 by transferring a patch of cells to 30 ml liquid BG-11 media in 100 ml Erlenmeyer flasks. Cultures were shaken at 120 rpm under constant white illumination at 50 µmol photons m^{-2} s^{-1} photon flux density at 30°C. In every study, pre-experimental cells in logarithmic growth phase were pelleted and re-inoculated in fresh BG-11 as experimental cultures.

In Paper I, pre-experimental culturing was performed in BG-11 buffered with 10 mM TES-KOH (pH 8.2) in air enriched with 3% CO_2. Experimental cultures were exposed to a downshift in CO_2 levels by re-inoculating the pre-culture cells in BG-11 (pH 8.2) at atmospheric CO_2. Growth at a photon flux density of 50 µmol photons m^{-2} s^{-1} light was then tested in the presence of initial glucose concentrations of (i) 0 mM glucose, (ii) 5 mM glucose and (iii) 10 mM glucose. Further light regimes of (iv) constant 10 µmol photons m^{-2} s^{-1} and (v) 15 min 50 µmol photons m^{-2} s^{-1} every 24 h were applied at initial level of 10 mM glucose. For photophysiological studies, conditions *iii* were applied. In paper II, pre-cultures were grown in BG-11 buffered with 20 mM Na-HEPES (pH 7.5) or 10 mM TES-KOH (pH 8.2) or 10 mM N-Cyclohexyl-2-aminoethanesulfonic acid (CHES, pH 9.0) in air enriched with 3% CO_2. Experimental cells were then exposed to a down-shift in CO_2 level by re-culturing cells at atmospheric CO_2 at the corresponding pH and various light regimes were applied to test growth, gas fluxes and changes in gene expression. In paper III, pre-experimental cultivation was done in BG-11 buffered by 20 mM Na-HEPES (pH 7.5) at atmospheric CO_2 and identical conditions were applied for experimental culturing. In paper IV, pre-cultures were kept at atmospheric CO_2 then re-cultured and cultivated at 50 µmol photons m^{-2} s^{-1} or 150 µmol photons m^{-2} s^{-1} constant light under identical conditions.

3.2 Determining cell properties

3.2.1 Cell size and number

The number and size of cells were evaluated by using the Nexcelcom Cellometer X2. Cell suspensions were diluted to OD_{750} 1, transferred to a counting plate provided by the manufacturer and brightfield images were captured. The average cell

size and number were determined by analysing the images with the Nexcelcom software (Paper I).

3.2.2 Concentration of intracellular chl

Concentration of chl was determined by measuring the absorbance of 90% (V/V) methanolic cell extracts at 663 nm. When indicated, the amounts of chl in cell suspensions were adjusted by resuspending given amounts of cells in fresh BG-11 prior to measurements (Paper I-IV).

3.2.3 Glucose consumption

Concentrations of glucose were determined in filtered (0.2 µM) spent media using the High Sensitivity Glucose Assay Kit (Sigma-Aldrich). The consumption of glucose was deduced from leftover glucose in the media and referenced against a given number of cells (Paper I).

3.3 Photosynthetic activity measurements

3.3.1 Fluorescence measurements and determining the redox kinetics of P700 and Cyt *f*

Whole-cell, NAD(P)H fluorescence, and oxidoreduction of P700 in intact cells was monitored using a pulse amplitude-modulated fluorometer (Dual-PAM-100, Walz). Prior to the measurements, samples were adjusted to 10-15 µg chl ml^{-1} and adapted to the dark at 30°C. Samples were measured in the presence of 10 mM glucose in an open quartz cuvette under atmospheric conditions (Paper I) or in an airtight quartz cuvette (Hellma) under anoxic conditions established by adding 10 U Glucose oxidase ml^{-1}, 20-40 U Catalase ml^{-1}, 5 mM glucose and flushing the gas phase with N_2 for 2 min (Paper III). When indicated, freshly prepared mQ water saturated with NO, or containing 10 mM methylmaleimide were added at a final concentration of 20 µM NO (Paper III) or 100 mM methylmaleimide (Paper IV), respectively. In Paper I, III and IV, P_m was determined by exposing dark-adapted cells to a multiple saturating light pulse (500 ms, 5000 µmol photons m^{-2} s^{-1}) under strong far-red illumination. Identical pulses were applied under periods of dark and actinic red light (50 µmol photons m^{-2} s^{-1}) to measure photosynthetic yields, as described previously (Klughammer and Schreiber, 2008a, 2008b). The rate constant of NADPH decay in dark was determined by fitting *via* $f = y_0 + a - b * x$ (Paper IV).

The decay of flash-induced yield of chl fluorescence in the dark was measured with a fluorometer (FL3500, PSI Instruments). The concentration of chl was set to 5

μg chl ml^{-1} then the cells were pre-adapted to the dark for 3 min. The following chemicals were added when indicated: 10 μM or 20 μM 3-(3,4-dichlorophenyl)-1,1-dimethylurea (DCMU); 25 μM 2,5-dibromo-3-methyl-6-isopropylbenzoquinone (DBMIB); or 1 μM or 20 μM NO (Paper I, III).

Whole-cell redox kinetics of Cyt *f* were determined by JTS-10 pump probe spectrophotometer (BioLogic). Prior to the measurements, the samples were adjusted to chl concentrations of 5 μg ml^{-1}, pre-adapted to the dark and exposed to green light at a photon flux density of 500 μmol photons m^{-2} s^{-1}. When indicated, 3-(3,4-dichlorophenyl)-1,1-dimethylurea (DCMU) was added to a final concentration of 20 μM (Paper I, III).

3.4 Monitoring gas exchange

3.4.1 Clark-type electrode measurements

Net O_2 production in whole cells were monitored with a Clark-type oxygen electrode in a temperature-regulated chamber equipped with stirrer (Hansatech). O_2 was calibrated in mQ water using a two-point calibration method. Cell suspensions were adjusted to chl concentration of 7.5 μg chl ml^{-1}, adapted to the dark, then supplemented with 0.5 mM 2,6-dichloro-p-benzoquinone (DCBQ). The production of O_2 was then measured under white light at 1000 μmol photons m^{-2} s^{-1}. Rates were calculated using the Hansatech software (Paper I).

3.4.2 Membrane inlet mass spectrometry measurements

Gas fluxes in intact cells were monitored by applying MIMS. During the measurements, samples were kept under physiological conditions in a home-built interface consisting of a temperature-regulated Hansatech chamber with a stirrer. The chamber was connected to the vacuum line of a mass spectrometer (Prima PRO model, Thermo Scientific) *via* a gas-permeable S4 polytetrafluoroethylene membrane (Hansatech). O_2 was calibrated similarly in Clark-type electrode measurements. Total inorganic carbon and NO was calibrated by injecting known amounts of HCO_3^- or NO into known volumes of growth media, respectively. Prior to the measurements, chl concentration of the samples were set to 10 μg chl ml^{-1} and freshly prepared aqueous $NaHCO_3$ was added at final concentration of 500-1500 μM. In paper III, anoxic conditions were established and NO μM was added as it was described for the chl fluorescence measurements. In paper I and II, samples were enriched with 98% (V/V) $^{18}O_2$ heavy isotope (CK Isotopes) and when indicated, supplemented with quinone analogues DBMIB or 2-heptyl-4-hydroxyquinoline-N-oxide (HQNO) at final concentrations of 25 μM and 50 μM, respectively.

Photosynthetic activity was followed under illumination at photon flux densities of 200-1500 µmol photons m^{-2} s^{-1}. Respiration was determined in pre- and post-illumination dark periods. Rates of gas fluxes were calculated as described earlier (Beckmann et al., 2009).

3.5 Transcriptomics

Relative changes in gene expressions were determined by real-time quantitative PCR (RT-qPCR). As a template, complementary DNA was applied that was synthetized with iScript cDNA Synthesis Kit (BioRad, USA) using total RNA isolated from *Synechocystis via* the hot-phenol method (Paper II).

3.6 Protein analysis

3.6.1 Western blotting

Cellular total protein fractions were prepared as described previously (Zhang et al., 2009). Proteins were separated by electrophoresis in 12 % (w/v) SDS-PAGE supplemented with 6 M urea, transferred to polyvinylidene difluoride membrane (Immobilon-P, Millipore) *via* semidry blotting and exposed to protein-specific primary antibodies. Secondary antibodies fused with Horseradish peroxidase were applied to tag primary antibodies. The antibody conjugates were then visualized by Amersham ECL Western Blotting Detection Reagent (GE Healthcare, Paper I and II).

3.6.2 Mass spectrometry and data-dependent analysis

Global label-free proteomics analysis of ΔCytM and wild type cells were performed using nanoscale liquid chromatography electrospray ionization tandem MS (nLC-MS/MS) using the data-dependent analysis (DDA) method (Paper I). Total proteins were isolated according to a method published earlier (Vuorijoki et al., 2016). Proteins were reduced, alkylated then precipitated in 1:1 acetone: ethanol solution and stored at –20° C until digestion. When resuspended, proteins were digested via in-solution digestion using 1 µg trypsin $µl^{-1}$, 5 % (V/V) acetonitrile and 50 mM Tris-HCl (pH 8). Peptides were separated in a nano-liquid chromatography system (EasyNanoLC 1000, Thermo Fisher Scientific), ionized by positive ionization then fragmented by high-energy collision dissociation. MS QExactive (Thermo Fisher Scientific) and Thermo Xcalibur (Thermo Fisher Scientific) software were used to register the mass-to-charge spectra in the range 300 to 2000 mass-to-charge ratio and the MS/MS scans for the 10 most intense peaks. Raw data was referenced against

the genome of *Synechocystis* (Kaneko et al., 1996) using an in-house Mascot search engine (Perkins et al., 1999). Search results were analysed with Proteome Discoverer software (Thermo Fisher Scientific) and further annotated with data downloaded from Uniprot. Quantification of MS data was performed using the Progenesis QI LC-MS 4.0 (Nonlinear Dynamics) software using a threshold of at least 2 detected peptides per protein. The abundance levels of the proteins were calculated based on the volumes of the peptide peaks representing the given proteins. The practical significance of differentially regulated proteins was set to FC > 1.5 (Paper I).

3.6.3 Kinetics parameters of the YqjM enzyme

The reductive rate of YqjM was determined via stopped flow spectroscopy under anoxic conditions in an anaerobic glovebox. Prior to the measurements, solutions were sparged with N_2. The reaction solution contained 25 μM purified YqjM protein, 30−1000 μM NADPH or NADH and 50 mM Tris-HCl (pH 7.5). Cofactor reduction was followed at 452 nm and 25 °C then reductive rate k_{red} and dissociation constant K_D was determined. To measure the oxidative rate k_{ox} of YqjM, the protein was reduced by equimolar amounts of NADPH. 20 μM reduced YqjM was then mixed with 25−500 μM methylmaleimide, buffered at 50 mM Tris-HCl (pH 7.5) and absorbance was followed at 452 nm and 25 °C (Paper IV).

3.7 Statistical analysis

Statistical significance was determined using the analysis of variance (ANOVA) method (Paper I-IV).

4 Main results

4.1 Deletion of CytM prevents the gradual inhibition of photosynthesis under photomixotrophic conditions

The effects of utilizing organic carbon on photosynthesis and the potential role of CytM in associated regulation were assessed in Paper I. Unmarked mutants of *Synechocystis* lacking the *cytM* gene (*sll1245*) were constructed according to a previously published method (Lea-Smith et al., 2016b). To evaluate whether deleting CytM affects growth, wild type and ΔCytM cells were cultivated at a photon flux density of 50 µmol photons m^{-2} s^{-1} in the absence or presence of glucose at an initial concentration of 10 mM. Based on optical density (OD_{750}) measurements (Fig. 1A in Paper I), no difference in growth was observed between the wild type and ΔCytM under photoautotrophic conditions. When supplemented with glucose, both strains grew faster than those cultured photoautotrophically. On the third day ΔCytM had however 1.9 ± 0.4 higher OD_{750} than the wild type. The observed growth advantage of ΔCytM over the wild type under photomixotrophic conditions is in line with previous reports (Hiraide et al., 2015).

Next, it was investigated how photomixotrophic culturing altered the photosynthetic apparatus and whether deleting CytM prevented this change. The functionality of PSII was tested by determining rates of net O_2 production in intact cells via the Clarke-type electrode (Fig. 3E in Paper I). Strikingly, wild type cells exposed to 1000 µmol photons m^{-2} s^{-1} white light demonstrated only marginal net production of O_2 when cultured photomixotrophically for 3 days. The O_2 evolving capacity increased when the artificial electron acceptor DCBQ was added to the cells prior to the measurements, albeit not to the level observed in the DCBQ-treated photoautotrophic wild type. This suggests that the functionality of PSII is fairly retained under photomixotrophic conditions, but the electron transfer downstream of PSII may be blocked, likely by a strongly reduced PQ pool. In contrast, net production of O_2 in photomixotrophic ΔCytM was similar to that in the photoautotrophic wild type, suggesting that the loss of CytM conserves net photosynthetic activity. We then assessed how the wild type lost and ΔCytM retained PSII activity during photomixotrophic cultivation. The redox kinetics of the PSII

primary electron acceptor Q_A^- was determined by daily measurements of flash-induced fluorescence yield decay kinetics (Fig. 4 in Paper I). Typical relaxation curves were observed under photoautotrophic conditions, and on day 1 of photomixotrophic culturing both in wild type and ΔCytM cells. On the second day, Q_A^- reoxidation in the wild type was substantially slower than on day 1, and on the third day nearly blocked. Such a gradual slow-down in Q_A^- reoxidation was not observed in photomixotrophic ΔCytM.

To evaluate whether different efficiencies in CO_2 assimilation or Mehler-like activity accounted for such differences between the wild type and ΔCytM on day 3, we probed real-time cellular gas fluxes (Fig. 7 in Paper I). Samples were supplemented with 1.5 mM $NaHCO_3$ and enriched with $^{18}O_2$ isotopologue then changes in total inorganic carbon (Ci) and O_2 levels were followed via MIMS under dark/200 μmol photons m^{-2} s^{-1} light/dark regime. This method enabled us to estimate the activity of Rubisco, and differentiate between gross $^{16}O_2$ production by PSII and $^{18}O_2$ consumption by FDPs (and RTOs). By calculating the difference between $^{18}O_2$ consumption in light and dark, we determined light-induced O_2 consumption that accounts for the Mehler-like activity. Importantly, residual gross $^{16}O_2$ production was observed in the photomixotrophic wild type exposed to the light. We detected nearly equal $^{18}O_2$ consumption in the light, therefore electrons originating from PSII may have been circulating via the water-water cycle, possibly driven by RTOs. In line with this, light-induced $^{18}O_2$ consumption and total Ci uptake was negligible. Compared to the photomixotrophic wild type, ΔCytM displayed a substantially higher gross production of $^{16}O_2$, light-induced $^{18}O_2$ consumption, and total Ci uptake. In summary, activities of FDPs and Rubisco in the wild type was negligible likely due to arrested flow of photosynthetic electrons. It remains ambiguous whether this blockage was triggered by limitations at PSII directly or indirectly via feedback repression originating downstream of PSI. Nevertheless, deleting the CytM protein effectively alleviated the blockage on PET by an as yet unknown mechanism.

4.2 Photomixotrophically cultured ΔCytM accumulates proteins of nutrient uptake systems and cofactor biosynthetic pathways

To reveal differences in the metabolism of wild type and ΔCytM cultivated under photomixotrophic conditions, the total proteome was analysed by nLC MS/MS and the DDA method (Fig. 8 in Paper I). In total, we identified 2415 proteins, out of which 634 were quantified. 162 proteins differed in abundance between ΔCytM and the wild type at a fold change (FC) less than -1.5 or more than 1.5 (Supplemental dataset S1-3 in Paper I). Differentially regulated proteins were grouped by molecular function. The most pronounced differences were observed in transporter proteins.

The most abundant proteins in the mutants were the constitutive low-affinity ABC-type phosphate transporters (pstA1, pstB1, pstB1', pstC) when compared to the wild type. Importantly, higher levels of a thylakoid *β*-type carbonic anhydrase, EcaB, were observed in ΔCytM compared to the wild type. EcaB was recently proposed to regulate the activity of NDH-1_3 and NDH-1_4 isoforms that are known to drive inducible or constitutive uptake of CO_2, respectively (Ogawa, 1991; Sun et al., 2019). Only a handful of enzymes participating in the central carbon metabolic enzymes were found to be differentially regulated in the mutant. A notable exemption is the phosphofructokinase enzyme (Pfk) which was less abundant in ΔCytM than in the wild type. Pfk operates in the EMP pathway by transferring a phosphoryl group from ATP to fructose-6-phosphate (F6P) yielding fructose 1,6-bisphosphate (FBP). Importantly, ΔCytM retained the Mg^{2+} transporter MgtE in higher amounts than the wild type. Mg^{2+} is a ligand of the tetrapyrrole ring in chlorophylls. Additionally, ChlL, a subunit of light-independent protochlorophyllide reductase (Wu and Vermaas, 1995) and ChlP, a geranylgeranyl reductase (Shpilyov et al., 2005) were found at higher levels in the mutant than in the wild type. The accumulation of transporter and biosynthetic proteins in ΔCytM plausibly reflects elevated nutrient requirements due to enhanced growth under photomixotrophic conditions. The key changes in protein abundances and bioenergetics processes in ΔCytM cells are summarized in Fig. 7.

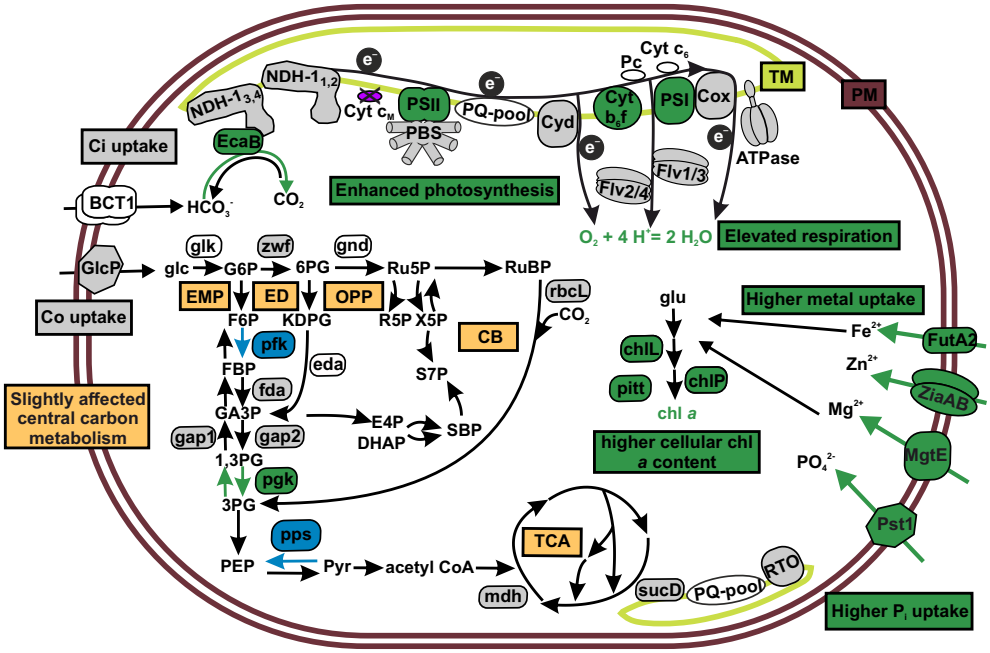

Figure 7. Schematics of the metabolism in ΔCytM cells cultivated under photomixotrophic conditions. BCT1, bicarbonate transporter 1; CB, Calvin-Benson-Bassham cycle; Ci uptake, inorganic carbon uptake; Co uptake, organic carbon uptake; eda, Entner-Doudoroff aldolase; fda, fructose-1,6-bisphosphate aldolase; FutA2, iron uptake protein A2; gap1-2, glyceraldehyde-3-phosphate dehydrogenase 1-2; glc, glucose; glcP, glucose transporter; glk, glucokinase; gnd, 6-phosphogluconate dehydrogenase; mdh, malate dehydrogenase; Pi uptake, inorganic phosphate uptake; pgk, phosphoglycerate kinase; PM, plasma membrane; pps, phosphoenolpyruvate synthase; Pyr, pyruvate; PEP, phosphoenolpyruvate; rbcL, Rubisco large chain, sucD, succinate-semialdehyde dehydrogenase; TCA, tricarboxylic acid cycle; TM, thylakoid membrane; ZiaAB, zinc transporter; zwf, glucose-6-phosphate 1-dehydrogenase. The drawing is adopted from Paper I and slightly modified (Solymosi et al., 2020).

4.3 Distinct *in vivo* activity of Flv1/Flv3 and Flv2/Flv4 in *Synechocystis* cultivated under atmospheric conditions

To distinguish between activities of Flv1/Flv3 and Flv2/Flv4 heterodimers, we investigated cellular gas fluxes in various *Synechocystis* mutants deficient in FDPs (Paper II). *In vivo* activity of FDPs was determined *via* MIMS similar to that in Paper I. First, we tested the wild type and ΔFlv1/Flv3 mutant (Figure 2 in Paper II) previously shown to be lacking Flv1 and Flv3 but retaining Flv2 and Flv4 proteins (Allahverdiyeva et al., 2011; Mustila et al., 2016). Cells were cultivated at pH 7.5 and atmospheric CO_2, which is known to induce the expression of all FDPs (Zhang et al., 2009). At the transition from dark to 500 μmol photons m^{-2} s^{-1} light, wild type cells displayed a prompt but transient increase in rates of O_2 consumption. Over time, this increase was followed by a rapid decay in rates then a quasi-stable state of O_2 consumption in light. In ΔFlv1/Flv3, rates of light-induced O_2 uptake were substantially lower than those in the wild type, but were not zero. This observation demonstrated that in *Synechocystis* cultured under atmospheric conditions, Flv1 and Flv3 are the major, but not the only, components driving O_2 photoreduction.

Next, we assessed whether the detected photoreduction of O_2 in the ΔFlv1/Flv3 mutant was driven by Flv2 and Flv4 proteins. The ΔFlv3/Flv4 mutant lacking all FDPs (Mustila et al., 2016) was exposed to light and Mehler-like activity was determined (Figure 2 in Paper II). We observed negligible light-induced consumption of O_2, demonstrating that the loss of FDPs completely abolish O_2 photoreduction activity in *Synechocystis*. This suggests that Flv2 and Flv4 substantially contribute to the Mehler-like reaction.

We then evaluated whether Flv2 and Flv4 transferred electrons to O_2 from the acceptor side of PSII or the PQ pool (Figure 3—figure supplement 1 in Paper II) as it was proposed earlier (Bersanini et al., 2014; Zhang et al., 2012). Given that Cyd proteins are capable of O_2 photoreduction by oxidizing the PQ pool (Ermakova et al., 2016), we applied the ΔCyd mutant. To block electron transfer downstream of PQ pool, ΔCyd cells were exposed to 25 μM DBMIB, which is known to inhibit Cyt

b$_6$*f* (Roberts and Kramer, 2001). Importantly, O_2 consumption in light was negligible, implying that Flv2 and Flv4 (or any other cellular components in ΔCyd) are unable to oxidize the acceptor side of PSII *via* O_2 photoreduction. All FDPs therefore reduce O_2 by electrons originating downstream of PSI.

The capacities of Flv1/Flv3 and Flv2/Flv4 were tested by determining rates of O_2 uptake in wild type, ΔFlv1/Flv3, and ΔFlv4 cells exposed to different light intensities (Figure 5 in Paper II). While ΔFlv4 is deficient in both Flv2 and Flv4 it expresses Flv1 and Flv3 proteins (Paper II; Zhang et al., 2012). When illuminated, all strains displayed triphasic kinetics in consumption of O_2. The most pronounced difference was observed in maximal rates of light-induced O_2 consumption at dark-to-light transitions. In the wild type, maximal rates at light intensities of 1000 and 1500 μmol photons m^{-2} s^{-1} were 2 and 2.3 times higher than that under 500 μmol photons m^{-2} s^{-1} illumination. Such fold changes were slightly lower in ΔFlv4 and only minor in ΔFlv1/Flv3. These results demonstrated that the Flv1/Flv3 heterodimer is a rapid and high-capacity electron sink, whereas the Flv2/4 heterodimer assists in the slower steady-state photoreduction of O_2.

4.4 NO represses PSII and NDH-1 *in vivo*

FLVB, the homolog of Flv3 in *Chlamydomonas* was shown to catalyse light-induced NO reduction in *Chlamydomonas in vivo* (Burlacot et al., 2020). Whether NO can function as a sink of photosynthetic electrons in cyanobacteria depends on the impacts of NO photosynthesis. In paper III, photochemical activity of PSII and PSI was evaluated *in vivo* by monitoring whole-cell fluorescence and P700 redox kinetics in wild type *Synechocystis* in the absence or presence of 20 μM NO (Fig. 1 in Paper III). Under actinic red illumination, untreated cells demonstrated photochemical yields of PSII [Y(I)] and PSI [Y(I)] comparable to previously published values (Solymosi et al., 2020). To avoid oxidation of NO into NO_x species, anoxic conditions were established. In anoxic cells exposed to actinic light, effective Y(II) was initially 67.4% ± 12.2% lower than that in cells under atmospheric conditions. Over 2 min illumination however, effective Y(II) increased and was only 36.2% ± 13.8% lower when compared to that in control cells. In line with this, donor side limitation at PSI [Y(ND)] was initially 18.0% ± 7.3% higher than that under atmospheric conditions but recovered to near control levels. Similar to effective Y(II), effective Y(I) was initially lower than in the control cells but improved over the 2 min of actinic illumination. Partial recovery of PSII and PSI activity may have been elicited by higher levels of O_2 that alleviated substrate limitation of FDPs and RTOs, leading to a more oxidized PQ pool.

Next, 20 μM NO was added to the cells 2 min prior to the measurement in the dark (Figure 1 in Paper III). When exposed to actinic light, anoxic cells treated with

NO demonstrated negligible effective Y(II). This is in line with previous *in vivo* studies reporting decreased Y(II) in pea leaves exposed to GSNO under atmospheric conditions (Wodala et al., 2008). The loss of Y(II) observed here was reflected in Y(ND), which was markedly higher than in the wild type under anoxic or atmospheric conditions. Consequently, only minor effective Y(I) was observed in cells treated with NO under anoxic conditions. These results demonstrate the detrimental effects of NO on PSII and PSI in cyanobacteria *in vivo*.

We then investigated the effects of NO on the redox kinetics of Q_A (Fig. 2 in Paper III). Anoxic cells were untreated or treated with 1 µM or 20 µM NO and exposed to a short saturating flash. Changes in fluorescence yield were subsequently monitored in the dark. In the absence of NO, anoxic cells displayed waving kinetics previously observed in *Synechocystis* under microoxic conditions and *Chlamydomonas* under H_2-producing conditions (Deák et al., 2014; Krishna et al., 2019). The wave feature comprises an initial decrease in the fluorescence yield, reflecting transient re-oxidation of Q_A^- by Q_B, and a subsequent rise, corresponding to re-reduction of the PQ pool by NDH-1 in the dark (Deák et al., 2014). When anoxic cells were exposed to NO, the transient rise was nearly eliminated. This suggests that NDH-1 is repressed by NO.

4.5 Deleting Flv1 or Flv3 enhances light-driven whole-cell biotransformation

To assess whether the loss of Flv1 or Flv3 proteins increase the availability of reducing equivalents for the ene reductase YqjM in *Synechocystis*, heterologous YqjM was expressed under the regulation of promoter P_{cpc} in wild type (Syn::P_{cpc}YqjM), ΔFlv1 (ΔFlv1::P_{cpc}YqjM) and ΔFlv3 (ΔFlv3::P_{cpc}YqjM) genetic backgrounds (Paper IV). Conversion of 2-methylmaleimide to 2-methylsuccinimide by YqjM was used as a model reaction. However, maleimides are known to modify proteins *via* binding to Cys residues (Zaffagnini et al., 2019). Therefore, we first evaluated the effects of the substrate 2-methylmaleimide on the photosynthetic apparatus (Fig. 5A, B in Paper IV). The wild type, and mutants Syn::P_{cpc}YqjM, ΔFlv1, and ΔFlv1::P_{cpc}YqjM were exposed to 400 µmol photons m^{-2} s^{-1} illumination for 15 min in the presence or absence of 10 mM 2-methylmaleimide. To determine photochemical yields of PSII and PSI, we monitored changes in cellular fluorescence simultaneously with redox kinetics of P700 under periods of dark, far-red and actinic red light. When the substrate was absent, Y(II) and Y(I) was comparable between the wild type and the mutant Syn::P_{cpc}YqjM, ΔFlv1 and ΔFlv1::P_{cpc}YqjM. However, wild type and ΔFlv1 cells exposed to 10 mM substrate demonstrated substantially lower Y(II) when compared to untreated cells. Moreover, Y(I) was lower in treated cells of the wild type and ΔFlv1 exposed to dark and far-red light than those in

untreated cells. Such detrimental effects were not observed in Syn::P_{cpc}YqjM and ΔFlv1::YqjM mutants expressing YqjM, demonstrating that YqjM effectively alleviates substrate toxicity by consuming 2-methylmaleimide.

Next, it was evaluated whether the loss of Flv1 or Flv3 increased the conversion efficiency of 2-methylmaleimide into 2-methylsuccinimide in *Synechocystis* mutants expressing YqjM (Fig. 6 in Paper IV). Cells were cultivated under 150 µmol photons m^{-2} s^{-1} illumination, adjusted to OD_{750} 2 and exposed to 10 mM 2-methylmaleimide in light. The product formation rate and the whole cell specific activity in light conditions was comparable between Syn::P_{cpc}YqjM, ΔFlv1::YqjM and ΔFlv3::YqjM. When light-dependent production was tested at a more industrially relevant higher density (OD_{750} 10) Flv1/3-deficient mutants ΔFlv1::YqjM and ΔFlv3::YqjM demonstrated higher productivity than the control strain Syn::P_{cpc}YqjM. These results show that engineering innate electron sinks is a viable strategy for enhancing reactions of interest that utilize photosynthetic reductants.

5 Discussion

Microalgae are well placed to become frontrunners in green technologies. Driven by the inexhaustible solar energy, the photosynthetic apparatus converts naturally abundant materials such as water, CO_2 and N_2 into reducing cofactors that can be used for the biosynthesis of valuable compounds. However, microalgae evolved to survive in changing natural environments and not to operate as solar-driven living factories. Under controlled production conditions, photoprotective processes waste energy thus limiting productivity. Photoprotective processes can be removed. However, given the astounding complexity of photosynthesis, specialized knowledge and know-how are required. In this study, we sought to uncover regulatory processes of photosynthesis and demonstrate the applicability of such fundamental knowledge in realizing the potential of microalgae in bioindustrial applications.

5.1 Scientific dilemmas when re-designing photosynthesis

The inactivation of thylakoid electron sinks, such as FDP, is a promising strategy to provide proteins of interest a competitive advantage for photosynthetic electrons. Recent papers have demonstrated potential applicability in biotransformation, production of biofuels such as H_2, and carbon-derived chemicals (Paper IV; Jokel et al., 2019; Selão et al., 2020; Thiel et al., 2019). However, a potentially larger pool of available reductants may not necessarily translate into higher yields of the targeted carbon-derived chemicals due to: (i) regulatory feedback repressions that may limit the apparent photosynthetic activity; or (ii) rearrangements in the metabolism to utilize the surplus reductants by "housekeeping" reactions. Therefore, the potential applicability of improving light reactions can be better assessed by evaluating targeted reactions that are directly coupled to the Fd pool such as the photoproduction of H_2 by innate hydrogenases. These proteins directly compete for electrons with innate sinks such as FDP and FNR. *Synechocystis* possesses [NiFe]-hydrogenases that are generally considered to be less efficient than e.g., the [Fe-Fe]-hydrogenase of *Chlamydomonas*, due to slower catalysis and bidirectionality. The latter is, the capacity to both generate and consume H_2 (Bothe et al., 2010; Peters et

al., 2015). As such, photoproduction of H_2 in *Chlamydomonas* is the most insightful case to demonstrate the applicability and complexity of electron sink engineering.

The loss of FLVB improves long-term photoproduction of H_2 in *Chlamydomonas* when exposed to a train of strong but short light pulses superimposed over a dark background (Jokel et al., 2019). Plausibly, such improvements are—at least partly—the result of eliminating a competitor of the hydrogenase. However, given that loss of FDP is known to delay *pmf* generation (Section 1.2.3; Paper V), other factors must play a role in increasing H_2 photoproduction in the mutant (Paper V). Indeed, delay in generating *pmf* likely translates into a less strict photosynthetic control, thereby: (i) limiting CET, a competitor pathway of the hydrogenase, and (ii) enabling active water splitting at PSII (Steinbeck et al., 2015), which is the primary electron supplier of hydrogenase in long-term H_2 photoproduction (Kosourov et al., 2020). In line with this, it was shown that long-term photoproduction of H_2 increased when *pmf* was artificially compromised by applying uncouplers or deleting PGR5 or PGRL1 in S-deprived *Chlamydomonas* (Antal et al., 2009; Steinbeck et al., 2015; Tolleter et al., 2011). Moreover, compromised *pmf* may translate into altered ATP/NADPH ratios influencing the initiation of the CBB cycle that is currently considered to be a major limitation in the photoproduction of H_2 (Kosourov et al., 2021; Tóth and Yacoby, 2019). It is important to note that hydrogenases are extremely sensitive to O_2 (Happe and Naber, 1993; Swanson et al., 2015) thus photoproduction of H_2 is primarily facilitated under anoxic conditions. We have shown that in *Synechocystis*, exposure to anoxia substantially affects the photosynthetic electron flux (Paper III). Therefore, engineering electron sinks—at least in cyanobacteria—likely have different effects under atmospheric conditions.

Introducing an exceptionally strong artificial electron sink in the thylakoid of cyanobacteria or green algae may eliminate feedback reactions and, when outcompeting innate sinks, simplify the electron transport. Biotransformation driven by photosynthesis is thus a promising approach to utilize photosynthetic reductants for targeted reactions and, simultaneously, enhance the effective photochemical work. The NADPH-dependent YqjM protein recently has recently been employed in a cyanobacterial whole-cell biotransformation platform (Paper IV). YqjM is a promising candidate for such an artificial electron sink, however, its substrate specificity could be narrower. A potential approach to improve substrate specificity is protein engineering *via* side-directed mutagenesis. This technique has been successfully applied to enhance enzymatic activity and substrate specificity of several oxidoreductases e.g., Cyt P450 proteins (Li et al., 2020).

In summary, understanding the interrelation between the photosynthetic apparatus and thylakoid electron sinks is key to successfully apply electron sink

engineering in a wider range of applications thus bringing microalgae closer to feasible applicability in bioindustry.

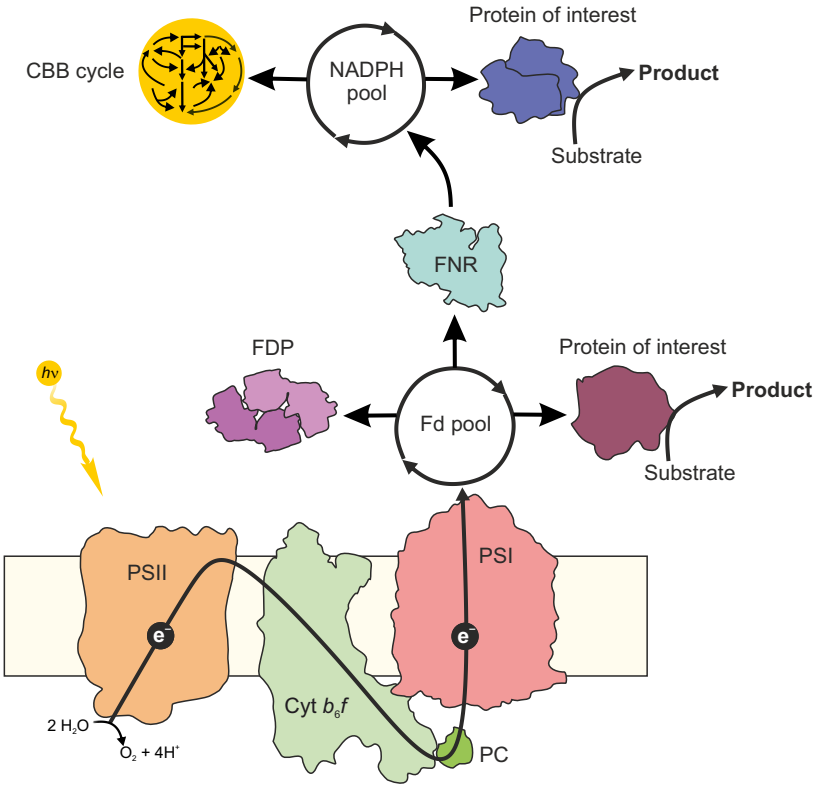

Figure 8. Schematics of reductant pools (Fd and NADPH) in *Synechocystis* and *Chlamydomonas*. Proteins of interest which can utilize Fd or NADPH for production of targeted compounds are competing with innate electron sinks such as FDP or the CBB cycle.

5.2 Inventive activity related to photosynthesis

Engineering photosynthesis has the longest history in crop plant development. To feed the predicted 10 billion-strong human population in 2050 *sustainably*, gaps in food production, arable land, and emission mitigation have to be closed. By applying gene-editing techniques on plants, strenuous efforts are devoted to improve crop yields and, decrease land and water usage by eliminating inefficiencies in CO_2 fixation, and improving utilization of light energy (Evans, 2013; Foyer et al., 2017; Murchie and Niyogi, 2011; Ort et al., 2015). A promising engineering approach is to enhance the energy-efficiency of CO_2 fixation. Introducing a highly efficient metabolic pathway alternative to the wasteful native photorespiratory pathway, plant productivity was boosted by 40% (South et al., 2019). However, the uptake of

technological achievements in European agriculture is limited due to restrictive legislation towards commercializing genetically modified crops [Regulation (EC) No 1829/2003]. Curiously, the attitude is more permissive towards patenting gene-edited crops and related findings [Article 53(b) EPC]. The controversy between GM and patent law is seldom discussed and creates unique regulatory challenges in the European Union (Jiang, 2020).

Contained use of genetically engineered microorganisms, such as microalgae, are permitted (Council Directive 90/219/EEC). A patent report in the space of algae-related technologies revealed that the number of yearly patents grew at a rate of 11-13% between 1995 and 2013, demonstrating the increasing interest in microalgae. The majority of these patents are related to growing and harvesting technologies, and proprietary strains. Applications were predominantly filed in Asia (75%), aiming for nutritional or medicinal uses, and the United States (13%), intending to produce biofuels (World Intellectual Property Organization, 2016). The global market of algal products (including those from seaweed) is forecast to grow at a compound annual growth rate of 5.4% reaching $5.17 billion by 2023 (Markets and Markets, 2018).

5.3 Is algae-tech economically feasible and environmentally sustainable?

In the last decades, the production of biofuels (bioethanol, biodiesel) in the United States was one of the most capital-intensive activities related to the algae-tech space. However, producing biofuels are yet to become commercially viable (Chen et al., 2018; Ruiz et al., 2016). A major bottleneck preventing economic feasibility is low biomass productivity due to e.g., the unrealized potential in photosynthetic photon-to-product conversion efficiency: only 1-3% is met out of the theoretical maximum of 10-13% (Melis, 2009; Radakovits et al., 2010). By remodelling 34 microalgal biofuel production platforms *via* life cycle assessment and techno-economic analysis, it was found that costs of biofuel production decrease 30-40% when biomass productivity is doubled in the currently common range of12.5 to 30 g dry weight (DW) biomass m^{-2} day^{-1}. However, further increasing biomass productivity to ~50 g DW biomass m^{-2} day^{-1} gains only 15-20% additional cost reduction, and still cannot lead to economically viable production. Importantly, the majority of the modelled platforms missed sustainability targets when a common sustainability metric, the global warming potential (GWP, expressed in emitted g CO_2 equivalent to MJ_{fuel}^{-1}) was calculated. According to the models, increasing biomass productivity would lead to no or only minor improvements in GWP. Diminishing returns in production cost or sustainability were due to extra environmental, capital, and operating burdens (Cruce et al., 2021). Indeed, it was demonstrated by an actual 100-

ha microalgal facility producing feed and biofuel that high energy requirements and fertilizer demand are major barriers preventing feasible and sustainable biofuel production (Beal et al., 2015). Thus, reducing material and energy input is key in maturing microalgae technology.

The current consensus for offsetting the high production costs is developing multi-pathway biorefineries that co-produce a range of valuable compounds (e.g., proteins) with biofuels (Ruiz et al., 2016; Zhu, 2015). Based on a recent modelling study, production costs markedly decreased when biomass fractionation was applied to co-produce valuable proteins with biodiesel (Cruce and Quinn, 2019). The consumer demand for food-grade microalgal proteins will be tested in the coming years. Recently, a United Kingdom-based algae-tech company Algenuity reported to partner with Unilever, a €50 billion-worth food industry giant, to commercialize vegetarian food additives based on a proprietary *Chlorella vulgaris* strain (find the patent as WO2020105001 in the WIPO IP Portal). Apart from proteins, microalgae are potential sources of various highly valuable fine chemicals and pharmaceuticals (Laurens et al., 2017). However, a wider value chain in microalgae biorefineries cannot solve sustainability issues. Access to renewable energy and efficient nutrient recycling are crucial to the path towards sustainable microalgae biorefineries (Ruiz et al., 2016).

6 Conclusions and future perspectives

The photosynthetic machinery is controlled by an intricate hierarchical regulatory network. By targeting master regulators with an engineering approach, the photosynthetic electron flow may be redirected towards the biosynthesis of targeted chemicals. Here, it has been uncovered that the CytM protein and the small molecule NO plays a role in controlling the photosynthetic capacity (Paper I, III). It has been revealed that the regulatory proteins Flv1/Flv3 and Flv2/Flv4 have distinct electron sink activities (Paper II). The potential applicability of such knowledge has been demonstrated by the enhanced efficiency of whole-cell biotransformation *via Synechocystis* lacking Flv1 or Flv3 (Paper IV). Finally, the regulation of microalgal photosynthesis and the efforts of its engineering has been reviewed in light of the recent developments (Paper V).

The complexity of metabolism is both the opportunity and the threat in microalgal biotechnology. An emerging trend is to increase complexity by employing microbial consortia to produce chemicals of interest (Sgobba and Wendisch, 2020). A seldom explored strategy in microalgal research is decreasing complexity. By redesigning the genome of the bacterium *Mycoplasma mycoides*, it was demonstrated that 473 genes are sufficient for a primitive prokaryote to function and reproduce (Hutchison et al., 2016). In the future, a minimalistic microalgae chassis may assist in developing robust microalgal production platforms.

Acknowledgements

This work was conducted in the laboratories of Molecular Plant Biology unit at the University of Turku. I am grateful to Eva-Mari Aro for the opportunity to work here. Financial support from Academy of Finland Centre of Excellence in Molecular Biology of Primary Producers Project (no. 307335), NordForsk Nordic Center of Excellence "NordAqua" Towards Versatility of Aquatic Production Platforms: Unlocking the Value of Nordic Bioresources Project (no. 82845), The Finnish Academy of Science and Letters, and the University of Turku Graduate School Doctoral Programme in Molecular Life Sciences is gratefully acknowledged.

First and foremost, I express my most sincere gratitude to my supervisor Yagut Allahverdiyeva for the guidance, support, and trust and my colleagues in the Photomicrobes group for the stimulating and supportive environment that enabled me to succeed with my doctoral research. The results of this book are fruits of devoted and tireless team work of the Photomicrobes group, the labs of Molecular Plant Biology unit and collaborators in the group of David Lea-Smith at the University of East Anglia, Chris J. Howe at the University of Cambridge and Robert Kourist at the Graz University of Technology. Special thanks to research director Eevi Rintamäki for guiding my studies and helping with administration duties.

The critical revision of the dissertation by Joanna Kargul and Francisco J. Florencio is greatly appreciated.

My heartfelt gratitude to fellow PhD students and post-docs in our unit for the time we spent together in lunch and coffee breaks, pubs, saunas, at Shitty Movie Nights and dinner parties. These times I will always remember warmly as the 'good old days'.

I will be forever grateful for the immeasurable support I have from Aliisa. Your love gives me reference that no matter how science, technology and politics are, I share a life with you, and at the end of the day that matters the most.

Végső de nem utolsó sorban szeretném megköszönni szüleimnek, testvéreimnek és régi magyar barátaimnak a támogatást amit minden formában nyújtanak. Ti itt vagytok nekem 2000 km távolságból is és tudom, hogy ha minden kötél szakad, rátok mindig számíthatok.

03.11.2021

List of References

Agarwal, R., Matros, A., Melzer, M., Mock, H.P., Sainis, J.K., 2010. Heterogeneity in thylakoid membrane proteome of Synechocystis 6803. J. Proteomics 73, 976–991.

Albarrán, C., Navarro, J.A., Molina-Heredia, F.P., Murdoch, P.D.S., De La Rosa, M.A., Hervás, M., 2005. Laser flash-induced kinetic analysis of cytochrome f oxidation by wild-type and mutant plastocyanin from the cyanobacterium Nostoc sp. PCC 7119. Biochemistry 44, 11601–11607.

Alboresi, A., Storti, M., Morosinotto, T., 2019. Balancing protection and efficiency in the regulation of photosynthetic electron transport across plant evolution. New Phytol. 221, 105–109.

Allahverdiyeva, Y., Ermakova, M., Eisenhut, M., Zhang, P., Richaud, P., Hagemann, M., Cournac, L., Aro, E.M., 2011. Interplay between flavodiiron proteins and photorespiration in Synechocystis sp. PCC 6803. J. Biol. Chem. 286, 24007–24014.

Allahverdiyeva, Y., Isojärvi, J., Zhang, P., Aro, E.M., 2015a. Cyanobacterial oxygenic photosynthesis is protected by flavodiiron proteins. Life.

Allahverdiyeva, Y., Mustila, H., Ermakova, M., Bersanini, L., Richaud, P., Ajlani, G., Battchikova, N., Cournac, L., Aro, E.M., 2013. Flavodiiron proteins Flv1 and Flv3 enable cyanobacterial growth and photosynthesis under fluctuating light. Proc. Natl. Acad. Sci. U. S. A. 110, 4111–4116.

Allahverdiyeva, Y., Suorsa, M., Tikkanen, M., Aro, E.M., 2015b. Photoprotection of photosystems in fluctuating light intensities. J. Exp. Bot. 66, 2427–2436.

Antal, T.K., Volgusheva, A.A., Kukarskih, G.P., Krendeleva, T.E., Rubin, A.B., 2009. Relationships between H2 photoproduction and different electron transport pathways in sulfur-deprived Chlamydomonas reinhardtii. Int. J. Hydrogen Energy 34, 9087–9094.

Asada, K., 1999. The water-water cycle in chloroplasts: Scavenging of active oxygens and dissipation of excess photons. Annu. Rev. Plant Biol. 50, 601–639.

Assil-Companioni, L., Büchsenschütz, H.C., Solymosi, D., Dyczmons-Nowaczyk, N.G., Bauer, K.K.F., Wallner, S., Macheroux, P., Allahverdiyeva, Y., Nowaczyk, M.M., Kourist, R., 2020. Engineering of NADPH Supply Boosts Photosynthesis-Driven Biotransformations. ACS Catal. 10, 11864–11877.

Astier, J., Rasul, S., Koen, E., Manzoor, H., Besson-Bard, A., Lamotte, O., Jeandroz, S., Durner, J., Lindermayr, C., Wendehenne, D., 2011. S-nitrosylation: An emerging post-translational protein modification in plants. Plant Sci.

Astier, J., Rossi, J., Chatelain, P., Klinguer, A., Besson-Bard, A., Rosnoblet, C., Jeandroz, S., Nicolas-Francès, V., Wendehenne, D., 2021. Nitric oxide production and signalling in algae. J. Exp. Bot. 72, 781–792.

Badger, M.R., Price, G.D., 2003. CO2 concentrating mechanisms in cyanobacteria: Molecular components, their diversity and evolution. J. Exp. Bot.

Baers, L.L., Breckels, L.M., Mills, L.A., Gatto, L., Deery, M.J., Stevens, T.J., Howe, C.J., Lilley, K.S., Lea-Smith, D.J., 2019. Proteome mapping of a cyanobacterium reveals distinct compartment organization and cell-dispersed metabolism. Plant Physiol. 181, 1721–1738.

Bassi, R., Dall'Osto, L., 2021. Dissipation of Light Energy Absorbed in Excess: The Molecular Mechanisms. Annu. Rev. Plant Biol. 72, 47–76.

Baymann, F., Rappaport, F., Joliot, P., Kallas, T., 2001. Rapid electron transfer to photosystem I and unusual spectral features of cytochrome c6 in Synechococcus sp. PCC 7002 in vivo. Biochemistry 40, 10570–10577.

Beal, C.M., Gerber, L.N., Sills, D.L., Huntley, M.E., Machesky, S.C., Walsh, M.J., Tester, J.W., Archibald, I., Granados, J., Greene, C.H., 2015. Algal biofuel production for fuels and feed in a 100-ha facility: A comprehensive techno-economic analysis and life cycle assessment. Algal Res. 10, 266–279.

Beckmann, K., Messinger, J., Badger, M.R., Wydrzynski, T., Hillier, W., 2009. On-line mass spectrometry: Membrane inlet sampling. Photosynth. Res. 102, 511–522.

Benschop, J.J., Badger, M.R., Price, G.D., 2003. Characterisation of CO2 and HCO3- uptake in the cyanobacterium Synechocystis sp. PCC6803. Photosynth. Res. 77, 117–126.

Berepiki, A., Gittins, J.R., Moore, C.M., Bibby, T.S., 2018. Rational engineering of photosynthetic electron flux enhances light-powered cytochrome P450 activity. Synth. Biol. 3.

Berepiki, A., Hitchcock, A., Moore, C.M., Bibby, T.S., 2016. Tapping the Unused Potential of Photosynthesis with a Heterologous Electron Sink. ACS Synth. Biol. 5, 1369–1375.

Berla, B.M., Saha, R., Immethun, C.M., Maranas, C.D., Moon, T.S., Pakrasi, H.B., 2013. Synthetic biology of cyanobacteria: unique challenges and opportunities. Front. Microbiol. 4, 246.

Bernroitner, M., Tangl, D., Lucini, C., Furtmüller, P.G., Peschek, G.A., Obinger, C., 2009. Cyanobacterial cytochrome cM: Probing its role as electron donor for CuA of cytochrome c oxidase. Biochim. Biophys. Acta - Bioenerg. 1787, 135–143.

Berry, S., Schneider, D., Vermaas, W.F.J., Rögner, M., 2002. Electron transport routes in whole cells of Synechocystis sp. Strain PCC 6803: The role of the cytochrome bd-type oxidase. Biochemistry 41, 3422–3429.

Bersanini, L., Allahverdiyeva, Y., Battchikova, N., Heinz, S., Lespinasse, M., Ruohisto, E., Mustila, H., Nickelsen, J., Vass, I., Aro, E.M., 2017. Dissecting the Photoprotective Mechanism Encoded by the flv4-2 Operon: a Distinct Contribution of Sll0218 in Photosystem II Stabilization. Plant Cell Environ. 40, 378–389.

Bersanini, L., Battchikova, N., Jokel, M., Rehman, A., Vass, I., Allahverdiyeva, Y., Aro, E.-M., 2014. Flavodiiron protein Flv2/Flv4-related photoprotective mechanism dissipates excitation pressure of PSII in cooperation with phycobilisomes in Cyanobacteria. Plant Physiol. 164, 805–18.

Beuf, L., Bédu, S., Durand, M.C., Joset, F., 1994. A protein involved in co-ordinated regulation of inorganic carbon and glucose metabolism in the facultative photoautotrophic cyanobacterium Synechocystis PCC6803. Plant Mol. Biol. 25, 855–864.

Bhatti, A.F., Choubeh, R.R., Kirilovsky, D., Wientjes, E., van Amerongen, H., 2020. State transitions in cyanobacteria studied with picosecond fluorescence at room temperature. Biochim. Biophys. Acta - Bioenerg. 1861, 148255.

Bhatti, A.F., Kirilovsky, D., van Amerongen, H., Wientjes, E., 2021. State transitions and photosystems spatially resolved in individual cells of the cyanobacterium Synechococcus elongatus . Plant Physiol. 186, 569–580.

Bialek, W., Krzywda, S., Zatwarnicki, P., Jaskolski, M., Kolesinski, P., Szczepaniak, A., 2014. Insights into the relationship between the haem-binding pocket and the redox potential of c 6 cytochromes: Four atomic resolution structures of c 6 and c 6-like proteins from Synechococcus sp. PCC 7002. Acta Crystallogr. Sect. D Biol. Crystallogr. 70, 2823–2832.

Bialek, W., Nelson, M., Tamiola, K., Kallas, T., Szczepaniak, A., 2008. Deeply branching c6-like cytochromes of cyanobacteria. Biochemistry 47, 5515–5522.

Bialek, W., Szczepaniak, A., Kolesinski, P., Kallas, T., 2016. Cryptic c 6-Like and c M Cytochromes of Cyanobacteria. In: Cytochrome Complexes: Evolution, Structures, Energy Transduction, and Signaling. Dordrecht: Springer, pp. 713–734.

Bloye, S.A., Silman, N.J., Mann, N.H., Carr, N.G., 1992. Bicarbonate concentration by synechocystis PCC6803: Modulation of protein phosphorylation and inorganic carbon transport by glucose. Plant Physiol. 99, 601–606.

Borisov, V.B., Gennis, R.B., Hemp, J., Verkhovsky, M.I., 2011. The cytochrome bd respiratory oxygen reductases. Biochim. Biophys. Acta - Bioenerg. 1807, 1398–1413.

Borisov, V.B., Siletsky, S.A., Paiardini, A., Hoogewijs, D., Forte, E., Giuffrè, A., Poole, R.K., 2020. Bacterial Oxidases of the Cytochrome bd Family: Redox Enzymes of Unique Structure, Function, and Utility As Drug Targets . Antioxid. Redox Signal. ars.2020.8039.

Bothe, H., Schmitz, O., Yates, M.G., Newton, W.E., 2010. Nitrogen Fixation and Hydrogen Metabolism in Cyanobacteria. Microbiol. Mol. Biol. Rev. 74, 529–551.

Boyer, P.D., 1997. The ATP synthase - A splendid molecular machine. Annu. Rev. Biochem. 66, 717–749.

Brinkert, K., De Causmaecker, S., Krieger-Liszkay, A., Fantuzzi, A., Rutherford, A.W., 2016. Bicarbonate-induced redox tuning in Photosystem II for regulation and protection. Proc. Natl. Acad. Sci. U. S. A. 113, 12144–12149.

Brown, K.A., Guo, Z., Tokmina-Lukaszewska, M., Scott, L.W., Lubner, C.E., Smolinski, S., Mulder, D.W., Bothner, B., King, P.W., 2019. The oxygen reduction reaction catalyzed by: Synechocystis sp. PCC 6803 flavodiiron proteins. Sustain. Energy Fuels 3, 3191–3200.

Bruce, D., Biggins, J., Steiner, T., Thewalt, M., 1985. Mechanism of the light state transition in photosynthesis. IV. Picosecond fluorescence spectroscopy of Anacystis nidulans and Porphyridium cruentum in state 1 and state 2 at 77 K. BBA - Bioenerg. 806, 237–246.

Buchert, F., Mosebach, L., Gäbelein, P., Hippler, M., 2020. PGR5 is required for efficient Q cycle in the cytochrome b6f complex during cyclic electron flow. Biochem. J. 477, 1631–1650.

Burlacot, A., Richaud, P., Gosset, A., Li-Beisson, Y., Peltier, G., 2020. Algal photosynthesis converts nitric oxide into nitrous oxide. Proc. Natl. Acad. Sci. U. S. A. 117, 2704–2709.

Burlacot, A., Sawyer, A., Cuiné, S., Auroy-Tarrago, P., Blangy, S., Happe, T., Peltier, G., 2018. Flavodiiron-mediated O 2 photoreduction links H 2 production with CO 2 fixation during the anaerobic induction of photosynthesis. Plant Physiol. 177, 1639–1649.

Büsch, A., Friedrich, B., Cramm, R., 2002. Characterization of the norB gene, encoding nitric oxide reductase, in the nondenitrifying cyanobacterium Synechocystis sp. strain PCC6803. Appl. Environ. Microbiol. 68, 668–672.

Cabeza, M.S., Guerrero, S.A., Iglesias, A.A., Arias, D.G., 2015. New enzymatic pathways for the reduction of reactive oxygen species in Entamoeba histolytica. Biochim. Biophys. Acta - Gen. Subj. 1850, 1233–1244.

Calzadilla, P.I., Kirilovsky, D., 2020. Revisiting cyanobacterial state transitions. Photochem. Photobiol. Sci. 19, 585–603.

Calzadilla, P.I., Zhan, J., Sétif, P., Lemaire, C., Solymosi, D., Battchikova, N., Wang, Q., Kirilovskya, D., 2019. The cytochrome b6f complex is not involved in cyanobacterial state transitions. Plant Cell 31, 911–931.

Cape, J.L., Bowman, M.K., Kramer, D.M., 2006. Understanding the cytochrome bc complexes by what they don't do. The Q-cycle at 30. Trends Plant Sci.

Cardona, T., Sedoud, A., Cox, N., Rutherford, A.W., 2012. Charge separation in Photosystem II: A comparative and evolutionary overview. Biochim. Biophys. Acta - Bioenerg. 1817, 26–43.

Chamizo-Ampudia, A., Sanz-Luque, E., Llamas, Á., Ocaña-Calahorro, F., Mariscal, V., Carreras, A., Barroso, J.B., Galván, A., Fernández, E., 2016. A dual system formed by the ARC and NR molybdoenzymes mediates nitrite-dependent NO production in Chlamydomonas. Plant Cell Environ. 39, 2097–2107.

Chaux, F., Burlacot, A., Mekhalfi, M., Auroy, P., Blangy, S., Richaud, P., Peltier, G., 2017. Flavodiiron proteins promote fast and transient O2 photoreduction in chlamydomonas. Plant Physiol. 174, 1825–1836.

Checchetto, V., Segalla, A., Allorent, G., La Rocca, N., Leanza, L., Giacometti, G.M., Uozumi, N., Finazzi, G., Bergantino, E., Szabò, I., 2012. Thylakoid potassium channel is required for efficient photosynthesis in cyanobacteria. Proc. Natl. Acad. Sci. U. S. A. 109, 11043–11048.

Chen, J., Li, J., Dong, W., Zhang, X., Tyagi, R.D., Drogui, P., Surampalli, R.Y., 2018. The potential of microalgae in biodiesel production. Renew. Sustain. Energy Rev. 90, 336–346.

Chen, X., Schreiber, K., Appel, J., Makowka, A., Fähnrich, B., Roettger, M., Hajirezaei, M.R., Sönnichsen, F.D., Schönheit, P., Martin, W.F., Gutekunst, K., 2016. The Entner-Doudoroff pathway is an overlooked glycolytic route in cyanobacteria and plants. Proc. Natl. Acad. Sci. U. S. A. 113, 5441–5446.

Cho, Y.S., Pakrasi, H.B., Whitmarsh, J., 2000. Cytochrome c(M) from Synechocystis 6803: Detection in cells, expression in Escherichia coli, purification and physical characterization. Eur. J. Biochem. 267, 1068–1074.

Cho, Y.S., Wang, Q.J., Krogmann, D., Whitmarsh, J., 1999. Extinction coefficients and midpoint potentials of cytochrome c6 from the cyanobacteria Arthrospira maxima, Microcystis aeruginosa, and Synechocystis 6803. Biochim. Biophys. Acta - Bioenerg. 1413, 92–97.

Chukhutsina, V., Bersanini, L., Aro, E.M., Van Amerongen, H., 2015. Cyanobacterial flv4-2 operon-encoded proteins optimize light harvesting and charge separation in photosystem II. Mol. Plant 8, 747–761.

Cohen, M., Ozer, E., Kushmaro, A., Alfonta, L., 2020. Cellular localization of cytochrome bd in cyanobacteria using genetic code expansion. Biotechnol. Bioeng. 117, 523–530.

Correa-Aragunde, N., Foresi, N., Del Castello, F., Lamattina, L., 2018. A singular nitric oxide synthase with a globin domain found in Synechococcus PCC 7335 mobilizes N from arginine to nitrate. Sci. Rep. 8, 1–11.

Cramer, W.A., Hasan, S.S., 2016. Structure-Function of the Cytochrome b 6 f Lipoprotein Complex. In: Cramer, W. A., Kallas, T. (Eds.), Cytochrome Complexes: Evolution, Structures, Energy Transduction, and Signaling. Springer Netherlands, pp. 177–207.

Cruce, J.R., Beattie, A., Chen, P., Quiroz, D., Somers, M., Compton, S., DeRose, K., Beckstrom, B., Quinn, J.C., 2021. Driving toward sustainable algal fuels: A harmonization of techno-economic and life cycle assessments. Algal Res. 54, 102169.

Cruce, J.R., Quinn, J.C., 2019. Economic viability of multiple algal biorefining pathways and the impact of public policies. Appl. Energy 233–234, 735–746.

Dann, M., Leister, D., 2019. Evidence that cyanobacterial Sll1217 functions analogously to PGRL1 in enhancing PGR5-dependent cyclic electron flow. Nat. Commun. 10.

De Causmaecker, S., Douglass, J.S., Fantuzzi, A., Nitschke, W., Rutherford, A.W., 2019. Energetics of the exchangeable quinone, QB, in Photosystem II. Proc. Natl. Acad. Sci. U. S. A. 116, 19458–19463.

De La Cerda, B., Díaz-Quintana, A., Navarro, J.A., Hervás, M., De La Rosa, M.A., 1999. Site-directed mutagenesis of cytochrome c6 from Synechocystis sp. PCC 6803. The heme protein possesses a negatively charged area that may be isofunctional with the acidic patch of plastocyanin. J. Biol. Chem. 274, 13292–13297.

De La Rosa, M.A., Navarro, J.A., Díaz-Quintana, A., De La Cerda, B., Molina-Heredia, F.P., Balme, A., Murdoch, P.D.S., Díaz-Moreno, I., Durán, R. V., Hervás, M., 2002. An evolutionary analysis of the reaction mechanisms of photosystem I reduction by cytochrome c6 and plastocyanin. Bioelectrochemistry 55, 41–45.

De Mia, M., Lemaire, S.D., Choquet, Y., Wollmana, F.A., 2019. Nitric oxide remodels the photosynthetic apparatus upon S- starvation in Chlamydomonas reinhardtii. Plant Physiol. 179, 718–731.

Deák, Z., Sass, L., Kiss, É., Vass, I., 2014. Characterization of wave phenomena in the relaxation of flash-induced chlorophyll fluorescence yield in cyanobacteria. Biochim. Biophys. Acta - Bioenerg. 1837, 1522–1532.

Diner, B.A., Petrouleas, V., 1990. Formation by NO of nitrosyl adducts of redox components of the Photosystem II reaction center. II. Evidence that HCO-3/CO2 binds to the acceptor-side non-heme iron. BBA - Bioenerg. 1015, 141–149.

Duhamel, S., Van Wambeke, F., Lefevre, D., Benavides, M., Bonnet, S., 2018. Mixotrophic metabolism by natural communities of unicellular cyanobacteria in the western tropical South Pacific Ocean. Environ. Microbiol. 20, 2743–2756.

Durán, R. V., Hervás, M., De La Rosa, M.A., Navarro, J.A., 2004. The Efficient Functioning of Photosynthesis and Respiration in Synechocystis sp. PCC 6803 Strictly Requires the Presence of either Cytochrome c6 or Plastocyanin. J. Biol. Chem. 279, 7229–7233.

Eisenhut, M., Roell, M.S., Weber, A.P.M., 2019. Mechanistic understanding of photorespiration paves the way to a new green revolution. New Phytol. 223, 1762–1769.

Ermakova, M., Huokko, T., Richaud, P., Bersanini, L., Howe, C.J., Lea-Smith, D.J., Peltier, G., Allahverdiyeva, Y., 2016. Distinguishing the roles of thylakoid respiratory terminal oxidases in the cyanobacterium Synechocystis sp. PCC 6803. Plant Physiol. 171, 1307–1319.

Evans, J.R., 2013. Improving photosynthesis. Plant Physiol. 162, 1780–1793.

Farquhar, G.D., Caemmerer, S., Berry, J.A., 1980. A biochemical model of photosynthetic CO_2 assimilation in leaves of C_3 species. Planta 149, 78-90–90.

Finazzi, G., Furia, A., Barbagallo, R.P., Forti, G., 1999. State transitions, cyclic and linear electron transport and photophosphorylation in Chlamydomonas reinhardtii. Biochim. Biophys. Acta - Bioenerg. 1413, 117–129.

Fischer, W.W., Hemp, J., Johnson, J.E., 2016. Evolution of Oxygenic Photosynthesis. Annu. Rev. Earth Planet. Sci.

Folgosa, F., Martins, M.C., Teixeira, M., 2018. The multidomain flavodiiron protein from Clostridium difficile 630 is an NADH:oxygen oxidoreductase. Sci. Rep. 8, 10164.

Ford, P.C., Lorkovic, I.M., 2002. Mechanistic aspects of the reactions of nitric oxide with transition-metal complexes. Chem. Rev. 102, 993–1017.

Forte, E., Urbani, A., Saraste, M., Sarti, P., Brunori, M., Giuffrè, A., 2001. The cytochrome cbb3 from Pseudomonas stutzeri displays nitric oxide reductase activity. Eur. J. Biochem. 268, 6486–6491.

Foyer, C.H., Neukermans, J., Queval, G., Noctor, G., Harbinson, J., 2012. Photosynthetic control of electron transport and the regulation of gene expression. J. Exp. Bot.

Foyer, C.H., Ruban, A. V., Nixon, P.J., 2017. Photosynthesis solutions to enhance productivity. Philos. Trans. R. Soc. B Biol. Sci. 372.

Francisco, É.C., Franco, T.T., Wagner, R., Jacob-Lopes, E., 2014. Assessment of different carbohydrates as exogenous carbon source in cultivation of cyanobacteria. Bioprocess Biosyst. Eng. 37, 1497–1505.

García-Cañas, R., Giner-Lamia, J., Florencio, F.J., López-Maury, L., 2021. A protease-mediated mechanism regulates the cytochrome c6/plastocyanin switch in Synechocystis sp. PCC 6803. Proc. Natl. Acad. Sci. U. S. A. 118.

Gerotto, C., Alboresi, A., Meneghesso, A., Jokel, M., Suorsa, M., Aro, E.M., Morosinotto, T., 2016. Flavodiiron proteins act as safety valve for electrons in Physcomitrella patens. Proc. Natl. Acad. Sci. U. S. A. 113, 12322–12327.

Gomes, C.M., Giuffrè, A., Forte, E., Vicente, J.B., Saraiva, L.M., Brunori, M., Teixeira, M., 2002. A novel type of nitric-oxide reductase: Escherichia coli flavorubredoxin. J. Biol. Chem. 277, 25273–25276.

Gonçalves, V.L., Vicente, J.B., Saraiva, L.M., Teixeira, M., 2011. Bioenergetic Processes of Cyanobacteria. Bioenerg. Process. Cyanobacteria 631–653.

Goussias, C., Ioannidis, N., Petrouleas, V., 1997. Low-temperature nteractions of NO with the S1 and S2 states of the water-oxidizing complex of photosystem II. A novel Mn-multiline EPR signal derived from the S1 state. Biochemistry 36, 9261–9266.

Gupta, R., He, Z., Luan, S., 2002. Functional relationship of cytochrome c6 and plastocyanin in Arabidopsis. Nature 417, 567–571.

Haimovich-Dayan, M., Kahlon, S., Hihara, Y., Hagemann, M., Ogawa, T., Ohad, I., Lieman-Hurwitz, J., Kaplan, A., 2011. Cross-talk between photomixotrophic growth and CO2-concentrating mechanism in Synechocystis sp. strain PCC 6803. Environ. Microbiol. 13, 1767–1777.

Hart, S.E., Schlarb-Ridley, B.G., Bendall, D.S., Howe, C.J., 2005. Terminal oxidases of cyanobacteria. In: Biochemical Society Transactions. pp. 832–835.

Haury, J.F., Spiller, H., 1981. Fructose uptake and influence on growth of and nitrogen fixation by Anabaena variabilis. J. Bacteriol. 147, 227–235.

Hayashi, T., Caranto, J.D., Wampler, D.A., Kurtz, D.M., Moënne-Loccoz, P., 2010. Insights into the nitric oxide reductase mechanism of flavodiiron proteins from a flavin-free enzyme. Biochemistry 49, 7040–7049.

Helman, Y., Barkan, E., Eisenstadt, D., Luz, B., Kaplan, A., 2005. Fractionation of the three stable oxygen isotopes by oxygen-producing and oxygen-consuming reactions in photosynthetic organisms. Plant Physiol. 138, 2292–2298.

Helman, Y., Tchernov, D., Reinhold, L., Shibata, M., Ogawa, T., Schwarz, R., Ohad, I., Kaplan, A., 2003. Genes encoding A-type flavoproteins are essential for photoreduction of O2 in cyanobacteria. Curr. Biol. 13, 230–235.

Hervás, M., Navarro, J.A., Díaz, A., Bottin, H., De la Rosa, M.A., 1995. Laser-Flash Kinetic Analysis of the Fast Electron Transfer from Plastocyanin and Cytochrome ce to Photosystem I. Experimental Evidence on the Evolution of the Reaction Mechanism. Biochemistry 34, 11321–11326.

Hienerwadel, R., Berthomieu, C., 1995. Bicarbonate Binding to the Non-Heme Iron of Photosystem II Investigated by Fourier Transform Infrared Difference Spectroscopy and 13C-Labeled Bicarbonate. Biochemistry 34, 16288–16297.

Hihara, Y., Ikeuchi, M., 1997. Mutation in a novel gene required for photomixotrophic growth leads to enhanced photoautotrophic growth of Synechocystis sp. PCC 6803. Photosynth. Res. 53, 243–252.

Hihara, Y., Sonoike, K., Ikeuchi, M., 1998. A novel gene, pmgA, specifically regulates photosystem stoichiometry in the cyanobacterium Synechocystis species PCC 6803 in response to high light. Plant Physiol. 117, 1205–1216.

Hillmann, F., Riebe, O., Fischer, R.J., Mot, A., Caranto, J.D., Kurtz, D.M., Bahl, H., 2009. Reductive dioxygen scavenging by flavo-diiron proteins of Clostridium acetobutylicum. FEBS Lett. 583, 241–245.

Hippler, M., Drepper, F., Farah, J., Rochaix, J.D., 1997. Fast electron transfer from cytochrome c6 and plastocyanin to photosystem I of Chlamydomonas reinhardtii requires PsaF. Biochemistry 36, 6343–6349.

Hiraide, Y., Oshima, K., Fujisawa, T., Uesaka, K., Hirose, Y., Tsujimoto, R., Yamamoto, H., Okamoto, S., Nakamura, Y., Terauchi, K., Omata, T., Ihara, K., Hattori, M., Fujita, Y., 2015. Loss of cytochrome c M stimulates cyanobacterial heterotrophic growth in the dark. Plant Cell Physiol. 56, 334–345.

Howe, C.J., Nimmo, R.H., Barbrook, A.C., Bendall, D.S., 2016. Cytochrome c 6A of Chloroplasts. In: Cramer, W.A., Kallas, T. (Eds.), Cytochrome Complexes: Evolution, Structures, Energy Transduction, and Signaling. Springer, Dordrecht, pp. 701–712.

Howe, C.J., Schlarb-Ridley, B.G., Wastl, J., Purton, S., Bendall, D.S., 2006. The novel cytochrome c6 of chloroplasts: A case of evolutionary bricolage? J. Exp. Bot. 57, 13–22.

Huang, F., Parmryd, I., Nilsson, F., Persson, A.L., Pakrasi, H.B., Andersson, B., Norling, B., 2002. Proteomics of Synechocystis sp. strain PCC 6803: identification of plasma membrane proteins. Mol. Cell. Proteomics 1, 956–966.

Hutchison, C.A., Chuang, R.Y., Noskov, V.N., Assad-Garcia, N., Deerinck, T.J., Ellisman, M.H., Gill, J., Kannan, K., Karas, B.J., Ma, L., Pelletier, J.F., Qi, Z.Q., Richter, R.A., Strychalski, E.A., Sun, L., Suzuki, Y., Tsvetanova, B., Wise, K.S., Smith, H.O., Glass, J.I., Merryman, C., Gibson, D.G., Venter, J.C., 2016. Design and synthesis of a minimal bacterial genome. Science (80-.). 351.

Ittekkot, V., Brockmann, U., Michaelis, W., Degens, E., 1981. Dissolved Free and Combined Carbohydrates During a Phytoplankton Bloom in the Northern North Sea. Mar. Ecol. Prog. Ser. 4, 299–305.

Iwata, S., Ostermeier, C., Ludwig, B., Michel, H., 1995. Structure at 2.8 Å resolution of cytochrome c oxidase from paracoccus denitrificans. Nature 376, 660–669.

Jansén, T., Kurian, D., Raksajit, W., York, S., Summers, M.L., Mäenpää, P., 2010. Characterization of trophic changes and a functional oxidative pentose phosphate pathway in Synechocystis sp. PCC 6803. Acta Physiol. Plant. 32, 511–518.

Jiang, L., 2020. Commercialization of the gene-edited crop and morality: challenges from the liberal patent law and the strict GMO law in the EU. New Genet. Soc. 39, 191–218.

Jokel, M., Johnson, X., Peltier, G., Aro, E.M., Allahverdiyeva, Y., 2018. Hunting the main player enabling Chlamydomonas reinhardtii growth under fluctuating light. Plant J. 94, 822–835.

Jokel, M., Nagy, V., Tóth, S.Z., Kosourov, S., Allahverdiyeva, Y., 2019. Elimination of the flavodiiron electron sink facilitates long-term H2 photoproduction in green algae. Biotechnol. Biofuels 12, 280.

Joshua, S., Mullineaux, C.W., 2004. Phycobilisome diffusion is required for light-state transitions in cyanobacteria. Plant Physiol. 135, 2112–2119.

Kämäräinen, J., Huokko, T., Kreula, S., Jones, P.R., Aro, E.-M., Kallio, P., 2016. Pyridine nucleotide transhydrogenase PntAB is essential for optimal growth and photosynthetic integrity under low-light mixotrophic conditions in Synechocystis sp. PCC 6803. New Phytol. 194–204.

Kaneko, T., Sato, S., Kotani, H., Tanaka, A., Asamizu, E., Nakamura, Y., Miyajima, N., Hirosawa, M., Sugiura, M., Sasamoto, S., Kimura, T., Hosouchi, T., Matsuno, A., Muraki, A., Nakazaki, N., Naruo, K., Okumura, S., Shimpo, S., Takeuchi, C., Wada, T., Watanabe, A., Yamada, M., Yasuda, M., Tabata, S., 1996. Sequence analysis of the genome of the unicellular cyanobacterium synechocystis sp. strain PCC6803. II. Sequence determination of the entire genome and assignment of potential protein-coding regions. DNA Res. 3, 109–136.

Kang, R., Wang, J., Shi, D., Cong, W., Cai, Z., Ouyang, F., 2004. Interactions between organic and inorganic carbon sources during mixotrophic cultivation of Synechococcus sp. Biotechnol. Lett. 26, 1429–1432.

Kanno, M., Atsumi, S., 2017. Engineering an Obligate photoautotrophic cyanobacterium to utilize glycerol for growth and chemical production. ACS Synth. Biol. 6, 69–75.

Kanno, M., Carroll, A.L., Atsumi, S., 2017. Global metabolic rewiring for improved CO2 fixation and chemical production in cyanobacteria. Nat. Commun. 8, 1–11.

Kaplan, A., Reinhold, L., 1999. CO2 concentrating mechanisms in photosynthetic microorganisms. Annu. Rev. Plant Biol. 50, 539–570.

Keeling, P.J., 2010. The endosymbiotic origin, diversification and fate of plastids. Philos. Trans. R. Soc. B Biol. Sci.

Kerfeld, C.A., Krogmann, D.W., 1998. PHOTOSYNTHETIC CYTOCHROMES c IN CYANOBACTERIA, ALGAE, AND PLANTS. Annu. Rev. Plant Physiol. Plant Mol. Biol. 49, 397–425.

Kerfeld, C.A., Melnicki, M.R., 2016. Assembly, function and evolution of cyanobacterial carboxysomes. Curr. Opin. Plant Biol.

Kerfeld, C.A., Melnicki, M.R., Sutter, M., Dominguez-Martin, M.A., 2017. Structure, function and evolution of the cyanobacterial orange carotenoid protein and its homologs. New Phytol. 215, 937–951.

Khetkorn, W., Incharoensakdi, A., Lindblad, P., Jantaro, S., 2016. Enhancement of poly-3-hydroxybutyrate production in Synechocystis sp. PCC 6803 by overexpression of its native biosynthetic genes. Bioresour. Technol. 214, 761–768.

Khorobrykh, S., Havurinne, V., Mattila, H., Tyystjärvi, E., 2020. Oxygen and ROS in photosynthesis. Plants.

Kirilovsky, D., Kaňa, R., Prášil, O., 2014. Mechanisms Modulating Energy Arriving at Reaction Centers in Cyanobacteria. Springer, Dordrecht, pp. 471–501.

Klughammer, C., Schreiber, U., 2008a. Saturation Pulse method for assessment of energy conversion in PS I. PAM Appl. Notes 1, 11–14.

Klughammer, C., Schreiber, U., 2008b. Complementary PS II quantum yields calculated from simple fluorescence parameters measured by PAM fluorometry and the Saturation Pulse method. PAM Appl. Notes 1, 27–35.

Knoop, H., Gründel, M., Zilliges, Y., Lehmann, R., Hoffmann, S., Lockau, W., Steuer, R., 2013. Flux balance analysis of cyanobacterial metabolism: the metabolic network of Synechocystis sp. PCC 6803. PLoS Comput. Biol. 9, e1003081.

Koepke, J., Olkhova, E., Angerer, H., Müller, H., Peng, G., Michel, H., 2009. High resolution crystal structure of Paracoccus denitrificans cytochrome c oxidase: New insights into the active site and the proton transfer pathways. Biochim. Biophys. Acta - Bioenerg. 1787, 635–645.

Kolbert, Z., Barroso, J.B., Brouquisse, R., Corpas, F.J., Gupta, K.J., Lindermayr, C., Loake, G.J., Palma, J.M., Petřivalský, M., Wendehenne, D., Hancock, J.T., 2019. A forty year journey: The generation and roles of NO in plants. Nitric Oxide - Biol. Chem.

Köninger, K., Gómez Baraibar, Á., Mügge, C., Paul, C.E., Hollmann, F., Nowaczyk, M.M., Kourist, R., 2016. Recombinant Cyanobacteria for the Asymmetric Reduction of C=C Bonds Fueled by the Biocatalytic Oxidation of Water. Angew. Chemie - Int. Ed. 55, 5582–5585.

Kosourov, S., Böhm, M., Senger, M., Berggren, G., Stensjö, K., Mamedov, F., Lindblad, P., Allahverdiyeva, Y., 2021. Photosynthetic hydrogen production: Novel protocols, promising engineering approaches and application of semi-synthetic hydrogenases. Physiol. Plant.

Kosourov, S., Nagy, V., Shevela, D., Jokel, M., Messinger, J., Allahverdiyeva, Y., 2020. Water oxidation by photosystem II is the primary source of electrons for sustained H 2 photoproduction in nutrient-replete green algae. Proc. Natl. Acad. Sci. 117, 202009210.

Kozuleva, M.A., Ivanov, B.N., 2010. Evaluation of the participation of ferredoxin in oxygen reduction in the photosynthetic electron transport chain of isolated pea thylakoids. Photosynth. Res. 105, 51–61.

Kozuleva, M.A., Ivanov, B.N., Vetoshkina, D. V., Borisova-Mubarakshina, M.M., 2020. Minimizing an Electron Flow to Molecular Oxygen in Photosynthetic Electron Transfer Chain: An Evolutionary View. Front. Plant Sci. 11, 211.

Kramer, D.M., Avenson, T.J., Edwards, G.E., 2004. Dynamic flexibility in the light reactions of photosynthesis governed by both electron and proton transfer reactions. Trends Plant Sci. 9, 349–357.

Kramer, D.M., Cruz, J.A., Kanazawa, A., 2003. Balancing the central roles of the thylakoid proton gradient. Trends Plant Sci. 8, 27–32.

Kranzler, C., Lis, H., Finkel, O.M., Schmetterer, G., Shaked, Y., Keren, N., 2014. Coordinated transporter activity shapes high-affinity iron acquisition in cyanobacteria. ISME J. 8, 409–417.

Krieger, A., Rutherford, A.W., Johnson, G.N., 1995. On the determination of redox midpoint potential of the primary quinone electron acceptor, QA, in Photosystem II. BBA - Bioenerg. 1229, 193–201.

Krishna, P.S., Styring, S., Mamedov, F., 2019. Photosystem ratio imbalance promotes direct sustainable H2 production in: Chlamydomonas reinhardtii. Green Chem. 21, 4683–4690.

Lamotte, O., Bertoldo, J.B., Besson-Bard, A., Rosnoblet, C., AimÃ©, S., Hichami, S., Terenzi, H., Wendehenne, D., 2015. Protein S-nitrosylation: specificity and identification strategies in plants. Front. Chem. 2, 114.

Laurens, L.M.L., Markham, J., Templeton, D.W., Christensen, E.D., Van Wychen, S., Vadelius, E.W., Chen-Glasser, M., Dong, T., Davis, R., Pienkos, P.T., 2017. Development of algae biorefinery concepts for biofuels and bioproducts; a perspective on process-compatible products and their impact on cost-reduction. Energy Environ. Sci. 10, 1716–1738.

Lea-Smith, D.J., Bombelli, P., Vasudevan, R., Howe, C.J., 2016a. Photosynthetic, respiratory and extracellular electron transport pathways in cyanobacteria. Biochim. Biophys. Acta - Bioenerg. 1857, 247–255.

Lea-Smith, D.J., Ross, N., Zori, M., Bendall, D.S., Dennis, J.S., Scott, S.A., Smith, A.G., Howe, C.J., 2013. Thylakoid terminal oxidases are essential for the cyanobacterium Synechocystis sp. PCC 6803 to survive rapidly changing light intensities. Plant Physiol. 162, 484–495.

Lea-Smith, D.J., Vasudevan, R., Howe, C.J., 2016b. Generation of marked and markerless mutants in model cyanobacterial species. J. Vis. Exp. 2016.

Lee, S., Ryu, J.Y., Soo, Y.K., Jeon, J.H., Ji, Y.S., Cho, H.T., Choi, S.B., Choi, D., De Marsac, N.T., Park, Y. Il, 2007. Transcriptional regulation of the respiratory genes in the cyanobacterium Synechocystis sp. PCC 6803 during the early response to glucose feeding. Plant Physiol. 145, 1018–1030.

Lee, T.C., Xiong, W., Paddock, T., Carrieri, D., Chang, I.F., Chiu, H.F., Ungerer, J., Hank Juo, S.H., Maness, P.C., Yu, J., 2015. Engineered xylose utilization enhances bio-products productivity in the cyanobacterium Synechocystis sp. PCC 6803. Metab. Eng. 30, 179–189.

Li, C., Zhang, R., Wang, J., Wilson, L.M., Yan, Y., 2020. Protein Engineering for Improving and Diversifying Natural Product Biosynthesis. Trends Biotechnol.

Lindermayr, C., Saalbach, G., Durner, J., 2005. Proteomic identification of S-nitrosylated proteins in arabidopsis. Plant Physiol. 137, 921–930.

Loll, B., Kern, J., Saenger, W., Zouni, A., Biesiadka, J., 2005. Towards complete cofactor arrangement in the 3.0 Å resolution structure of photosystem II. Nature 438, 1040–1044.

Lyons, J.A., Aragão, D., Slattery, O., Pisliakov, A. V., Soulimane, T., Caffrey, M., 2012. Structural insights into electron transfer in caa 3-type cytochrome oxidase. Nature 487, 514–518.

Makowka, A., Nichelmann, L., Schulze, D., Spengler, K., Wittmann, C., Forchhammer, K., Gutekunst, K., 2020. Glycolytic Shunts Replenish the Calvin–Benson–Bassham Cycle as Anaplerotic Reactions in Cyanobacteria. Mol. Plant 13, 471–482.

Malakhov, M.P., Malakhova, O.A., Murata, N., 1999. Balanced regulation of expression of the gene for cytochrome c(M) and that of genes for plastocyanin and cytochrome c6 in Synechocystis. FEBS Lett. 444, 281–284.

Malakhov, M.P., Wada, H., Los, D.A., Semenenko, V.E., Murata, N., 1994. A New Type of Cytochrome c from Synechocystis PCC6803. J. Plant Physiol. 144, 259–264.

Mallén-Ponce, M.J., Huertas, M.J., Sánchez-Riego, A.M., Florencio, F.J., 2021. Depletion of m -type thioredoxin impairs photosynthesis, carbon fixation, and oxidative stress in cyanobacteria . Plant Physiol.

Mallick, N., Rai, L.C., Mohn, F.H., Soeder, C.J., 1999. Studies on nitric oxide (NO) formation by the green alga Scenedesmus obliquus and the diazotrophic cyanobacterium Anabaena doliolum. Chemosphere 39, 1601–1610.

Malone, L.A., Proctor, M.S., Hitchcock, A., Hunter, C.N., Johnson, M.P., 2021. Cytochrome b6f – Orchestrator of photosynthetic electron transfer. Biochim. Biophys. Acta - Bioenerg.

Manna, P., Vermaas, W., 1997. Lumenal proteins involved in respiratory electron transport in the cyanobacterium Synechocystis sp. PCC6803. Plant Mol. Biol. 35, 407–416.

Marcaida, M.J., Schlarb-Ridley, B.G., Worrall, J.A.R., Wastl, J., Evans, T.J., Bendall, D.S., Luisi, B.F., Howe, C.J., 2006. Structure of Cytochrome c6A, a Novel Dithio-cytochrome of Arabidopsis thaliana, and its Reactivity with Plastocyanin: Implications for Function. J. Mol. Biol. 360, 968–977.

Margulis, K., Zer, H., Lis, H., Schoffman, H., Murik, O., Shimakawa, G., Krieger-Liszkay, A., Keren, N., 2020. Over Expression of the Cyanobacterial Pgr5-Homologue Leads to Pseudoreversion in a Gene Coding for a Putative Esterase in Synechocystis 6803. Life 10, 174.

Markets and Markets, 2018. Algae products market by type (lipids, carrageenan, carotenoids, alginate, and algal protein), application (food & beverages, nutraceuticals & dietary supplements, personal care, feed and pharmaceuticals), source, form and region – Global forecast to 2023.

Marquez, F.J., Sasaki, K., Kakizono, T., Nishio, N., Nagai, S., 1993. Growth characteristics of Spirulina platensis in mixotrophic and heterotrophic conditions. J. Ferment. Bioeng. 76, 408–410.

Matson, M.M., Atsumi, S., 2018. Photomixotrophic chemical production in cyanobacteria. Curr. Opin. Biotechnol. 50, 65–71.

McConnell, M.D., Koop, R., Vasil'ev, S., Bruce, D., 2002. Regulation of the distribution of chlorophyll and phycobilin-absorbed excitation energy in cyanobacteria. A structure-based model for the light state transition. Plant Physiol. 130, 1201–1212.

Melis, A., 2009. Solar energy conversion efficiencies in photosynthesis: Minimizing the chlorophyll antennae to maximize efficiency. Plant Sci. 177, 272–280.

Meyer, Y., Belin, C., Delorme-Hinoux, V., Reichheld, J.P., Riondet, C., 2012. Thioredoxin and glutaredoxin systems in plants: Molecular mechanisms, crosstalks, and functional significance. Antioxidants Redox Signal. 17, 1124–1160.

Miller, N.T., Vaughn, M.D., Burnap, R.L., 2021. Electron flow through NDH-1 complexes is the major driver of cyclic electron flow-dependent proton pumping in cyanobacteria. Biochim. Biophys. Acta - Bioenerg. 1862, 148354.

Mills, L.A., McCormick, A.J., Lea-Smith, D.J., 2020. Current knowledge and recent advances in understanding metabolism of the model cyanobacterium Synechocystis sp. PCC 6803. Biosci. Rep. 40.

Molina-Heredia, F.P., Balme, A., Hervás, M., Navarro, J.A., De la Rosa, M.A., 2002. A comparative structural and functional analysis of cytochrome cM, cytochrome c6 and plastocyanin from the cyanobacterium Synechocystis sp. PCC 6803. FEBS Lett. 517, 50–54.

Molina-Heredia, F.P., Hervás, M., Navarro, J.A., De La Rosa, M.A., 1998. Cloning and correct expression in Escherichia coli of the petE and petJ genes respectively encoding plastocyanin and cytochrome c6 from the cyanobacterium Anabaena sp. PCC 7119. Biochem. Biophys. Res. Commun. 243, 302–306.

Molina-Heredia, F.P., Wastl, J., Navarro, J.A., Bendall, D.S., Hervás, M., Howe, C.J., De la Rosa, M.A., 2003. A new function for an old cytochrome? Nature 424, 33–34.

Moore, L.R., 2013. More mixotrophy in the marine microbial mix. Proc. Natl. Acad. Sci. U. S. A. 110, 8323–8324.

Morisse, S., Zaffagnini, M., Gao, X.H., Lemaire, S.D., Marchand, C.H., 2014. Insight into protein S-nitrosylation in Chlamydomonas reinhardtii. Antioxid. Redox Signal. 21, 1271–1284.

Mosebach, L., Heilmann, C., Mutoh, R., Gäbelein, P., Steinbeck, J., Happe, T., Ikegami, T., Hanke, G., Kurisu, G., Hippler, M., 2017. Association of Ferredoxin:NADP+ oxidoreductase with the photosynthetic apparatus modulates electron transfer in Chlamydomonas reinhardtii. Photosynth. Res. 134, 291–306.

Mulkidjanian, A.Y., 2007. Proton translocation by the cytochrome bc1 complexes of phototrophic bacteria: Introducing the activated Q-cycle. Photochem. Photobiol. Sci. 6, 19–34.

Mullineaux, C.W., 2014. Co-existence of photosynthetic and respiratory activities in cyanobacterial thylakoid membranes. Biochim. Biophys. Acta - Bioenerg. 1837, 503–511.

Mullineaux, C.W., Allen, J.F., 1990. State 1-State 2 transitions in the cyanobacterium Synechococcus 6301 are controlled by the redox state of electron carriers between Photosystems I and II. Photosynth. Res. 23, 297–311.

Mullineaux, C.W., Tobin, M.J., Jones, G.R., 1997. Mobility of photosynthetic complexes in thylakoid membranes. Nature 390, 421–424.

Muñoz-Marín, M.C., Gómez-Baena, G., López-Lozano, A., Moreno-Cabezuelo, J.A., Díez, J., García-Fernández, J.M., 2020. Mixotrophy in marine picocyanobacteria: use of organic compounds by Prochlorococcus and Synechococcus. ISME J. 14, 1065–1073.

Murchie, E.H., Niyogi, K.K., 2011. Manipulation of photoprotection to improve plant photosynthesis. Plant Physiol. 155, 86–92.

Mustila, H., Paananen, P., Battchikova, N., Santana-Sánchez, A., Muth-Pawlak, D., Hagemann, M., Aro, E.-M., Allahverdiyeva, Y., 2016. The Flavodiiron Protein Flv3 Functions as a Homo-Oligomer During Stress Acclimation and is Distinct from the Flv1/Flv3 Hetero-Oligomer Specific to the O2 Photoreduction Pathway. Plant Cell Physiol. 57, 1468–1483.

Muzzopappa, F., Kirilovsky, D., 2020. Changing Color for Photoprotection: The Orange Carotenoid Protein. Trends Plant Sci. 25, 92–104.

Nakajima, T., Kajihata, S., Yoshikawa, K., Matsuda, F., Furusawa, C., Hirasawa, T., Shimizu, H., 2014. Integrated metabolic flux and omics analysis of Synechocystis sp. PCC 6803 under mixotrophic and photoheterotrophic conditions. Plant Cell Physiol. 55, 1606–1612.

Nieva, M., Valiente, E.F., 1996. Inorganic carbon transport and fixation in cells of Anabaena variabilis adapted to mixotrophic conditions. Plant Cell Physiol. 37, 1–7.

Nikkanen, L., Santana Sánchez, A., Ermakova, M., Rögner, M., Cournac, L., Allahverdiyeva, Y., 2020. Functional redundancy between flavodiiron proteins and NDH-1 in Synechocystis sp. PCC 6803. Plant J. 103, 1460–1476.

Nishijima, Y., Kanesaki, Y., Yoshikawa, H., Ogawa, T., Sonoike, K., Nishiyama, Y., Hihara, Y., 2015. Analysis of spontaneous suppressor mutants from the photomixotrophically grown pmgA-disrupted mutant in the cyanobacterium Synechocystis sp. PCC 6803. Photosynth. Res. 126, 465–475.

Ogawa, T., 1991. A gene homologous to the subunit-2 gene of NADH dehydrogenase is essential to inorganic carbon transport of Synechocystis PCC6803. Proc. Natl. Acad. Sci. U. S. A. 88, 4275–4279.

Ogawa, T., Aiba, S., 1981. Bioenergetic analysis of mixotrophic growth in Chlorella vulgaris and Scenedesmus acutus. Biotechnol. Bioeng. 23, 1121–1132.

Okayama, S., 1976. Redox potential of plastoquinone A in spinach chloroplasts. BBA - Bioenerg. 440, 331–336.

Olive, J., Ajlani, G., Astier, C., Recouvreur, M., Vernotte, C., 1997. Ultrastructure and light adaptation of phycobilisome mutants of synechocystis PCC 6803. Biochim. Biophys. Acta - Bioenerg. 1319, 275–282.

Ördög, A., Wodala, B., Rózsavölgyi, T., Tari, I., Horváth, F., 2013. Regulation of guard cell photosynthetic electron transport by nitric oxide. J. Exp. Bot. 64, 1357–1366.

Ort, D.R., Merchant, S.S., Alric, J., Barkan, A., Blankenship, R.E., Bock, R., Croce, R., Hanson, M.R., Hibberd, J.M., Long, S.P., Moore, T.A., Moroney, J., Niyogi, K.K., Parry, M.A.J., Peralta-Yahya, P.P., Prince, R.C., Redding, K.E., Spalding, M.H., Van Wijk, K.J., Vermaas, W.F.J., Von Caemmerer, S., Weber, A.P.M., Yeates, T.O., Yuan, J.S., Zhu, X.G., 2015. Redesigning photosynthesis to sustainably meet global food and bioenergy demand. Proc. Natl. Acad. Sci. U. S. A. 112, 8529–8536.

Patel, A.K., Singhania, R.R., Sim, S.J., Dong, C. Di, 2021. Recent advancements in mixotrophic bioprocessing for production of high value microalgal products. Bioresour. Technol. 320, 124421.

Peltier, G., Tolleter, D., Billon, E., Cournac, L., 2010. Auxiliary electron transport pathways in chloroplasts of microalgae. Photosynth. Res. 106, 19–31.

Perez-Garcia, O., Bashan, Y., Bashan, Y., Bashan, Y., 2015. Microalgal heterotrophic and mixotrophic culturing for bio-refining: From metabolic routes to techno-economics. Algal Biorefineries Vol. 2 Prod. Refin. Des. 61–131.

Perkins, D.N., Pappin, D.J.C., Creasy, D.M., Cottrell, J.S., 1999. Probability-based protein identification by searching sequence databases using mass spectrometry data. Electrophoresis 20, 3551–3567.

Peters, J.W., Schut, G.J., Boyd, E.S., Mulder, D.W., Shepard, E.M., Broderick, J.B., King, P.W., Adams, M.W.W., 2015. [FeFe]- and [NiFe]-hydrogenase diversity, mechanism, and maturation. Biochim. Biophys. Acta - Mol. Cell Res. 1853, 1350–1369.

Petrouleas, V., Diner, B.A., 1990. Formation by NO of nitrosyl adducts of redox components of the Photosystem II reaction center. I. NO binds to the acceptor-side non-heme iron. BBA - Bioenerg. 1015, 131–140.

Pils, D., Gregor, W., Schmetterer, G., 1997. Evidence for in vivo activity of three distinct respiratory terminal oxidases in the cyanobacterium Synechocystis sp. strain PCC6803. FEMS Microbiol. Lett. 152, 83–88.

Pils, D., Schmetterer, G., 2001. Characterization of three bioenergetically active respiratory terminal oxidases in the cyanobacterium Synechocystis sp. strain PCC 6803. FEMS Microbiol. Lett. 203, 217–222.

Planchet, E., Gupta, K.J., Sonoda, M., Kaiser, W.M., 2005. Nitric oxide emission from tobacco leaves and cell suspensions: Rate limiting factors and evidence for the involvement of mitochondrial electron transport. Plant J. 41, 732–743.

Radakovits, R., Jinkerson, R.E., Darzins, A., Posewitz, M.C., 2010. Genetic engineering of algae for enhanced biofuel production. Eukaryot. Cell 9, 486–501.

Ranade, S., Zhang, Y., Kaplan, M., Majeed, W., He, Q., 2015. Metabolic engineering and comparative performance studies of Synechocystis sp. PCC 6803 strains for effective utilization of xylose. Front. Microbiol. 6, 1484.

Ranjbar Choubeh, R., Wientjes, E., Struik, P.C., Kirilovsky, D., van Amerongen, H., 2018. State transitions in the cyanobacterium Synechococcus elongatus 7942 involve reversible quenching of the photosystem II core. Biochim. Biophys. Acta - Bioenerg. 1859, 1059–1066.

Rexroth, S., Nowaczyk, M.M., Rögner, M., 2017. Cyanobacterial photosynthesis: The light reactions. In: Modern Topics in the Phototrophic Prokaryotes: Metabolism, Bioenergetics, and Omics. Springer International Publishing, pp. 163–191.

Reyes-Sosa, F.M., Gil-Martínez, J., Molina-Heredia, F.P., 2011. Cytochrome c 6-like protein as a putative donor of electrons to photosystem I in the cyanobacterium Nostoc sp. PCC 7119. Photosynth. Res. 110, 61–72.

Reyes, J.C., Chavez, S., Muro-Pastor, M.I., Candau, P., Florencio, F.J., 1993. Effect of glucose utilization on nitrite excretion by the unicellular cyanobacterium Synechocystis sp. strain PCC 6803. Appl. Environ. Microbiol. 59, 3161–3163.

Rippka, R., 1972. Photoheterotrophy and chemoheterotrophy among unicellular blue-green algae. Arch. Mikrobiol. 87, 93–98.

Rippka, R., Deruelles, J., Waterbury, J.B., Herdman, M., Stanier, R.Y., 1979. Generic Assignments, Strain Histories and Properties of Pure Cultures of Cyanobacteria. J. Gen. Microbiol. 111, 1–61.

Roberts, A.G., Kramer, D.M., 2001. Inhibitor “double occupancy” in the Qo pocket of the chloroplast cytochrome b6f complex. Biochemistry 40, 13407–13412.

Romão, C. V., Vicente, J.B., Borges, P.T., Frazão, C., Teixeira, M., 2016. The dual function of flavodiiron proteins: Oxygen and/or nitric oxide reductases. J. Biol. Inorg. Chem. 21, 39–52.

Ruiz, J., Olivieri, G., De Vree, J., Bosma, R., Willems, P., Reith, J.H., Eppink, M.H.M., Kleinegris, D.M.M., Wijffels, R.H., Barbosa, M.J., 2016. Towards industrial products from microalgae. Energy Environ. Sci. 9, 3036–3043.

Safarian, S., Hahn, A., Mills, D.J., Radloff, M., Eisinger, M.L., Nikolaev, A., Meier-Credo, J., Melin, F., Miyoshi, H., Gennis, R.B., Sakamoto, J., Langer, J.D., Hellwig, P., Kühlbrandt, W., Michel, H., 2019. Active site rearrangement and structural divergence in prokaryotic respiratory oxidases. Science (80-.). 366, 100–104.

Safarian, S., Rajendran, C., Müller, H., Preu, J., Langer, J.D., Ovchinnikov, S., Hirose, T., Kusumoto, T., Sakamoto, J., Michel, H., 2016. Structure of a bd oxidase indicates similar mechanisms for membraneintegrated oxygen reductases. Science (80-.). 352, 583–586.

Sakihama, Y., Nakamura, S., Yamasaki, H., 2002. Nitric oxide production mediated by nitrate reductase in the green alga Chlamydomonas reinhardtii: An alternative NO production pathway in photosynthetic organisms. Plant Cell Physiol. 43, 290–297.

Sakuragi, Y., Maeda, H., DellaPenna, D., Bryant, D.A., 2006. α-Tocopherol plays a role in photosynthesis and macronutrient homeostasis of the cyanobacterium Synechocystis sp. PCC 6803 that is independent of its antioxidant function. Plant Physiol. 141, 508–521.

Santana-Sanchez, A., Solymosi, D., Mustila, H., Bersanini, L., Aro, E.-M., Allahverdiyeva, Y., 2019. Flavodiiron proteins 1–to-4 function in versatile combinations in O2 photoreduction in cyanobacteria. Elife 8, 1–22.

Santos-Merino, M., Singh, A.K., Ducat, D.C., 2019. New applications of synthetic biology tools for cyanobacterial metabolic engineering. Front. Bioeng. Biotechnol.

Santos-Merino, M., Torrado, A., Davis, G.A., Rottig, A., Bibby, T.S., Kramer, D.M., Ducat, D.C., 2021. Improved photosynthetic capacity and photosystem I oxidation via heterologous metabolism engineering in cyanobacteria. Proc. Natl. Acad. Sci. U. S. A. 118, 2021.

Sanz-Luque, E., Chamizo-Ampudia, A., Llamas, A., Galvan, A., Fernandez, E., 2015a. Understanding nitrate assimilation and its regulation in microalgae. Front. Plant Sci.

Sanz-Luque, E., Ocaña-Calahorro, F., De Montaigu, A., Chamizo-Ampudia, A., Llamas, Á., Galván, A., Fernández, E., 2015b. THB1, a truncated hemoglobin, modulates nitric oxide levels and nitrate reductase activity. Plant J. 81, 467–479.

Sarrou, J., Isgandarova, S., Kern, J., Zouni, A., Renger, G., Lubitz, W., Messinger, J., 2003. Nitric oxide-induced formation of the S-2 state in the oxygen-evolving complex of photosystem II from Synechococcus elongatus. Biochemistry 42, 1016–1023.

Schansker, G., Goussias, C., Petrouleas, V., William Rutherford, A., 2002. Reduction of the Mn cluster of the water-oxidizing enzyme by nitric oxide: Formation of an S-2 state. Biochemistry 41, 3057–3064.

Schirrmeister, B.E., Gugger, M., Donoghue, P.C.J., 2015. Cyanobacteria and the Great Oxidation Event: Evidence from genes and fossils. Palaeontology 58, 769–785.

Schneegurt, M.A., Sherman, D.M., Sherman, L.A., 1997. Growth, physiology, and ultrastructure of a diazotrophic cyanobacterium, Cyanothece sp. strain ATCC 51142, in mixotrophic and chemoheterotrophic cultures. J. Phycol. 33, 632–642.

Schultze, M., Forberich, B., Rexroth, S., Dyczmons, N.G., Roegner, M., Appel, J., 2009. Localization of cytochrome b6f complexes implies an incomplete respiratory chain in cytoplasmic membranes of the cyanobacterium Synechocystis sp. PCC 6803. Biochim. Biophys. Acta - Bioenerg. 1787, 1479–1485.

Scott, N.L., Falzone, C.J., Vuletich, D.A., Zhao, J., Bryant, D.A., Lecomte, J.T.J., 2002. Truncated hemoglobin from the cyanobacterium Synechococcus sp. PCC 7002: Evidence for hexacoordination and covalent adduct formation in the ferric recombinant protein. Biochemistry 41, 6902–6910.

Scott, N.L., Lecomte, J.T.J., 2008. Cloning, expression, purification, and preliminary characterization of a putative hemoglobin from the cyanobacterium synechocystis sp. PCC 6803. Protein Sci. 9, 587–597.

Selão, T.T., Jebarani, J., Ismail, N.A., Norling, B., Nixon, P.J., 2020. Enhanced Production of D-Lactate in Cyanobacteria by Re-Routing Photosynthetic Cyclic and Pseudo-Cyclic Electron Flow. Front. Plant Sci. 10, 1700.

Sétif, P., Shimakawa, G., Krieger-Liszkay, A., Miyake, C., 2020. Identification of the electron donor to flavodiiron proteins in Synechocystis sp. PCC 6803 by in vivo spectroscopy. Biochim. Biophys. Acta - Bioenerg. 1861, 148256.

Sgobba, E., Wendisch, V.F., 2020. Synthetic microbial consortia for small molecule production. Curr. Opin. Biotechnol. 62, 72–79.

Shen, J.R., Inoue, Y., 1993. Binding and Functional Properties of Two New Extrinsic Components, Cytochrome c-550 and a 12-kDa Protein, in Cyanobacterial Photosystem II. Biochemistry 32, 1825–1832.

Shen, J.R., Qian, M., Inoue, Y., Burnap, R.L., 1998. Functional characterization of Synechocystis sp. PCC 6803 δpsbU and δpsbV mutants reveals important roles of cytochrome c-550 in cyanobacterial oxygen evolution. Biochemistry 37, 1551–1558.

Shevela, D., Do, H.N., Fantuzzi, A., Rutherford, A.W., Messinger, J., 2020. Bicarbonate-Mediated CO2Formation on Both Sides of Photosystem II. Biochemistry 59, 2442–2449.

Shimakawa, G., Ishizaki, K., Tsukamoto, S., Tanaka, M., Sejima, T., Miyake, C., 2017. The liverwort, Marchantia, drives alternative electron flow using a flavodiiron protein to protect PSI. Plant Physiol. 173, 1636–1647.

Shinde, S., Zhang, X., Singapuri, S.P., Kalra, I., Liu, X., Morgan-Kiss, R.M., Wang, X., 2020. Glycogen metabolism supports photosynthesis start through the oxidative pentose phosphate pathway in cyanobacteria. Plant Physiol. 182, 507–517.

Shpilyov, A. V., Zinchenko, V. V., Shestakov, S. V., Grimm, B., Lokstein, H., 2005. Inactivation of the geranylgeranyl reductase (ChlP) gene in the cyanobacterium Synechocystis sp. PCC 6803. Biochim. Biophys. Acta - Bioenerg. 1706, 195–203.

Silaghi-Dumitrescu, R., Coulter, E.D., Das, A., Ljungdahl, L.G., Jameson, G.N.L., Huynh, B.H., Kurtz, D.M., 2003. A flavodiiron protein and high molecular weight rubredoxin from Moorella thermoacetica with nitric oxide reductase activity. Biochemistry 42, 2806–2815.

Sim, S.J., Joun, J., Hong, M.E., Patel, A.K., 2019. Split mixotrophy: A novel cultivation strategy to enhance the mixotrophic biomass and lipid yields of Chlorella protothecoides. Bioresour. Technol. 291, 121820.

Sipka, G., Magyar, M., Mezzetti, A., Akhtar, P., Zhu, Q., Xiao, Y., Han, G., Santabarbara, S., Shen, J.-R., Lambrev, P.H., Garab, G., 2021. Light-adapted charge-separated state of photosystem II: structural and functional dynamics of the closed reaction center. Plant Cell.

Slater, B., Kosmützky, D., Nisbet, R.E.R., Howe, C.J., 2021. The evolution of the cytochrome c 6 family of photosynthetic electron transfer proteins . Genome Biol. Evol.

Smith, A.J., 1983. Modes of cyanobacterial carbon metabolism. Ann. l'Institut Pasteur Microbiol. 134, 93–113.

Solymosi, D., Nikkanen, L., Muth-Pawlak, D., Fitzpatrick, D., Vasudevan, R., Howe, C.J., Lea-Smith, D.J., Allahverdiyeva, Y., 2020. Cytochrome CMdecreases photosynthesis under photomixotrophy in synechocystis sp. PCC 6803. Plant Physiol. 183, 700–716.

Sonoda, M., Kitano, K., Katoh, A., Katoh, H., Ohkawa, H., Ogawa, T., 1997. Size of cotA and identification of the gene product in Synechocystis sp. strain PCC6803. J. Bacteriol. 179, 3845–3850.

South, P.F., Cavanagh, A.P., Liu, H.W., Ort, D.R., 2019. Synthetic glycolate metabolism pathways stimulate crop growth and productivity in the field. Science (80-.). 363.

Stal, L.J., Moezelaar, R., 1997. Fermentation in cyanobacteria. FEMS Microbiol. Rev. 21, 179–211.

Stanier, R.Y., Cohen-Bazire, G., 1977. Phototrophic prokaryotes: the cyanobacteria. Annu. Rev. Microbiol. 31, 225–274.

Stebegg, R., Wurzinger, B., Mikulic, M., Schmetterer, G., 2012. Chemoheterotrophic growth of the cyanobacterium anabaena sp. strain PCC 7120 dependent on a functional cytochrome c oxidase. J. Bacteriol. 194, 4601–4607.

Steinbeck, J., Nikolova, D., Weingarten, R., Johnson, X., Richaud, P., Peltier, G., Hermann, M., Magneschi, L., Hippler, M., 2015. Deletion of Proton Gradient Regulation 5 (PGR5) and PGR5-Like 1 (PGRL1) proteins promote sustainable light-driven hydrogen production in Chlamydomonas reinhardtii due to increased PSII activity under sulfur deprivation. Front. Plant Sci. 6.

Steinbeck, J., Ross, I.L., Rothnagel, R., Gäbelein, P., Schulze, S., Giles, N., Ali, R., Drysdale, R., Sierecki, E., Gambin, Y., Stahlberg, H., Takahashi, Y., Hippler, M., Hankamer, B., 2018. Structure of a PSI-LHCI-cyt b6f supercomplex in Chlamydomonas reinhardtii promoting cyclic electron flow under anaerobic conditions. Proc. Natl. Acad. Sci. U. S. A. 115, 10517–10522.

Stoecker, D.K., Hansen, P.J., Caron, D.A., Mitra, A., 2017. Mixotrophy in the Marine Plankton. Ann. Rev. Mar. Sci. 9, 311–335.

Sturms, R., DiSpirito, A.A., Fulton, D.B., Hargrove, M.S., 2011. Hydroxylamine reduction to ammonium by plant and cyanobacterial hemoglobins. Biochemistry 50, 10829–10835.

Sun, N., Han, X., Xu, M., Kaplan, A., Espie, G.S., Mi, H., 2019. A thylakoid-located carbonic anhydrase regulates CO 2 uptake in the cyanobacterium Synechocystis sp. PCC 6803. New Phytol. 222, 206–217.

Svensson-Ek, M., Abramson, J., Larsson, G., Törnroth, S., Brzezinski, P., Iwata, S., 2002. The X-ray crystal structures of wild-type and EQ(I-286) mutant cytochrome c oxidases from Rhodobacter sphaeroides. J. Mol. Biol. 321, 329–339.

Takahashi, H., Uchimiya, H., Hihara, Y., 2008. Difference in metabolite levels between photoautotrophic and photomixotrophic cultures of Synechocystis sp. PCC 6803 examined by capillary electrophoresis electrospray ionization mass spectrometry. J. Exp. Bot. 59, 3009–3018.

Tamoi, M., Miyazaki, T., Fukamizo, T., Shigeoka, S., 2005. The Calvin cycle in cyanobacteria is regulated by CP12 via the NAD(H)/NADP(H) ratio under light/dark conditions. Plant J. 42, 504–513.

Teeling, H., Fuchs, B.M., Becher, D., Klockow, C., Gardebrecht, A., Bennke, C.M., Kassabgy, M., Huang, S., Mann, A.J., Waldmann, J., Weber, M., Klindworth, A., Otto, A., Lange, J., Bernhardt, J., Reinsch, C., Hecker, M., Peplies, J., Bockelmann, F.D., Callies, U., Gerdts, G., Wichels, A., Wiltshire, K.H., Glöckner, F.O., Schweder, T., Amann, R., 2012. Substrate-controlled succession of marine bacterioplankton populations induced by a phytoplankton bloom. Science (80-.). 336, 608–611.

Theune, M.L., Hildebrandt, S., Steffen-Heins, A., Bilger, W., Gutekunst, K., Appel, J., 2020. In-vivo quantification of electron flow through photosystem I – cyclic electron transport makes up about 35% in a cyanobacterium. BBA - Bioenerg. 1862, 148353.

Thiel, K., Patrikainen, P., Nagy, C., Fitzpatrick, D., Pope, N., Aro, E.M., Kallio, P., 2019. Redirecting photosynthetic electron flux in the cyanobacterium Synechocystis sp. PCC 6803 by the deletion of flavodiiron protein Flv3. Microb. Cell Fact. 18, 1–16.

Thorsteinsson, M. V, Bevan, D.R., Potts, M., Dou, Y., Eich, R.F., Hargrove, M.S., Gibson, Q.H., Olson, J.S., 1999. A cyanobacterial hemoglobin with unusual ligand binding kinetics and stability properties. Biochemistry 38, 2117–2126.

Tolleter, D., Ghysels, B., Alric, J., Petroutsos, D., Tolstygina, I., Krawietz, D., Happe, T., Auroy, P., Adriano, J.M., Beyly, A., Cuiné, S., Plet, J., Reiter, I.M., Genty, B., Cournac, L., Hippler, M., Peltier, G., 2011. Control of hydrogen photoproduction by the proton gradient generated by cyclic electron flow in Chlamydomonas reinhardtii. Plant Cell 23, 2619–2630.

Toogood, H.S., Scrutton, N.S., 2018. Discovery, Characterization, Engineering, and Applications of Ene-Reductases for Industrial Biocatalysis. ACS Catal. 8, 3532–3549.

Torrado, A., Valladares, A., Puerto-Galán, L., Hervás, M., Navarro, J.A., Molina-Heredia, F.P., 2017. Cyt c6-3: A new isoform of photosynthetic Cyt c6 exclusive to heterocyst-forming cyanobacteria. Plant Cell Physiol. 58, 256–265.

Tóth, S.Z., Yacoby, I., 2019. Paradigm Shift in Algal H2 Production: Bypassing Competitive Processes. Trends Biotechnol.

Twigg, A.I., Baniulis, D., Cramer, W.A., Hendrich, M.P., 2009. EPR detection of an O2 surrogate bound to heme cn of the cytochrome b6f complex. J. Am. Chem. Soc. 131, 12536–12537.

Ueda, K., Nakajima, T., Yoshikawa, K., Toya, Y., Matsuda, F., Shimizu, H., 2018. Metabolic flux of the oxidative pentose phosphate pathway under low light conditions in Synechocystis sp. PCC 6803. J. Biosci. Bioeng. 126, 38–43.

Umena, Y., Kawakami, K., Shen, J.R., Kamiya, N., 2011. Crystal structure of oxygen-evolving photosystem II at a resolution of 1.9Å. Nature 473, 55–60.

Uppal, S., Khan, M.A., Kundu, S., 2020. Identification and characterization of a recombinant cognate hemoglobin reductase from Synechocystis sp. PCC 6803. Int. J. Biol. Macromol. 162, 1054–1063.

Vaccaro, R.F., Hicks, S.E., Jannasch, H.W., Carey, F.G., 1968. the Occurrence and Role of Glucose in Seawater. Limnol. Oceanogr. 13, 356–360.

Varman, A.M., Xiao, Y., Pakrasi, H.B., Tang, Y.J., 2013. Metabolic engineering of Synechocystis sp. Strain PCC 6803 for isobutanol production. Appl. Environ. Microbiol. 79, 908–914.

Vicente, J.B., Gomes, C.M., Wasserfallen, A., Teixeira, M., 2002. Module fusion in an A-type flavoprotein from the cyanobacterium Synechocystis condenses a multiple-component pathway in a single polypeptide chain. Biochem. Biophys. Res. Commun. 294, 82–87.

Vijay, D., Akhtar, M.K., Hess, W.R., 2019. Genetic and metabolic advances in the engineering of cyanobacteria. Curr. Opin. Biotechnol.

Viola, S., Sellés, J., Bailleul, B., Joliot, P., Wollman, F.-A., 2021. In vivo electron donation from plastocyanin and cytochrome c to PSI in Synechocystis sp. PCC6803. Biochim. Biophys. Acta - Bioenerg. 1862, 148449.

Vuorijoki, L., Isojärvi, J., Kallio, P., Kouvonen, P., Aro, E.M., Corthals, G.L., Jones, P.R., Muth-Pawlak, D., 2016. Development of a Quantitative SRM-Based Proteomics Method to Study Iron Metabolism of Synechocystis sp. PCC 6803. J. Proteome Res. 15, 266–279.

Wastl, J., Molina-Heredia, F.P., Hervás, M., Navarro, J.A., De La Rosa, M.A., Bendall, D.S., Howe, C.J., 2004. Redox properties of Arabidopsis cytochrome c6 are independent of the loop extension specific to higher plants. Biochim. Biophys. Acta - Bioenerg. 1657, 115–120.

Watanabe, M., Ikeuchi, M., 2013. Phycobilisome: Architecture of a light-harvesting supercomplex. Photosynth. Res.

Wei, L., Derrien, B., Gautier, A., Houille-Vernes, L., Boulouis, A., Saint-Marcoux, D., Malnoë, A., Rappaport, F., de Vitry, C., Vallon, O., Choquet, Y., Wollman, F.A., 2014. Nitric oxide-triggered remodeling of chloroplast bioenergetics and thylakoid proteins upon nitrogen starvation in Chlamydomonas reinhardtii. Plant Cell 26, 353–372.

Weigel, M., Varotto, C., Pesaresi, P., Finazzi, G., Rappaport, F., Salamini, F., Leister, D., 2003. Plastocyanin is indispensable for photosynthetic electron flow in Arabidopsis thaliana. J. Biol. Chem. 278, 31286–31289.

Williams, J.G.K., 1988. Construction of Specific Mutations in Photosystem II Photosynthetic Reaction Center by Genetic Engineering Methods in Synechocystis 6803. Methods Enzymol. 167, 766–778.

Wodala, B., Deák, Z., Vass, I., Erdei, L., Altorjay, I., Horváth, F., 2008. In vivo target sites of nitric oxide in photosynthetic electron transport as studied by chlorophyll fluorescence in pea leaves. Plant Physiol. 146, 1920–1927.

World Intellectual Property Organization, 2016. Patent Landscape Report on Microalgae-Related Technologies. Pat. Landsc. Reports.

Worrall, J.A.R., Schlarb-Ridley, B.G., Reda, T., Marcaida, M.J., Moorlen, R.J., Wastl, J., Hirst, J., Bendall, D.S., Luisi, B.F., Howe, C.J., 2007. Modulation of heme redox potential in the cytochrome c6 family. J. Am. Chem. Soc. 129, 9468–9475.

Wu, Q., Vermaas, W.F.J., 1995. Light-dependent chlorophyll a biosynthesis upon chlL deletion in wild-type and photosystem I-less strains of the cyanobacterium Synechocystis sp. PCC 6803. Plant Mol. Biol. 29, 933–945.

Xie, H., Buschmann, S., Langer, J.D., Ludwig, B., Michel, H., 2014. Biochemical and biophysical characterization of the two isoforms of cbb3-Type cytochrome c oxidase from Pseudomonas stutzeri. J. Bacteriol. 196, 472–482.

Yang, C., Hua, Q., Shimizu, K., 2002. Metabolic flux analysis in Synechocystis using isotope distribution from 13C-labeled glucose. Metab. Eng. 4, 202–216.

Yao, L., Shabestary, K., Björk, S.M., Asplund-Samuelsson, J., Joensson, H.N., Jahn, M., Hudson, E.P., 2020. Pooled CRISPRi screening of the cyanobacterium Synechocystis sp PCC 6803 for enhanced industrial phenotypes. Nat. Commun. 11, 1–13.

Yeremenko, N., Jeanjean, R., Prommeenate, P., Krasikov, V., Nixon, P.J., Vermaas, W.F.J., Havaux, M., Matthijs, H.C.P., 2005. Open reading frame ssr2016 is required for antimycin A-sensitive photosystem I-driven cyclic electron flow in the cyanobacterium Synechocystis sp. PCC 6803. Plant Cell Physiol. 46, 1433–1436.

Yoshikawa, K., Hirasawa, T., Ogawa, K., Hidaka, Y., Nakajima, T., Furusawa, C., Shimizu, H., 2013. Integrated transcriptomic and metabolomic analysis of the central metabolism of Synechocystis sp. PCC 6803 under different trophic conditions. Biotechnol. J. 8, 571–580.

You, L., Berla, B., He, L., Pakrasi, H.B., Tang, Y.J., 2014. 13C-MFA delineates the photomixotrophic metabolism of Synechocystis sp. PCC 6803 under light- and carbon-sufficient conditions. Biotechnol. J. 9, 684–692.

Young, J.D., Shastri, A.A., Stephanopoulos, G., Morgan, J.A., 2011. Mapping photoautotrophic metabolism with isotopically nonstationary 13C flux analysis. Metab. Eng. 13, 656–665.

Yu, H., Jia, S., Dai, Y., 2009. Growth characteristics of the cyanobacterium Nostoc flagelliforme in photoautotrophic, mixotrophic and heterotrophic cultivation. J. Appl. Phycol. 21, 127–133.

Zaffagnini, M., Fermani, S., Marchand, C.H., Costa, A., Sparla, F., Rouhier, N., Geigenberger, P., Lemaire, S.D., Trost, P., 2019. Redox Homeostasis in Photosynthetic Organisms: Novel and Established Thiol-Based Molecular Mechanisms. Antioxidants Redox Signal. 31, 155–210.

Zatwarnicki, P., Barciszewski, J., Krzywda, S., Jaskolski, M., Kolesinski, P., Szczepaniak, A., 2014. Cytochrome c6B of Synechococcus sp. WH 8102 - Crystal structure and basic properties of novel c6-like family representative. Biochem. Biophys. Res. Commun. 443, 1131–1135.

Zhang, P., Allahverdiyeva, Y., Eisenhut, M., Aro, E.M., 2009. Flavodiiron proteins in oxygenic photosynthetic organisms: Photoprotection of photosystem II by FIv2 and FIv4 in Synechocystis sp. PCC 6803. PLoS One 4, e5331.

Zhang, P., Eisenhut, M., Brandt, A.M., Carmel, D., Silén, H.M., Vass, I., Allahverdiyeva, Y., Salminen, T.A., Aro, E.M., 2012. Operon flv4-flv2 provides cyanobacterial photosystem ii with flexibility of electron transfer. Plant Cell 24, 1952–1971.

Zhu, L., 2015. Biorefinery as a promising approach to promote microalgae industry: An innovative framework. Renew. Sustain. Energy Rev. 41, 1376–1384.

Zilliges, Y., Dau, H., 2016. Unexpected capacity for organic carbon assimilation by Thermosynechococcus elongatus, a crucial photosynthetic model organism. FEBS Lett. 590, 962–970.

Zouni, A., Witt, H.T., Kern, J., Fromme, P., Krauss, N., Saenger, W., Orth, P., 2001. Crystal structure of photosystem II from Synechococcus elongatus at 3.8 Å resolution. Nature 409, 739–743.

Zubkov, M. V., Tarran, G.A., 2008. High bacterivory by the smallest phytoplankton in the North Atlantic Ocean. Nature 455, 224–226.

TURUN
YLIOPISTO
UNIVERSITY
OF TURKU

Painosalama Oy, Turku, Finland 2021

ISBN 978-951-29-8688-0 (PRINT)
ISBN 978-951-29-8689-7 (PDF)
ISSN 0082-7002 (Print)
ISSN 2343-3175 (Online)